CONTRACTOR REPORT

SAND88—7030
Unlimited Release
UC—276

The Development and Verification of the Perez Diffuse Radiation Model

Richard Perez, Ronald Stewart, Robert Seals, Ted Guertin
Atmospheric Sciences Research Center
SUNY at Albany
Albany, NY 12222

Prepared by Sandia National Laboratories Albuquerque, New Mexico 87185
and Livermore, California 94550 for the United States Department of Energy
under Contract DE-AC04-76DP00789

Printed October 1988

Issued by Sandia National Laboratories, operated for the United States Department of Energy by Sandia Corporation.

Printed in the United States of America
Available from
National Technical Information Service
U.S. Department of Commerce
5285 Port Royal Road
Springfield, VA 22161

NTIS price codes
Printed copy: A09
Microfiche copy: A01

Distribution
Category UC-276

SAND88-7030
Unlimited Release
Printed October 1988

THE DEVELOPMENT AND VERIFICATION OF THE PEREZ DIFFUSE RADIATION MODEL

Richard Perez, Ronald Stewart
Robert Seals, Ted Guertin

Atmospheric Sciences Research Center
SUNY at Albany
Albany, NY 12222

Sandia Contract 56-5434

ABSTRACT

The purpose of this work was to determine site specific coefficients (within the U.S.) for use with the Perez diffuse irradiance model. The model predicts diffuse irradiance on tilted planes of any orientation for all insolation conditions, based on the knowledge of direct and global (or diffuse) irradiance. This is a component of SNLA's photovoltaic simulation program PVFORM. The model consists of (1) a pre-set geometric framework that describes the main non-isotropic features of sky radiance - circumsolar and horizon/zenith effects - and (2) an experimentally derived component that describes the variations of these anisotropic effects with weather conditions. A measurement program was initiated to provide the data necessary for (1) deriving the model's experimental component for several US locations, (2) comparing model configuration and evaluating performance at these locations and (3) evaluating site dependency and recommending, if justified, model configurations adapted to particular environments/climates. Five environmentally distinct sites were selected based on their potential impact on model performance. In addition, work was performed to improve sky condition parameterization and eliminate all unjustified complexities of the original model. The main results of this work are the following: (1) the model algorithm has been greatly simplified while conserving original accuracy, (2) the physical soundness and effectiveness of the insolation parameterization method have been improved, (3) one unique model, with a fixed set of coefficients, has been shown to be sufficiently accurate to describe sites within the U.S.

ACKNOWLEDGEMENTS

We thank Dr. Pierre Ineichen of the University of Geneva, Switzerland, and Dr. Antoine Zelenka of the Swiss Meteorological Institute, for their constructive comments and discussions.

We also thank the SNLA and FSEC staff for their responsive interaction during station construction and data acquisition.

Trinity University, Georgia-Tech and SERI contributed to the project by loaning pyranometers.

Finally, daylight availability modeling work conducted at the ASRC on behalf of NYSERDA contributed to enhance the effort and results of this program.

TABLE OF CONTENTS

LIST OF TABLES

LIST OF FIGURES

INTRODUCTION

The Atmospheric Sciences Research Center of the State University of New York at Albany (ASRC) was contracted by Sandia National Laboratories (SNLA) in 1986 to further develop and perform a comprehensive validation of the slope irradiance algorithm proposed by Perez et al. [1]. This algorithm, now referred to as the Perez model, takes into account the anisotropy of the sky's diffuse irradiance to predict irradiance on tilted surfaces. It is a component of SNLA's photovoltaic simulation program, PVFORM [2].

The main goal of this program was to address remaining questions as to the site dependency of the model and to develop, if necessary, different versions of the model for specific environments.

A measurement program was designed and implemented to provide the experimental data base necessary to optimize and validate the model for the conterminous United States. Also, a substantial portion of the effort was directed toward improving and streamlining the algorithm.

This report is an overview of the program. It is divided into four main sections.

The first section reviews the changes performed on the model's algorithm since the onset of the program. This section also describes the current methodology used to fit the model to a given experimental data set.

The second section describes the measurement program and its implications for the modeling work.

Data analysis results are presented in the third section. They include a presentation and comparison of coefficients derived at each site along with model validation results.

The last section of this report focuses on interpretation and discussion of results and concludes with a set of recommendations.

I MODEL ALGORITHM

I.1 Derivation of a new, simpler algorithm.

The new algorithm is given in Eq. (1) below,

$$D_c = D_h \{ (1-F_1)[1+\cos(S)]/2 + F_1\, a/b + F_2 \sin(S) \}, \quad (1)$$

where D_c is the diffuse irradiance received by a tilted surface of slope S, D_h is the horizontal diffuse irradiance, F_1 and F_2 are respectively the circumsolar and horizon "reduced" brightness coefficients, and a and b are two terms describing the incidence-weighted solid angle sustained by the circumsolar region as seen respectively by the tilted surface and the horizontal.

The methodology and rationale for systematically reducing the complexity of the algorithm while maintaining the original performance [3] are presented in detail in Appendix C (pp. C-15 to C-26). This work which was also reported in Solar Energy [4].

Although the model's geometric framework and the methodology to derive coefficients have remained basically unchanged, considerable simplifications have been performed. First, a linear algorithm was substituted for the original equation by redefining brightness coefficients as fractions of horizontal diffuse irradiance rather than as radiance enhancement terms. Second, unneeded (and arbitrary) original geometric complexities were removed. For instance, the physical horizon band could be replaced by an arc of great circle, yielding a simpler analytic formulation with only negligible impact on energies computed for tilted planes. Concerning the circumsolar brightening, two model versions were proposed [3]; one keeping the original physical circular region and the other simply assuming a point source.

Results presented herein are based on the recommended simpler (point-source circumsolar) version. The recommendation is based on the following facts: (1) the knowledge of actual sky radiance distribution profiles is not an absolute requirement to achieve relatively high precision of the integrated (diffuse irradiance) value on a flat-plate collector with a large field of view; the effect may be accounted for by a series or point or extended sources; (2) a circumsolar point source is not less physically sound than a fixed-width, uniform-radiance circumsolar disc; (3) performance degradation from extended to point source was experimentally found to be negligible.

The new model framework is compared to the original in Figure 1.

Note that the above remarks are valid only for flat-plate collectors. Other applications, such as daylighting, involving more complex window/room geometries, are more sensitive to the actual radiance (luminance) gradients. An extrapolation of the current model for these applications is under development [5].

In this form, the terms a and b of Eq. (1) may be simply expressed as:

$$a = \text{Max}\,[0,\ \cos(\theta)],\ \text{and} \tag{2}$$

$$b = \text{Max}\,[\cos 85^{o},\ \cos(Z)], \tag{3}$$

where θ and Z are the solar incidence angles on the tilted surface and on the horizontal. The lower limit in the formulation of b is introduced to avoid possible distortions and to allow adequate model utilization for zenith angles higher than the validation domain of this study (5^{o}, 85^{o}).

I.2 Derivation of Brightness Coefficients

Coefficients are treated as functions of three quantities that parameterize the sky's condition. These quantities are the solar zenith angle, Z, the sky's clearness, ε, and the sky's brightness, Δ. The parameters ε and Δ are given by:

$$\varepsilon = 1 + \{[(D_h + I)/D_h + \kappa Z^3]/[1 + \kappa Z^3] - 1\} \tag{4}$$

where $\kappa = 1.041$ -- Z in radians --,

$$\text{and } \Delta = D_h\, m/I_o, \tag{5}$$

where I is the normal incident direct irradiance, m the optical air mass and I_o is the extraterrestrial normal incident irradiance.

It is important to remark that the three parameters are designed to describe all sky conditions from overcast to clear and are based on two measured quantities - global and direct (or diffuse) irradiance - which are necessary to compute irradiance on tilted surfaces regardless of the diffuse algorithm used.

Although some degree of interdependence exists between the three quantities, they are treated as independent dimensions of a sky condition's space.

Substantial work was done to enhance this independent character; the dependence of both ε and Δ on Z has been practically eliminated. Figure 2 shows the dependence of the original ε on Z and explains the Z^3 formulation in Eq. (4).

Dependence of ε on the site's altitude was also noted. A linear empirical altitude correction was used for this work after analyzing data from sites ranging from sea level to 1600 m. The corrective factor (1 - 0.00026h) was applied to ε. This is recommended for high-altitude sites such as Albuquerque, NM. However, additional investigation is needed to more precisely delineate altitude effect on the sky condition's parameter ε.

The functions used to describe the variations of F_1 and F_2 with these parameters have also been changed. Originally, these were discrete functions. The $\Delta - \varepsilon - Z$ space was divided into 240 categories. Each was assigned a pair of values for F_1 and F_2. A fully analytical approach was tried but rejected because its formulation would have been too complex and would have consumed too computer time (see Sandia's re;ated report [3] in Appendix C). A compromise was reached whereby analytical linear functions were used to describe variations with Δ and Z, and a discrete representation was used on the ε axis, which was divided into 8 intervals. The eight ε intervals are specified in Table I -- they have been optimized to balance the observed variations of F_1 and F_2 evenly between each interval. Model coefficients are formulated as:

$$F_1(\varepsilon) = \text{Max}\,[0,\ F_{11}(\varepsilon) + \Delta\, F_{12}(\varepsilon) + Z\, F_{13}(\varepsilon)] \quad \text{and} \quad (6)$$

$$F_2(\varepsilon) = F_{21}(\varepsilon) + \Delta\, F_{22}(\varepsilon) + Z\, F_{23}(\varepsilon). \quad (7)$$

The formulation of F_1 is made so as to avoid non-physical negative values that may occur and result in unacceptable distortions if the model is used for very low solar elevation angles beyond the present validation range.

A total of 48 coefficients is needed in the current model formulation (down from 480 in the original version).

These coefficients are obtained by least square fitting of Eq. (1) to experimental data recorded on tilted surfaces. The following methodology is used:

> Given **n** tilted sensors and **m** hourly (or shorter time step) events belonging to one of the eight ε ranges specified in Table I, let the values of global, direct and diffuse radiation for the jth hour be respectively G_j, I_j and D_{hj}, and the corresponding global values on tilted surfaces, G_{cij}, from i =1 to n. Let the expression R be defined as:

$$R = \sum_{j=1}^{m} \sum_{i=1}^{n} (G_{cij} - g_{cij})^2, \quad (8)$$

where g_{cij} is the global irradiance on the ith surface estimated by the Perez model as follows:

$$g_{cij} = I_j \cos(\theta_{ij}) + a_{ij} + b_{ij}\, F_1 + c_{ij}\, F_2, \quad (9)$$

where θ_{ij} is the solar incidence angle on the i^{th} surface at time j --this is of course assumed to be 90^o for incident angles exceeding 90^o. The terms a_{ij}, b_{ij} and c_{ij} are given by [see Eq. (1)]:

$$a_{ij} = D_{hj}\,[1 + \cos(S_i)]/2, \quad (10)$$

$$b_{ij} = D_{hj}\,[\cos(\theta_{ij})/\cos(Z_j)] - a_{ij}, \quad (11)$$

$$c_{ij} = D_{hj} \sin(S_i), \quad (12)$$

where S_i is the slope of the i^{th} surface and Z_j is the solar zenith angle at time j.

Given the expression selected for F_1 and F_2, the expression R may be written as:

$$R = \sum_{j=1}^{m}\sum_{i=1}^{n} [(A'_{ij} + B'_{ij}F_{11} + C'_{ij}F_{12} + D'_{ij}F_{13} + E'_{ij}F_{21} + F'_{ij}F_{22} + G'_{ij}F_{23})]^2, \quad (13)$$

where:

$$A'_{ij} = G_{cij} - I_j \cos(\theta_{ij}) - a_{ij}, \quad (12)$$

$$B'_{ij} = b_{ij}, \quad (13)$$

$$C'_{ij} = b_{ij}\,\Delta_j, \quad (14)$$

$$D'_{ij} = b_{ij}\,Z_j, \quad (16)$$

$$E'_{ij} = c_{ij}, \quad (17)$$

$$F'_{ij} = c_{ij}\,\Delta_j, \quad (18)$$

$$G'_{ij} = c_{ij}\,Z_j. \quad (19)$$

The six coefficients' ranges are then obtained by minimizing the expression R; that is, by solving the following system of linear equations:

$$\begin{aligned}
&A"B" + B"^2F_{11} + B"C"F_{12} + B"D"F_{13} + B"E"F_{21} + B"F"F_{22} + B"G"F_{23} = 0\\
&A"C" + B"C"F_{11} + C"^2F_{12} + C"D"F_{13} + C"E"F_{21} + C"F"F_{22} + C"G"F_{23} = 0\\
&A"D" + B"D"F_{11} + D"C"F_{12} + D"^2F_{13} + D"E"F_{21} + D"F"F_{22} + D"G"F_{23} = 0\\
&A"E" + B"E"F_{11} + E"C"F_{12} + E"D"F_{13} + E"^2F_{21} + E"F"F_{22} + E"G"F_{23} = 0\\
&A"F" + B"F"F_{11} + F"C"F_{12} + F"D"F_{13} + F"E"F_{21} + F"^2F_{22} + F"G"F_{23} = 0\\
&A"G" + B"G"F_{11} + G"C"F_{12} + G"D"F_{13} + G"E"F_{21} + G"F"F_{22} + G"^2F_{23} = 0,
\end{aligned} \quad (20)$$

where,

$$A"B" = \sum_{j=1}^{m}\sum_{i=1}^{n} [A'_{ij}B'_{ij}], \quad (21)$$

$$B"^2 = \sum_{j=1}^{m}\sum_{i=1}^{n} [B'^2], \quad (22)$$

.....

$$G"^2 = \sum_{j=1}^{m}\sum_{i=1}^{n} [G'^2], \text{ etc.} \quad (23)$$

The process is repeated for each of the eight ε categories so as to obtain a total of 48 coefficients.

Note that the use of the new algorithm greatly simplifies the coefficient determination process. The original model called for solving a set of nonlinear equations, a computer-demanding task that could lead to nonconverging solutions.

II EXPERIMENTAL DATA

As explained above, the derivation of coefficients for the model (as well as its validation) relies on the availability of radiation data for tilted surfaces. Four vertical surfaces facing four azimuths and a south facing 45° slope were suggested as a compromise that would not bias the results in any particular orientation while keeping the number of measurements reasonably small.

Although the model had already been validated independently [1,6,7] against several data sets worldwide, notably by the International Energy Agency [7], several questions remained as to the site-specific climatic and environmental effects on the model's coefficients and performance. These questions remained unanswered primarily because most validation data sets relied on different instrumentation, measurement techniques, quality assurance, etc.

This work represents a first attempt to systematically assemble a set of identical measurements, using identical instrumentation and set-up, in several locations nationwide, each being selected for its distinct climatic and environmental characteristics.

II.1 Selection of Sites

The site selection process included the following steps:

(1) Reviewing published literature on solar radiation climatology and mapping.

(2) Accounting for site-specific environmental factors thought to have a potential impact on model performance and coefficients; that is altitude, regional albedo and prevailing local aerosol content.

(3) Limiting final sites to those where Sandia National Laboratories already conducted experimental work (there are 13 such stations nationwide).

The selection process is presented in detail in Appendix C (pp. C-3 to C-14). It is briefly summarized here.

Literature review pointed out two traditional approaches to the division of a large area into distinct solar regions. The first is based on the region's energy yield (global, direct or diffuse) [8,9,10]. The second approach identifies regions by similarities in temporal variations and average, maximum

and minimum yield of the global component. The methodologies used for this second approach range from sophisticated principal component [11,12,13] or harmonic analysis [14] to classifications according to yearly energy yield amplitude and phase [15].

It was felt that few of the more sophisticated methods gave results applicable to the present analysis, primarily because the classifications -- often based on monthly data -- only reflect long-term variation patterns rather than the physical aspects of radiation relevant to the model's performance. The SERI direct/diffuse maps [10] and the Willmott's classification [11] were selected as most appropriate input to the present selection process; the former because the direct/diffuse gain of a region is indicative of the prevailing turbidity, the latter because Willmott's statistical regionalization was the only one using daily rather than monthly data thereby incorporating some information on sky condition.

In addition to literature review, the selection process included four site-specific environmental factors thought to have potential influence on model configuration and performance if not properly accounted for by the proposed insolation parameterization. These factors are only partially accounted for in the above statistical regionalizations. They are (1) the site's altitude; (2) the regional albedo as inferred from prevailing regional ground cover; (3) the site's air quality (particulate content); and (4) the site's prevailing atmospheric moisture content. The two first factors could have a possibly non-negligible impact on clear-day horizon brightening, while the third and fourth factors have a strong influence on circumsolar brightening.

Finally, after limiting final site selection to SNLA experimental facilities, the five following sites were selected:

(1) Albuquerque, New Mexico -- high altitude, arid.
(2) Phoenix, Arizona -- low altitude, arid.
(3) El Monte (Los Angeles), California -- continental arid and oceanic influence, presence of anthropogenic smog.
(4) Cape Canaveral, Florida -- sub-tropical, maritime.
(5) Osage, Kansas -- this last site was selected because it represented a transition zone between the arid western region investigated and mid-latitude temperate regions where model performance was assumed to be known.

II.2 Instrumentation and Data Acquisition

Measurements performed at each site consisted of global, direct and diffuse irradiance as well as ground-shielded global irradiance on a 45° south-facing slope and on vertical surfaces facing respectively north, east, south and west. A typical station set-up is shown in Figure 3. Instrumentation consisted of Eppley PSPs and NIPs. Ground shields were box-like structures, the interiors of which were covered with black-painted honey-comb so as to virtually eliminate the ground reflected component. Their rims were aligned with the center of the tilted detectors at a distance of 25 cm.

All instruments, except Cape Canaveral's, were cross-calibrated outdoors at a SNLA facility at the onset of the project. PSPs were calibrated horizontally under 45° solar incidence. Cape Canaveral's sensors were calibrated by the

Florida Solar Energy Center (FSEC).

In addition to irradiance sensors, the stations were also equipped with an equivalent set of quantum sensors measuring photon counts between 400 and 700 nm in order to begin assessing the extent of spectral effects. These data will be analyzed subsequently on behalf of the Solar Energy Research Institute.

Each site's collection period for data analyzed herein is given below:

Phoenix: 12/1/86 to 6/30/87
El Monte: 12/20/86 to 6/30/87
Osage: 3/5/86 to 5/30/87
Albuquerque: 1/3/87 to 6/30/87
Cape Canaveral: 3/9/87 to 11/15/87

With the exception of Osage, data are representative of most solar geometries existing at each site -- solstice-to-solstice.

Note: Post 7/16/87 Cape Canaveral data are analyzed separately in Appendix B, because of instrumentation questions still unresolved at reporting time.

All data were subjected to automatic quality control, which was extrapolated from recommendations prepared for the US Daylight Availability Measurement Working Group [16]. Secondary data QC based on the Perez model was also performed. This insured that differences between the calculated (global minus direct) and modeled diffuse value did not either exceed 50 W or 30%, whichever was largest (that is, over 3 to 4 times the known Perez RMSE). Also, manual quality control of data was performed during bi/tri-weekly site visits to clean instruments, verify tracking accuracy and report any pertinent events.

Also used in this report for comparison purposes are data from the Albany, NY Solar Energy Meteorological and Training Site (SEMRTS) [17] recorded between January 1979 and December 1983, data from Carpentras, France [18], recorded between January 1979 and December 1980 and data from Trappes, France [19], recorded between April 1979 and April 1981.

III DATA ANALYSIS -- RESULTS

III.1 Climatology of the Sites

The distribution of hourly events observed at each site with respect to insolation conditions (with the parameters Δ and ε for Z ~ constant) is plotted in Figures 5 through 9 for Phoenix, El Monte, Osage, Albuquerque and Cape Canaveral, respectively. Figure 4, in which distribution for Carpentras, France, is plotted, features descriptive labels that should be helpful in understanding these representations.

The dominance of very clear events (high ε) in Phoenix and Albuquerque is clearly marked. It is interesting to note the high peak in Albuquerque for the highest ε category is due both to the site's clearness and its altitude -- ε has not been corrected for altitude dependence in this plot to illustrate this point.

By contrast, El Monte exhibits a much higher frequency of high turbidity occurrences ($2 < \varepsilon < 5$), intermediate (partly cloudy/very high turbidity) events ($1 < \varepsilon < 2$) and overcast events ($\varepsilon = 1$). Conditions at Cape Canaveral are quite similar; however, the frequency of very clear events is noticeably lower than in the Los Angeles area. The Osage distribution is bimodal (i.e., two peaks; clear and overcast conditions). This confirms the transitional aspect of this site between the new regions investigated in this study and previously studied northeastern climates, where the bimodal distribution is extremely marked (as can be seen in Figure 10 where Albany's event distribution has been plotted).

Figures 4 and 11 describe event distribution at two sites where the model had been validated previously; that is, at Trappes and Carpentras, France. The latter exhibits characteristics reminiscent of the southwestern arid sites, although with a higher incidence of intermediate events. The former exhibits a distribution typical of oceanic Europe with a very high proportion of overcast and intermediate events.

III.2 Coefficients for the Model

A set of coefficients was derived for each of the five SNLA sites. Coefficients are presented in Tables 2 to 6 for Phoenix, El Monte, Osage, Albuquerque and Cape Canaveral respectively. A composite coefficient set, C_1, from the five sites was established and is presented in Table 7. In addition, coefficients derived from Albany data are presented in Table 8, and a composite set based on both SNLA and Albany data, C_2, is shown in Table 9. Coefficients for the two French sites are presented in Table 10. Finally the coef-

ficients for a composite file including the eight sites investigated are reported in Table 11.

Variations of F_1 and F_2 with sky clearness at ~ constant solar zenith angle ($45^o < Z < 60^o$) have been plotted in Figures 12 through 16 for each of the five SNLA sites. Figure 17 includes composite plots from all five sites. They are presented in scatter plot format. Each point was obtained by deriving best fit F_1 and F_2 for each hourly record analyzed.

These variations are consistent with previous results (e.g., Perez et al., [4]) insofar as their main characteristics can be observed at each site. These variations are

(1) The circumsolar brightening coefficient, F_1, increases gradually with ε until it peaks for intermediate ε values representative of high turbidity skies, and then decreases markedly with increased clearness -- this is particularly visible in Phoenix.

(2) The horizon brightening coefficient, F_2, is negative for overcast and low ε occurrences -- indicative of brightening of the zenithal region of the sky for these conditions. This becomes positive past intermediate conditions and increases substantially with clearness.

(3) Remarkably low data scatter is observed, notably for "intermediate conditions" which include a large possible combination of cloud type, amount, thickness and height as well as atmospheric turbidity.

Some differences between sites are also of interest; for instance, the strongly marked peak in El Monte for ε~2 is probably representative of the heavy smog events frequent in that area. Also, when comparing Albuquerque and Phoenix, both very similar, to El Monte, it is evident that circumsolar brightening in the latter site has a lesser tendency to decrease for very bright skies, which may be indicative of a persistence of large forward scattering aerosols for these conditions. However, the impact of these differences on energy modeling appears to be minimal, as indicated by the validation results.

III.3 Model Validation

Cross validation of the model, using coefficients from each site against all data sets, constitutes the most important tool to assess model performance, evaluate site dependency and evaluate the need for environment-dependent sets of coefficients.

Results are presented in Appendix A. They include the mean bias (MB) and root mean square (RMS) errors for each surface orientation, site and model coefficient set investigated; that is a total of 100 tests. Composite RMS and MB errors for all orientations are also presented.

The isotropic and two anisotropic models (Hay [20] and Klucher [21]) are used as reference standards. They are described in Perez et al. [1], which is

included as an appendix.

Validation results are summarized in Table 12, where composite errors for each US site and model have been summarized.

Several facts may be pointed out from the analysis of Appendix A and Table 12:

First, it is clear that the model based on a composite set of coefficients (C_1 or C_2) performs adequately for all sites studied. The root mean square error is kept under 16 W for all sites. This represents a performance gain of ~ 60% on the isotropic model and ~ 33% on the Hay model. The additional performance gain using site-specific coefficients is small (on the order of 1 W).

Second, the large errors obtained for the Osage-based model and, to a much lesser extent, for the Albany-based model are noteworthy and demonstrate the usefulness of the present study. Indeed, the very poor results obtained with the Osage-based model in Albuquerque and Phoenix are simply due to the fact that Osage, unlike the two south-western sites, included only very few high ε events and, because of the least square fitting method used to derive the coefficients, the resolution achieved for such events is totally unsatisfactory and allows for important distortions. Likewise, the small performance deterioration caused in all SNLA sites by the Albany-based model may be explained, in part, by the higher latitude of this site and the corresponding lack of very low solar zenith angle events. The fact that composite models perform adequately in both Osage and Albany, on the contrary, demonstrates that the model becomes very stable when this is not "tuned" to satisfy particular climatic conditions.

Table 13, which summarizes the cross validation performed with USA-composite and Trappes/Carpentras data sets, further illustrates the increased stability achieved by pooling several climatic environments to define the model.

Third, the best results among SNLA-based models are obtained with Phoenix coefficients and to a lesser extent, Albuquerque and El Monte coefficients. Likewise, these three sites also exhibit the smallest prediction errors. Although some degree of site dependency may be invoked, other reasons may be advanced to explain these small remaining differences: (1) In Cape Canaveral the main difference with other sites may be traced to the east vertical sensor, which exhibits unusually larger errors, whereas other orientations are adequately modeled -- the Table 12 composite error summary does not include the east sensor for that site; (2) Osage's coefficients' singularity was discussed above, but the larger model errors encountered at this site are likely to be caused by station maintenance, which proved more problematic than at other sites (lack of knowledgeable personnel, less frequent site visits).

Last, the largest isotropic errors (and largest relative model improvement) are found for El Monte where the high occurrence of high turbidity/thin cloudiness makes for a strongly anisotropic environment. The smallest isotropic errors are found in Albuquerque

and Phoenix; this is due both to the more isotropic nature of the very clear sky and the lower impact of the diffuse component in energy budgets at these two sites. Regardless of these differences, the model's performance limit appears to be 13-15 W RMSE, 0-5 W MBE, achieved at each of these sites. This is only slightly larger than the expected instrumentation precision for Class I sensors.

Another model validation question was addressed: that of the impact of instrumentation choice and set-up on model determination and therefore on the effectiveness of this validation study.

The impact of the efficacy of ground radiation removal was assessed: Table 14 presents model cross-validation performed with two Albuquerque data sets. The first contains data recorded from 11/5/86 to 12/31/87 before installation of honeycomb in the ground shields; the second contains data from 1/3/87 to 2/24/87 after installation. The two data sets have a comparable solar geometry as they are almost symmetrical with respect to the winter equinox. It is clear that the "no-honeycomb coefficients" cause the model to overestimate and vice-versa. However, performance deterioration is minimal and certainly does not raise questions as to the validity and conclusions of this and other studies. It is interesting to note that the overestimating model yields noticeably higher RMS errors than the more conservative "with honeycomb" model.

The impact of instrumentation choice will be studied as a follow-up to this work in cooperation with the University of Geneva [22]. This will provide data of high quality, with instrumentation set up similar to this program's, but using Kipp and Zonen CM10 pyranometers with different characteristics from Eppley PSPs.

IV CONCLUSIONS, RECOMMENDATIONS

The three main conclusions of this study are

(1) The original model was considerably streamlined without performance deterioration.

(2) The physical soundness and effectiveness of the parameterization for the sky's condition parameterization have been improved.

(3) No fundamental difference was noted among coefficients derived at any of the SNLA sites. A common set of coefficients based on the ensemble of sites was found to perform adequately for all locations. It would then appear that the sky-condition parameterization method used handles site differences adequately and that a single model is recommended.

(4) SNLA-derived coefficients were found to be more conservative than coefficients derived previously for Albany and two French sites. A model based on SNLA coefficients performs comparatively better on these data than vice versa.

The SNLA coefficient set (Table 8) is recommended as the unique set. The choice is not critical, because both Tables 9 (USA) and 11 (all sites available) also yield perfectly acceptable results. The preference for Table 8, despite the larger climatic base of Table 9 or 11, is based on the following discussion.

Both Albany SEMRTS and the French sites include a less satisfactory instrumentation set-up than the SNLA sites: silicon-based detectors were used in Albany for the four vertical planes; ground shields were black-painted but not coated with anti-reflective devices. No ground shields were available in Trappes and Carpentras -- the reflected component was removed using available measurements in the north and south vertical planes only; also these sites made partial use of older Kipp and Zonen CM3/5 pyranometers.

An extension of this program, currently undertaken in collaboration with the University of Geneva, should further address this question. New state-of-the-art data from Switzerland will be included to derive an updated coefficient set to be made available in the specialized literature.

V REFERENCES

1. R. Perez, R. Stewart, C. Arbogast, R. Seals and J. Scott, (1986): An Anisotropic Hourly Diffuse Radiation Model for Sloping Surfaces --Description, Performance Validation, Site Dependency Evaluation. Solar Energy, 36, 481-498.

2. D. Menicucci and J. Fernandez, (1988): PVFORM Version 3.3; A Photovoltaic System Simulation Program For Stand-Alone and Grid-interactive Applications. SAND85-0376 Sandia National Laboratories, Albuquerque, NM.

3. Sandia National Laboratories Project # 56-5434 (1986); Intermediate Report # 2. SNL, Albuquerque, NM.

4. R. Perez, R. Seals, P. Ineichen, R. Stewart and D. Menicucci, (1987): A New Simplified Version of the Perez Diffuse Irradiance Model for Tilted Surfaces. Solar Energy (In Press; Accepted 2/87).

5. R. Perez, (1987): Daylight Resource Availability. Phase II Final Report. New York State Energy Research and Development Authority, Albany, NY.

6. R. Hulstrom and R. Bird, (1985): Solar Irradiance Available to Various Photovoltaic Systems. SERI/TI-215-2525; Solar Energy Research Institute, Golden, CO.

7. International Energy Agency (1986): Task IX on Heating and Cooling. Subtask B on Solar Radiation Model Validation and Calculation of Solar Irradiance for Inclined Surfaces. Final Report. IEA, Paris, France.

8. J. Werner, (1982): Solartechnik in Verschiedenen Klimazonen der Welt. Sonnenenergie & Warmepumpe.

9. Solar Energy Climatic Analysis - Sandia National Laboratories Report no. RS-3141/20654.

10. Solar Radiation Energy Resource Atlas of the United States. SERI Report no. SERI/SP-642-1037 (1981).

11. C. J. Willmott and M. T. Vernon, (1980): Solar Climates of the Conterminous United States: A Preliminary Investigation. Solar Energy 24.

12. R. C. Balling and M. J. Vojtesak, (1983): Solar Climates of the United States Based on Long-Term Monthly Averaged Daily Insolation Values. Solar Energy, 31, 3.

13. O. E. Granger, (1980): Climatology of Global Solar Radiation in California and Interpolation Technique Based on Orthogonal Functions. Solar Energy, 24.

14. R. C. Balling, (1983): Harmonic Analysis of Monthly Insolation Levels in the United States. Solar Energy 31, 3.

15. W. H. Terjung, (1960): A Global Classification of Solar Radiation. Solar Energy, 13.

16. R. Perez, (1985): Data Quality Control and Processing Requirements, Chapter VII, United States Standard Practice for the Measurement and Reporting of Daylight Availability Data - Interim Standard. R. McCluney, Florida Solar Energy Center, Fla.

17. Solar Energy Meteorological Research and Training Site Region II. Hourly Insolation Data, 1979-1983. SUNY at Albany, Albany, NY.

18. Direction de la Meteorologie, Service Meteorologique Metropolitain. Fichiers Solaires Horaires, Station # 260, Paris, France.

19. Direction de la Meteorologie, Service Meteorologique Metropolitain. Fichiers Solaires Horaires, Station # 851, Paris, France.

20. J.E. Hay and J.A. Davies, (1980): Calculation of the Solar Radiation Incident on an Inclined Surface. Proc. 1st Canadian Solar Radiation Workshop, Toronto (Edited by J. E. Hay and T. K. Won), pp. 59-72.

21. T.M. Klucher, (1978): Evaluation of Models to Predict Insolation on Tilted Surfaces. Solar Energy 23, pp. 111-114.

22. O. Guisan and P. Ineichen, (1985-1988): Evaluation Differenciee du Rayonnement Solaire Diffus Pour Une Meilleure Connaissance Du Rayonnement Solaire Global. (Swiss DOE/Swiss National Foundation Research Project). University of Geneva, Geneva, Switzerland.

VI FIGURES AND TABLES

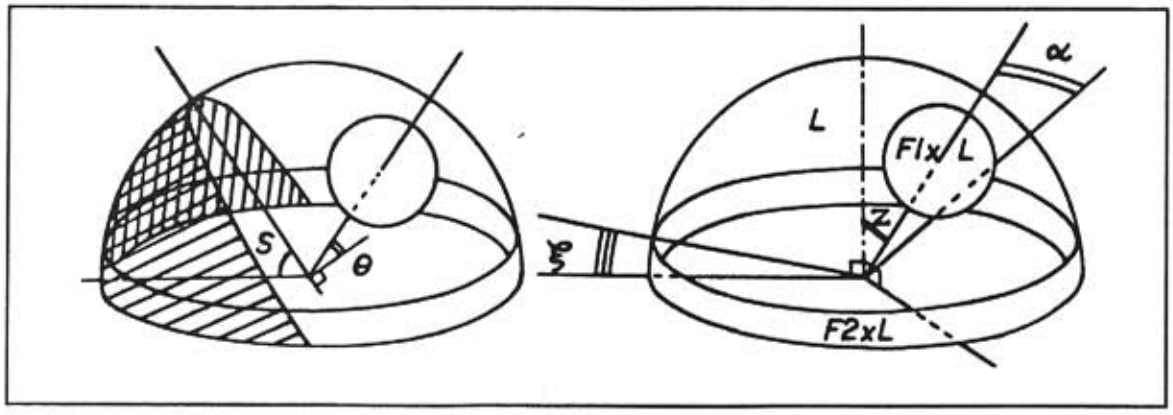

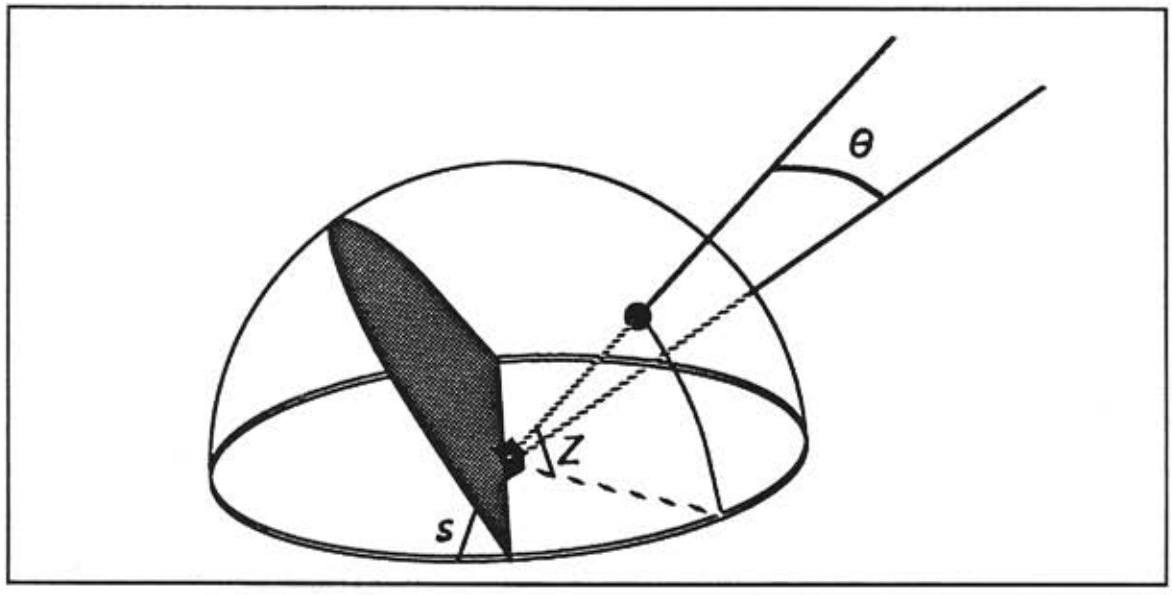

Figure 1 : Comparison of Original and Current Model Geometric Frameworks

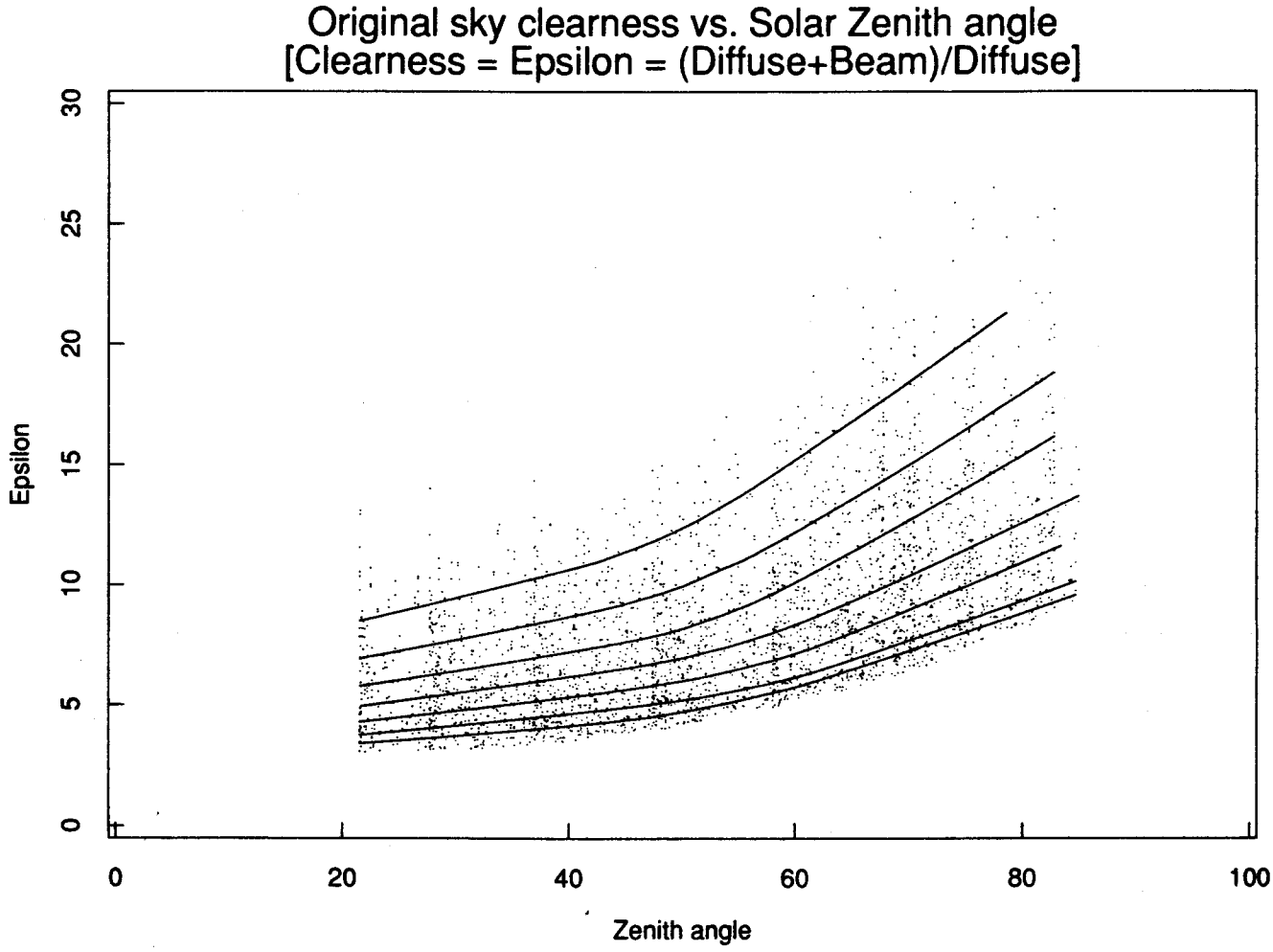

Figure 2: Variation of Original Sky Clearness with Solar Zenith Angle

Figure 3 : Typical Mobile Station (Osage, KS)

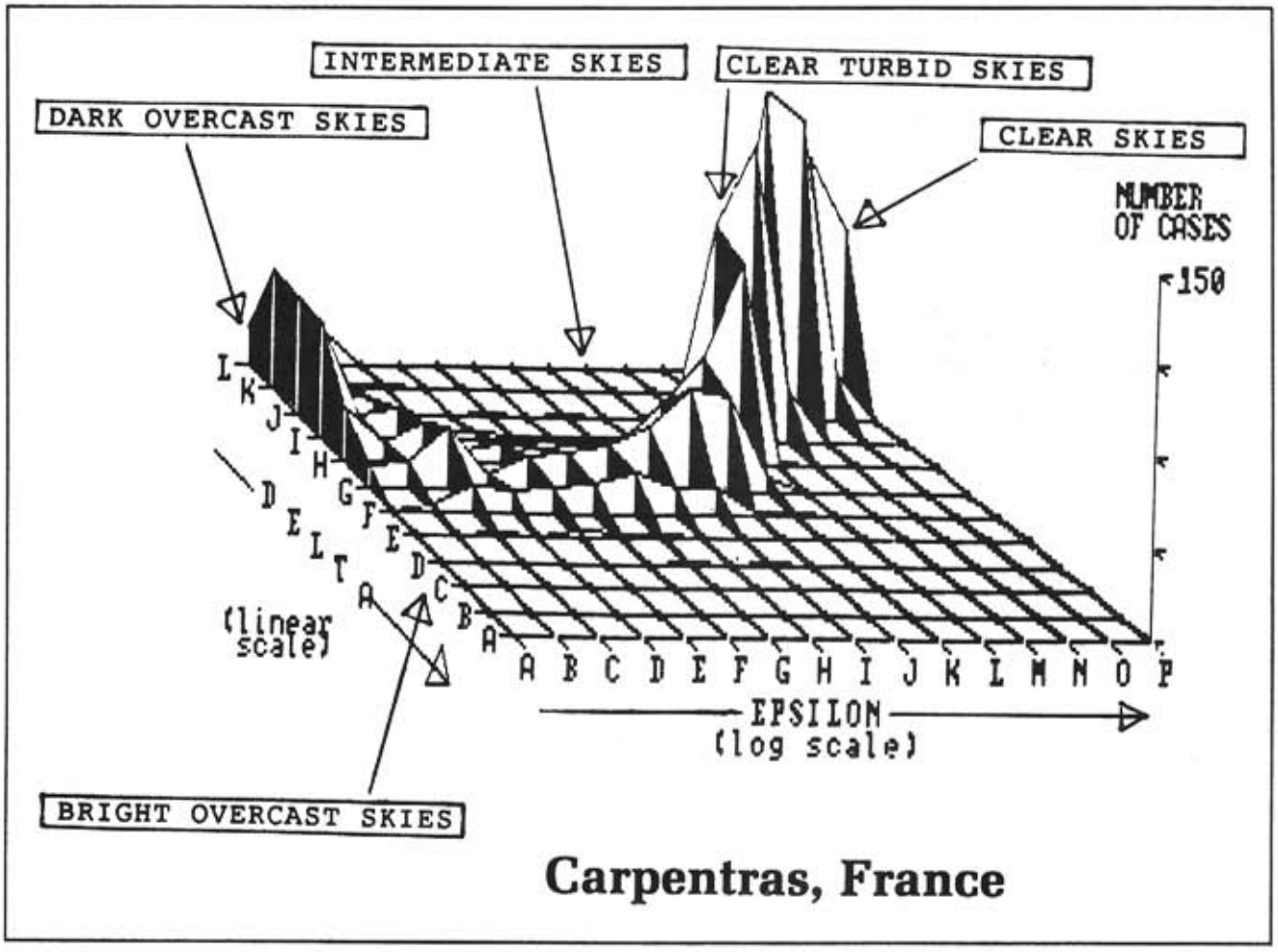

Legend (Interval Limits)		
	Epsilon	Delta
[A]	1.000-1.033	>0.66
[B]	1.033-1.065	0.60-0.66
[C]	1.065-1.148	0.54-0.60
[D]	1.148-1.230	0.48-0.54
[E]	1.230-1.365	0.42-0.48
[F]	1.365-1.500	0.36-0.42
[G]	1.500-1.725	0.30-0.36
[H]	1.725-1.950	0.24-0.30
[I]	1.950-2.375	0.18-0.24
[J]	2.375-2.800	0.12-0.18
[K]	2.800-3.650	0.06-0.12
[L]	3.650-4.500	0.00-0.06
[M]	4.500-5.350	
[N]	5.350-6.200	
[O]	6.200-8.000	
[P]	>8.000	

Figure 4 : Carpentras, France: Distribution of Observed Events with Sky Clearness ( ) and Sky Brightness (^) for Solar Zenith Angles ranging from 45 to 60

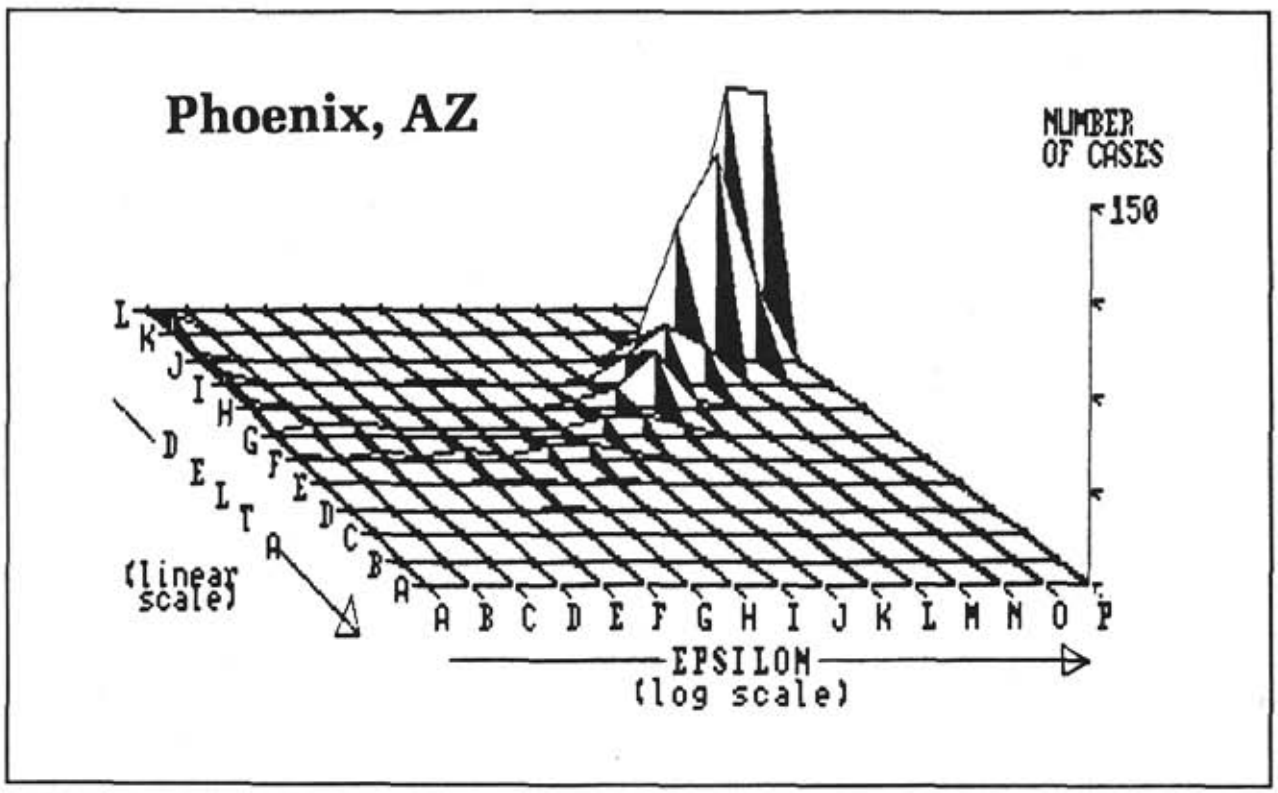

Legend (Interval Limits)	
Epsilon	Delta
[A]1.000-1.033	>0.66
[B]1.033-1.065	0.60-0.66
[C]1.065-1.148	0.54-0.60
[D]1.148-1.230	0.48-0.54
[E]1.230-1.365	0.42-0.48
[F] 1.365-1.500	0.36-0.42
[G]1.500-1.725	0.30-0.36
[H]1.725-1.950	0.24-0.30
[I] 1.950-2.375	0.18-0.24
[J] 2.375-2.800	0.12-0.18
[K]2.800-3.650	0.06-0.12
[L] 3.650-4.500	0.00-0.06
[M]4.500-5.350	
[N]5.350-6.200	
[O]6.200-8.000	
[P] >8.000	

Figure 5 : Same as Figure 4 but Phoenix, AZ

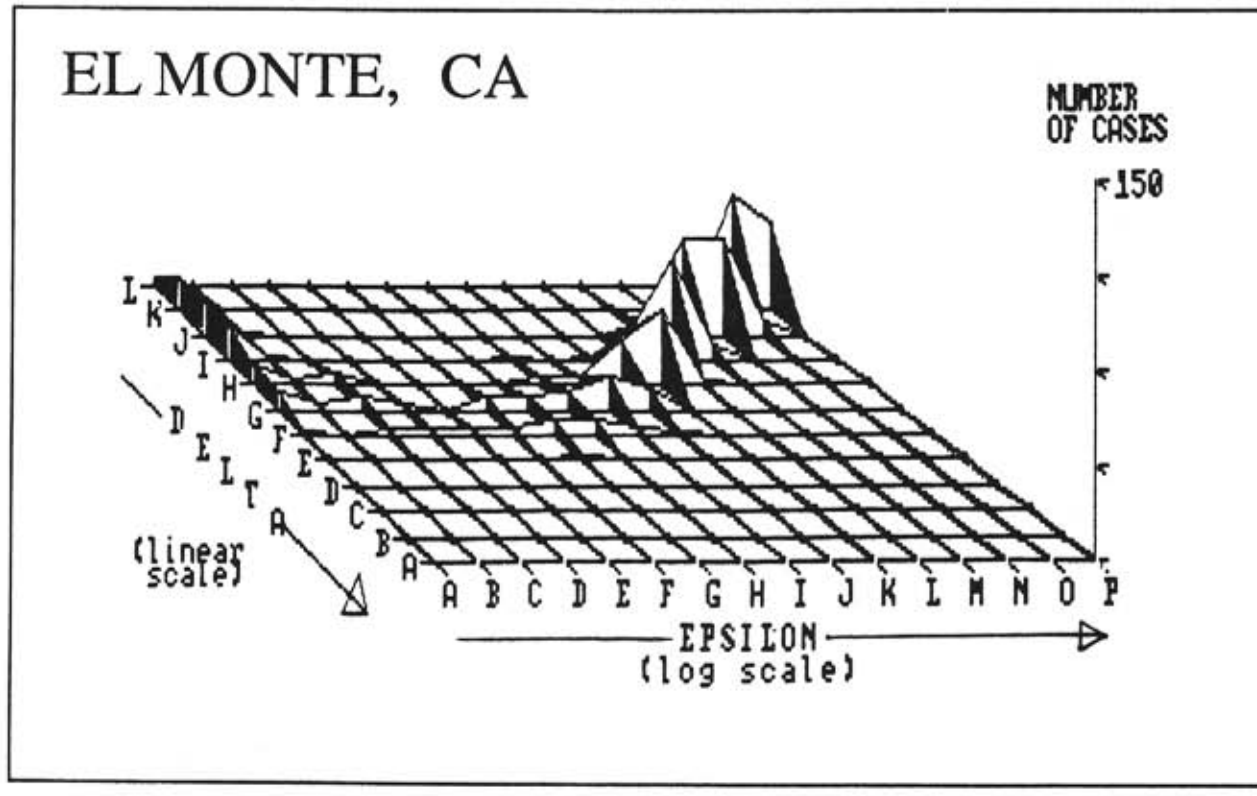

Legend (Interval Limits)		
	Epsilon	Delta
[A]	1.000-1.033	>0.66
[B]	1.033-1.065	0.60-0.66
[C]	1.065-1.148	0.54-0.60
[D]	1.148-1.230	0.48-0.54
[E]	1.230-1.365	0.42-0.48
[F]	1.365-1.500	0.36-0.42
[G]	1.500-1.725	0.30-0.36
[H]	1.725-1.950	0.24-0.30
[I]	1.950-2.375	0.18-0.24
[J]	2.375-2.800	0.12-0.18
[K]	2.800-3.650	0.06-0.12
[L]	3.650-4.500	0.00-0.06
[M]	4.500-5.350	
[N]	5.350-6.200	
[O]	6.200-8.000	
[P]	>8.000	

Figure 6 : Same as Figure 4 but El Monte, CA

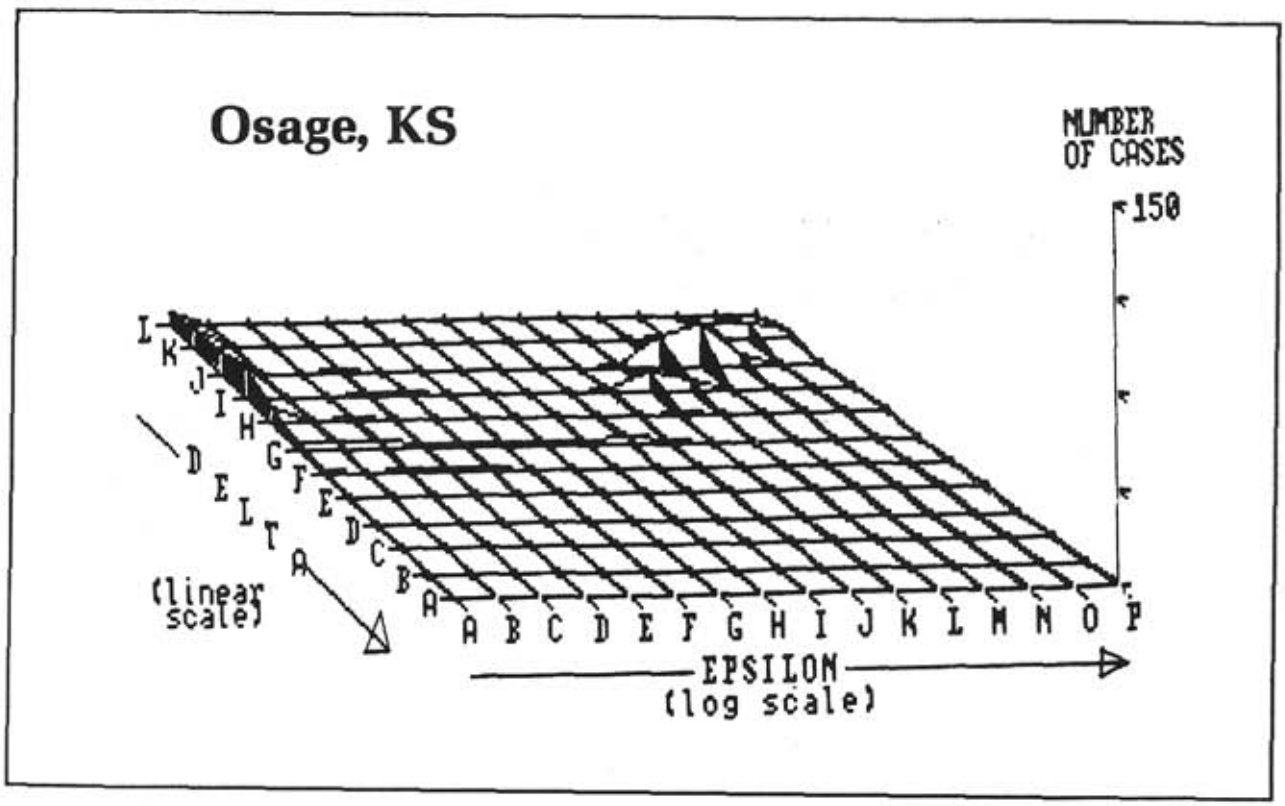

Legend (Interval Limits)	
Epsilon	Delta
[A] 1.000-1.033	>0.66
[B] 1.033-1.065	0.60-0.66
[C] 1.065-1.148	0.54-0.60
[D] 1.148-1.230	0.48-0.54
[E] 1.230-1.365	0.42-0.48
[F] 1.365-1.500	0.36-0.42
[G] 1.500-1.725	0.30-0.36
[H] 1.725-1.950	0.24-0.30
[I] 1.950-2.375	0.18-0.24
[J] 2.375-2.800	0.12-0.18
[K] 2.800-3.650	0.06-0.12
[L] 3.650-4.500	0.00-0.06
[M] 4.500-5.350	
[N] 5.350-6.200	
[O] 6.200-8.000	
[P] >8.000	

Figure 7 : Same as Figure 4 but Osage, KS

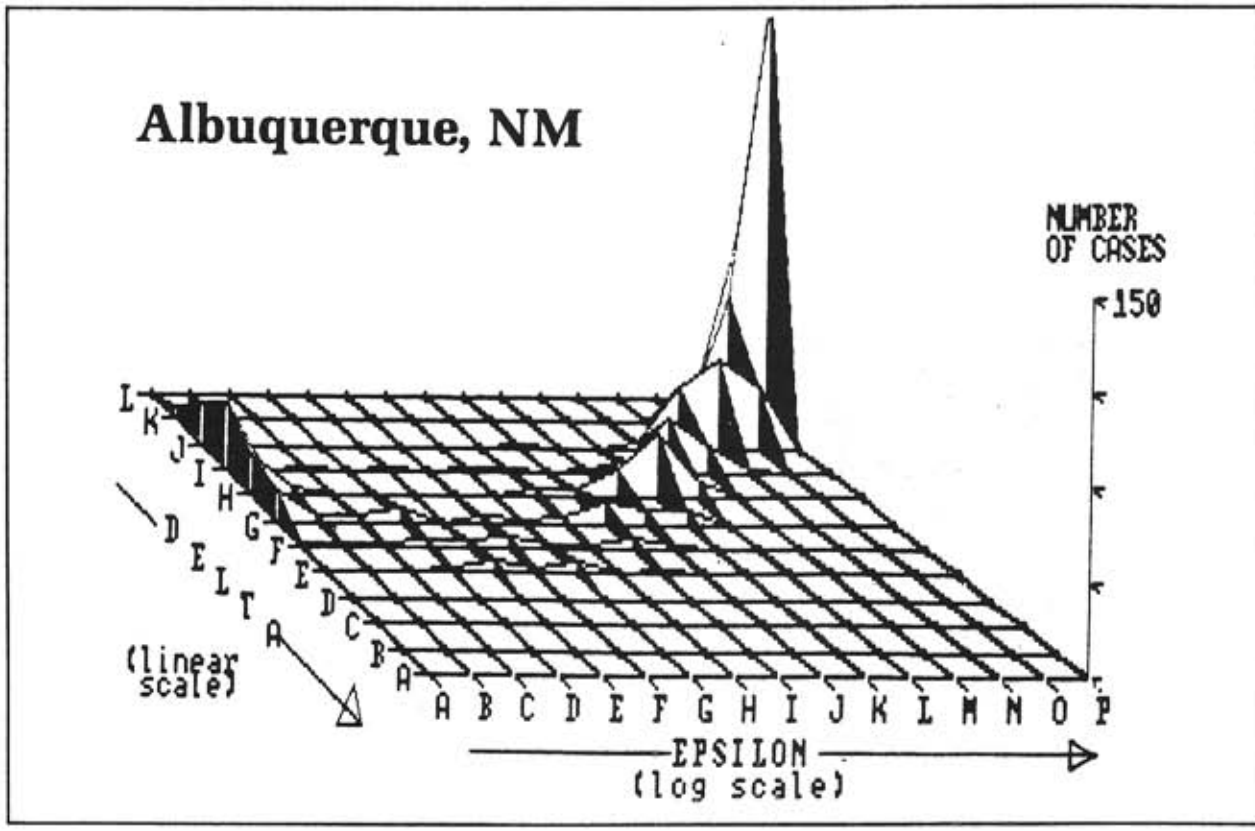

Legend (Interval Limits)	
Epsilon	Delta
[A]1.000-1.033	>0.66
[B]1.033-1.065	0.60-0.66
[C]1.065-1.148	0.54-0.60
[D]1.148-1.230	0.48-0.54
[E]1.230-1.365	0.42-0.48
[F] 1.365-1.500	0.36-0.42
[G]1.500-1.725	0.30-0.36
[H]1.725-1.950	0.24-0.30
[I] 1.950-2.375	0.18-0.24
[J] 2.375-2.800	0.12-0.18
[K]2.800-3.650	0.06-0.12
[L] 3.650-4.500	0.00-0.06
[M]4.500-5.350	
[N]5.350-6.200	
[O]6.200-8.000	
[P] >8.000	

Figure 8 : Same as Figure 4 but Albuquerque, NM

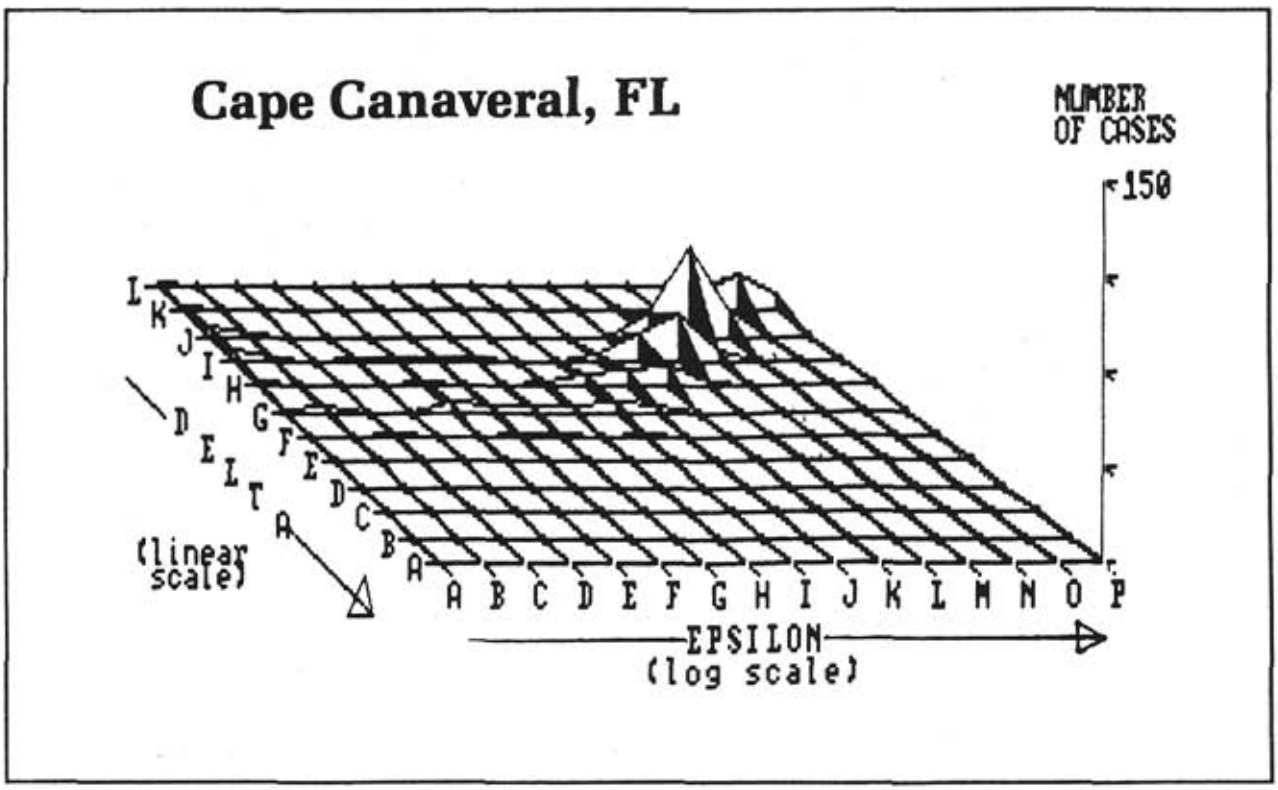

Legend (Interval Limits)	
Epsilon	Delta
[A] 1.000-1.033	>0.66
[B] 1.033-1.065	0.60-0.66
[C] 1.065-1.148	0.54-0.60
[D] 1.148-1.230	0.48-0.54
[E] 1.230-1.365	0.42-0.48
[F] 1.365-1.500	0.36-0.42
[G] 1.500-1.725	0.30-0.36
[H] 1.725-1.950	0.24-0.30
[I] 1.950-2.375	0.18-0.24
[J] 2.375-2.800	0.12-0.18
[K] 2.800-3.650	0.06-0.12
[L] 3.650-4.500	0.00-0.06
[M] 4.500-5.350	
[N] 5.350-6.200	
[O] 6.200-8.000	
[P] >8.000	

Figure 9 : Same as Figure 4 but Cape Canaveral, FLA

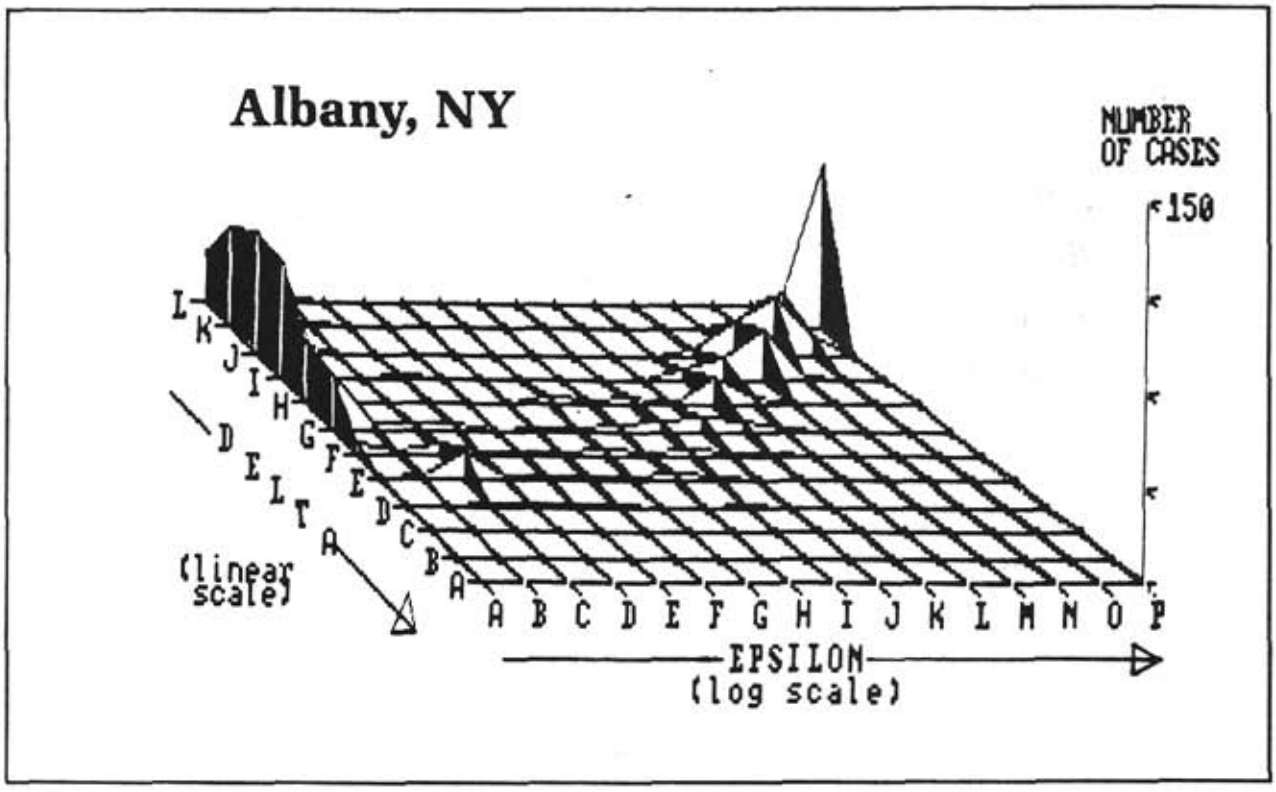

Legend (Interval Limits)	
Epsilon	Delta
[A]1.000-1.033	>0.66
[B]1.033-1.065	0.60-0.66
[C]1.065-1.148	0.54-0.60
[D]1.148-1.230	0.48-0.54
[E]1.230-1.365	0.42-0.48
[F] 1.365-1.500	0.36-0.42
[G]1.500-1.725	0.30-0.36
[H]1.725-1.950	0.24-0.30
[I] 1.950-2.375	0.18-0.24
[J] 2.375-2.800	0.12-0.18
[K]2.800-3.650	0.06-0.12
[L] 3.650-4.500	0.00-0.06
[M]4.500-5.350	
[N]5.350-6.200	
[O]6.200-8.000	
[P] >8.000	

Figure 10 : Same as Figure 4 but Albany, NY

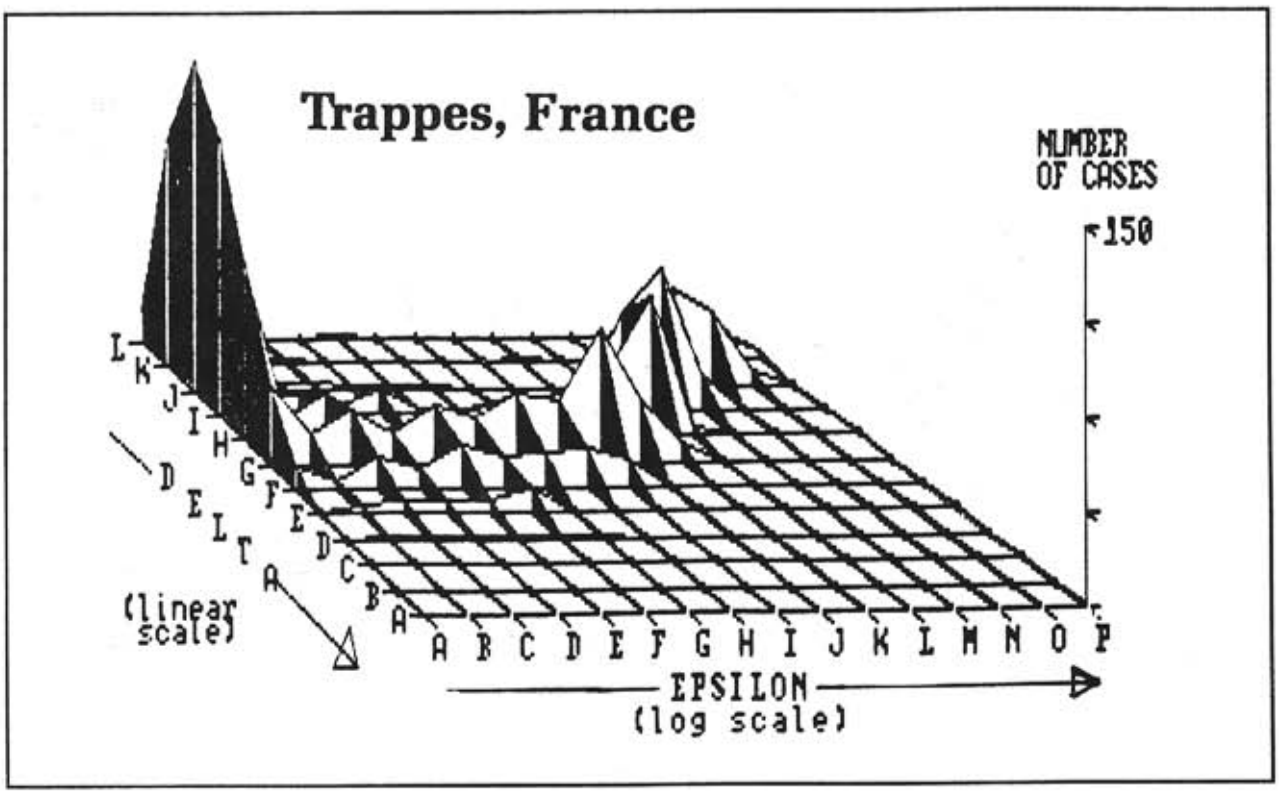

Legend (Interval Limits)	
Epsilon	Delta
[A] 1.000-1.033	>0.66
[B] 1.033-1.065	0.60-0.66
[C] 1.065-1.148	0.54-0.60
[D] 1.148-1.230	0.48-0.54
[E] 1.230-1.365	0.42-0.48
[F] 1.365-1.500	0.36-0.42
[G] 1.500-1.725	0.30-0.36
[H] 1.725-1.950	0.24-0.30
[I] 1.950-2.375	0.18-0.24
[J] 2.375-2.800	0.12-0.18
[K] 2.800-3.650	0.06-0.12
[L] 3.650-4.500	0.00-0.06
[M] 4.500-5.350	
[N] 5.350-6.200	
[O] 6.200-8.000	
[P] >8.000	

Figure 11 : Same as Figure 4 but Trappes, France

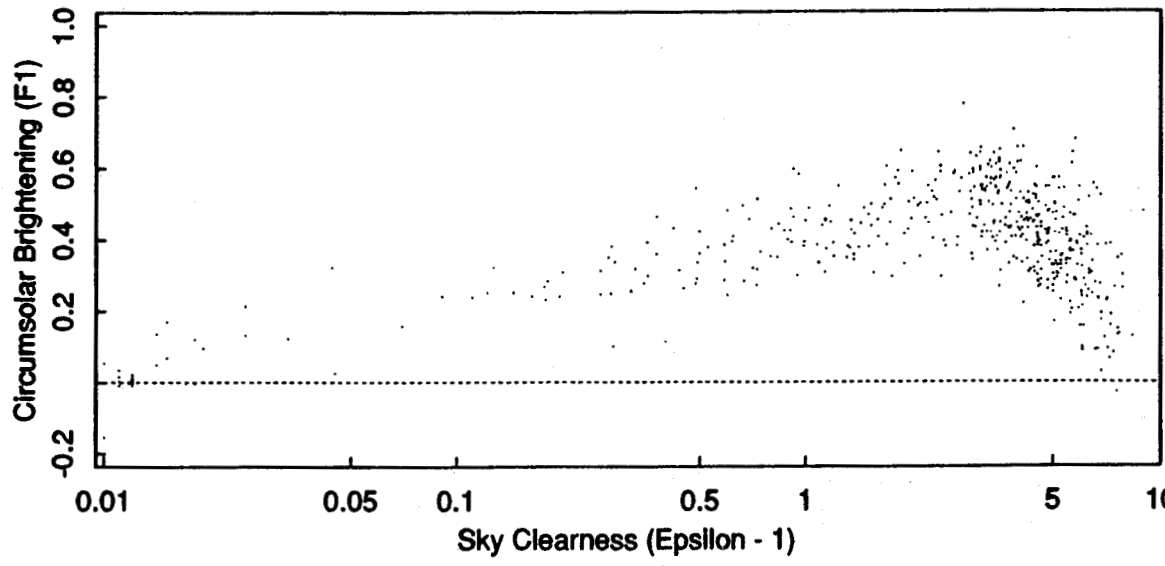

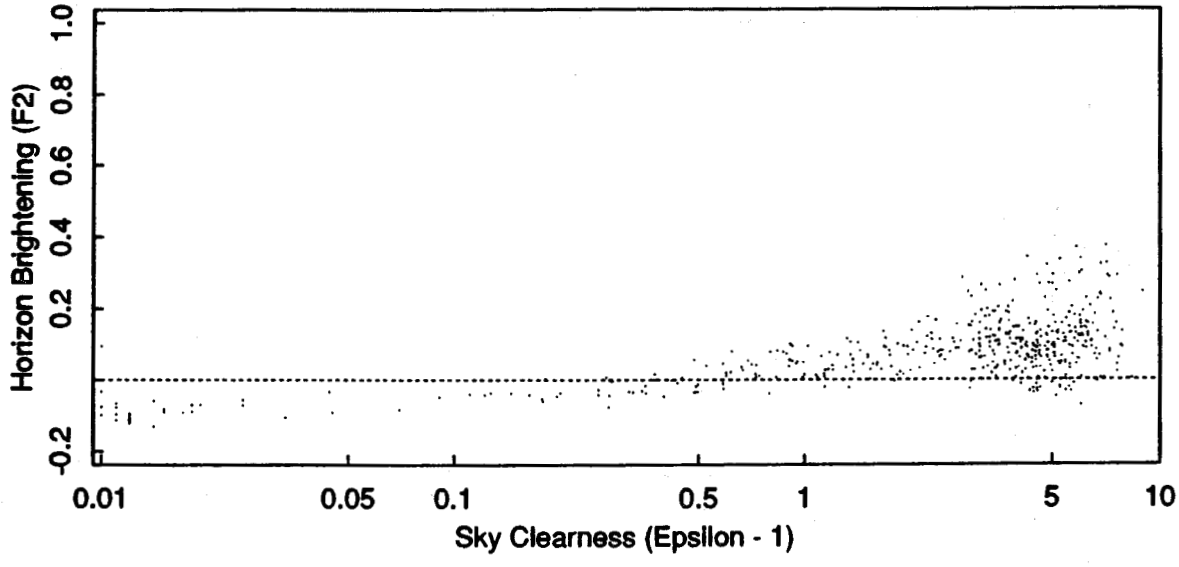

Figure 12: Phoenix, AZ: Variation of F1 and F2 with Sky Clearness ( ) for Solar Zenith Angles Ranging from 45 to 60

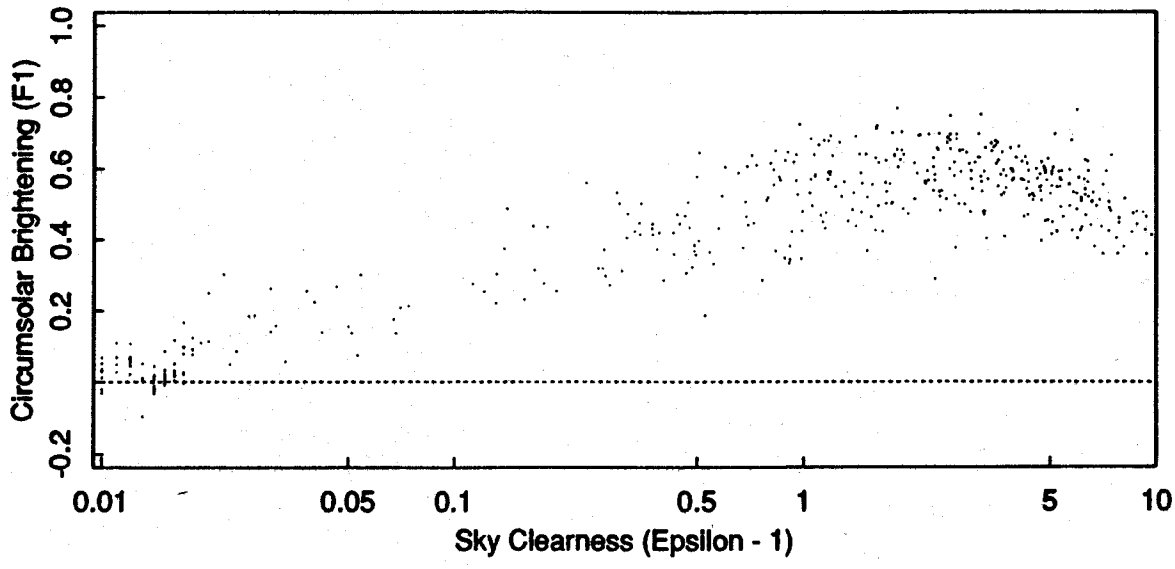

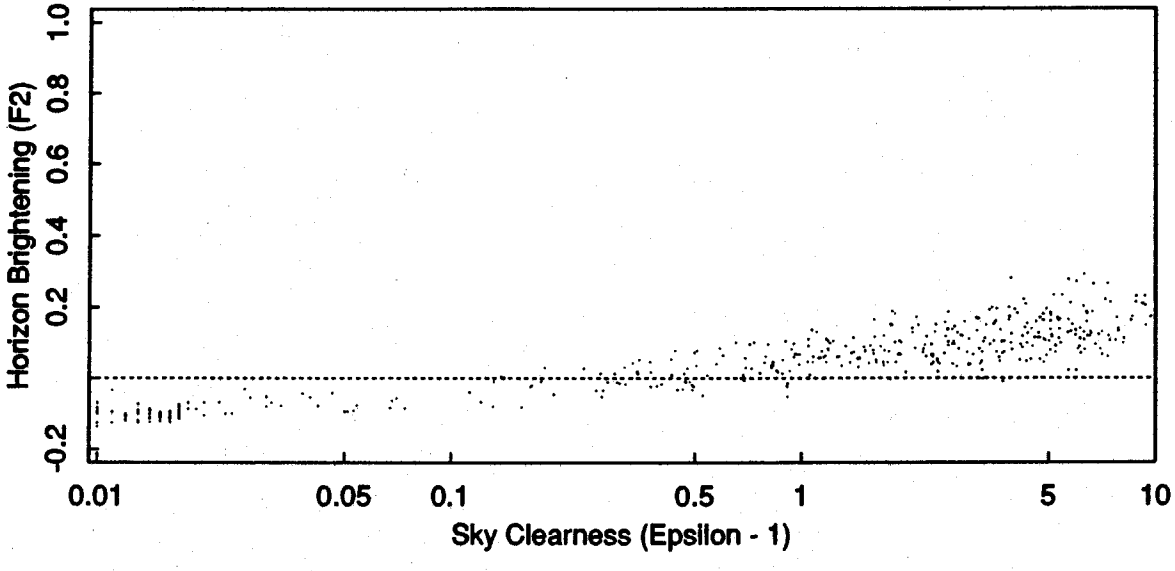

Figure 13: Same as Figure 12 but El Monte, CA

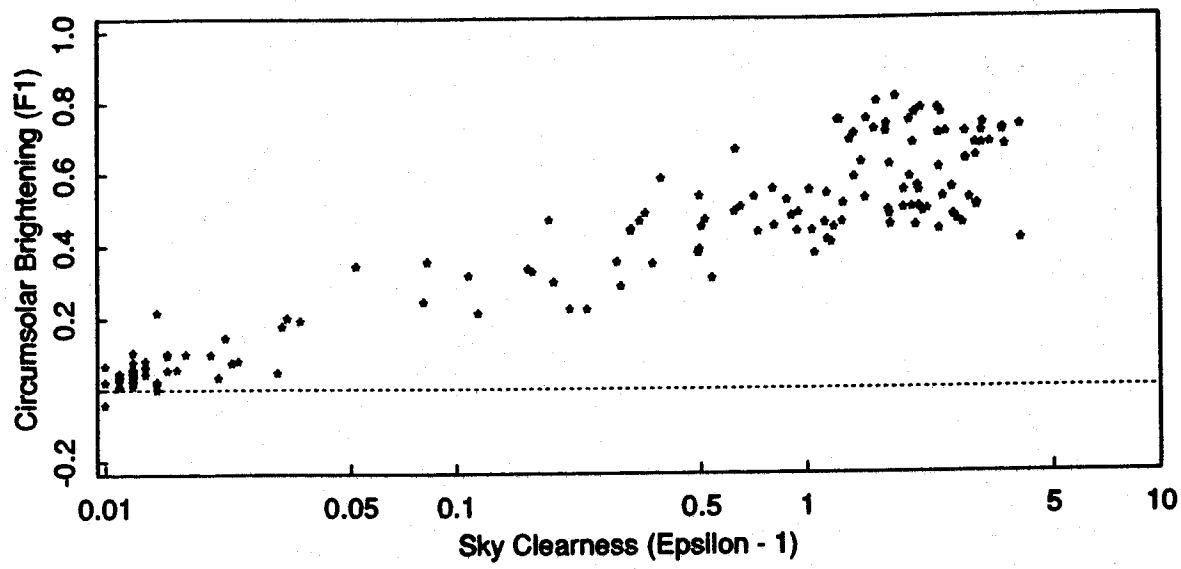

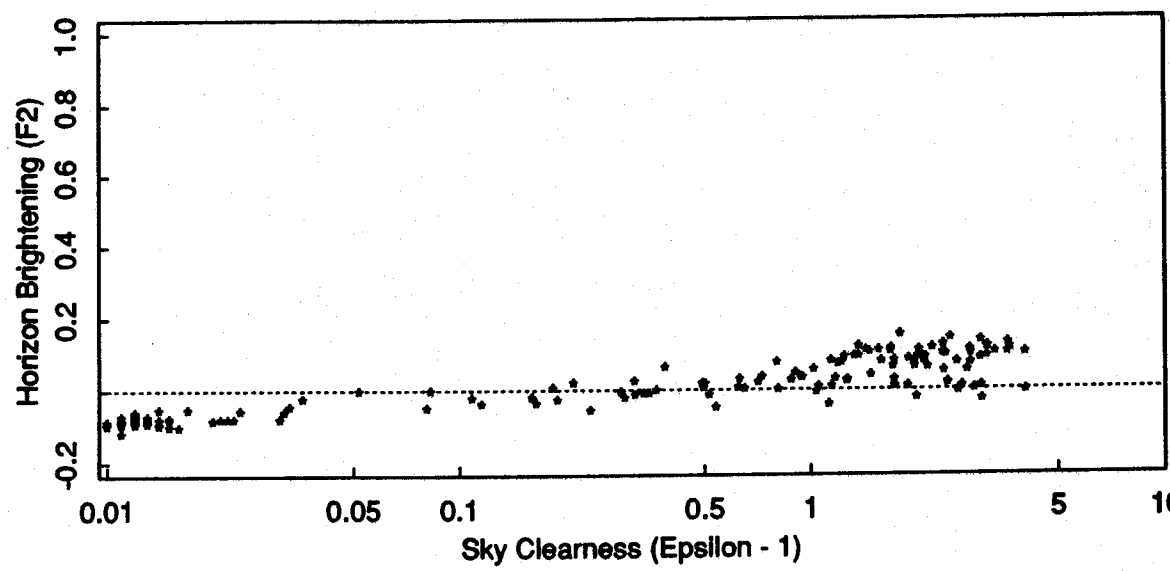

Figure 14: Same as Figure 12 but Osage, KS

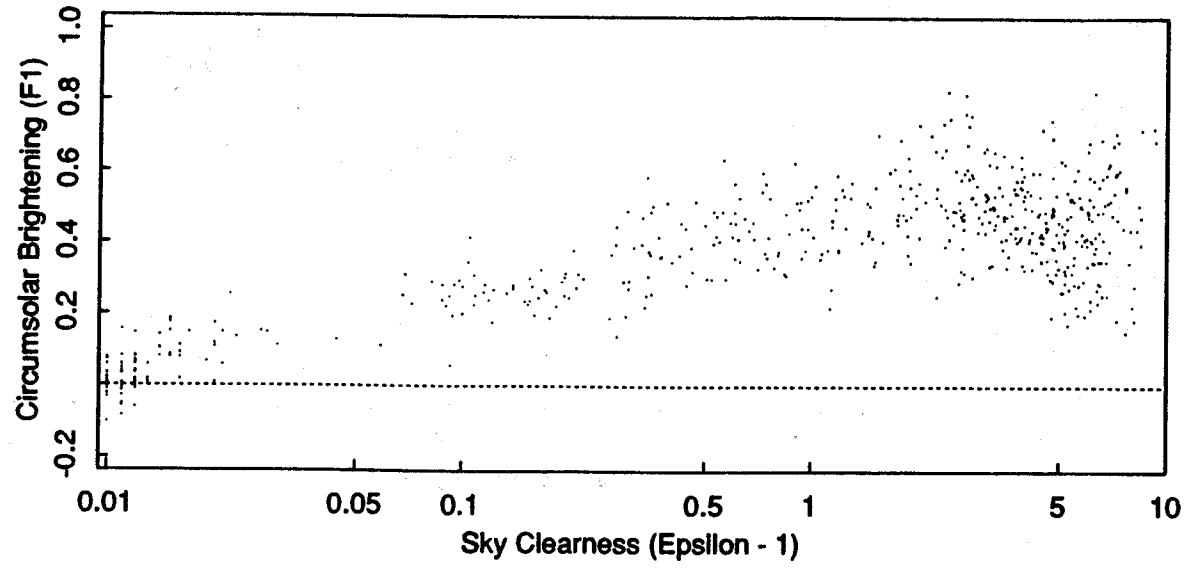

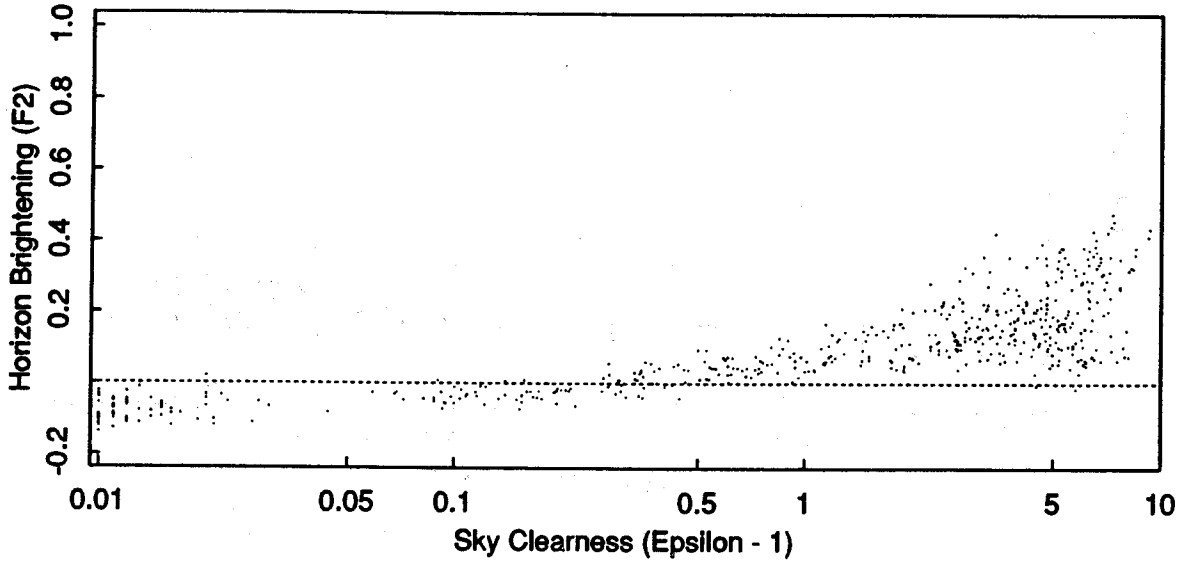

Figure 15: Same as Figure 12 but Albuquerque, NM

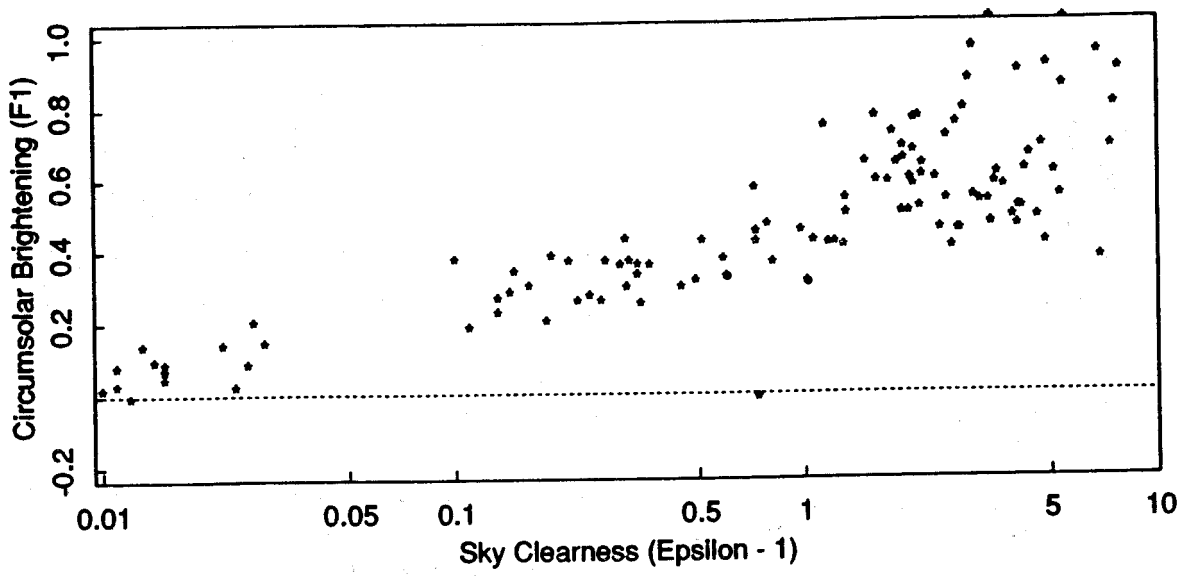

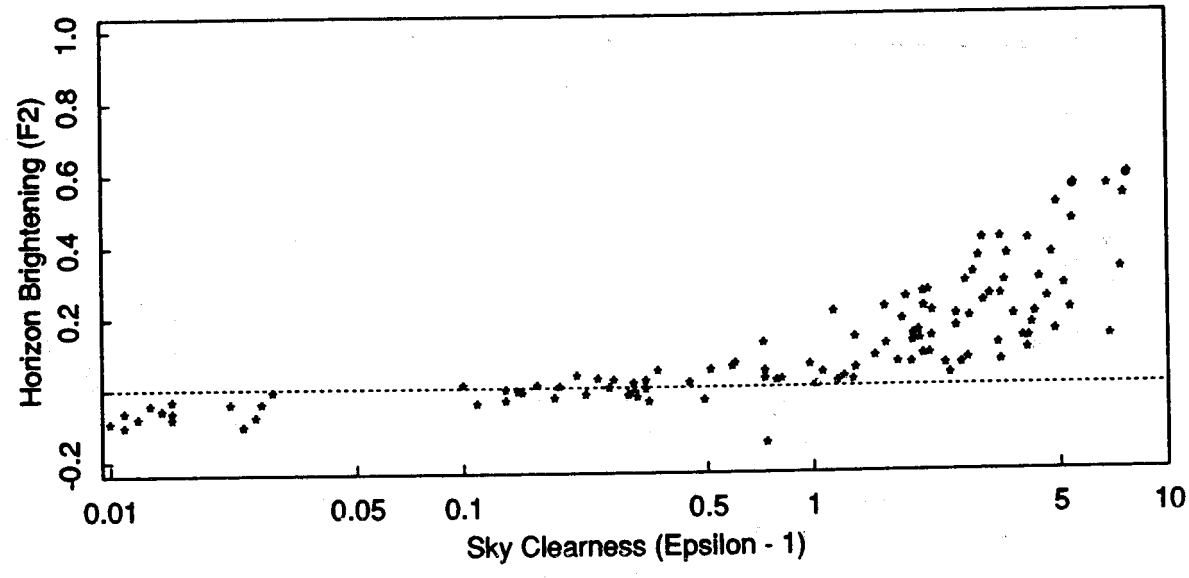

Figure 16: Same as Figure 12 but Cape Canaveral, FLA

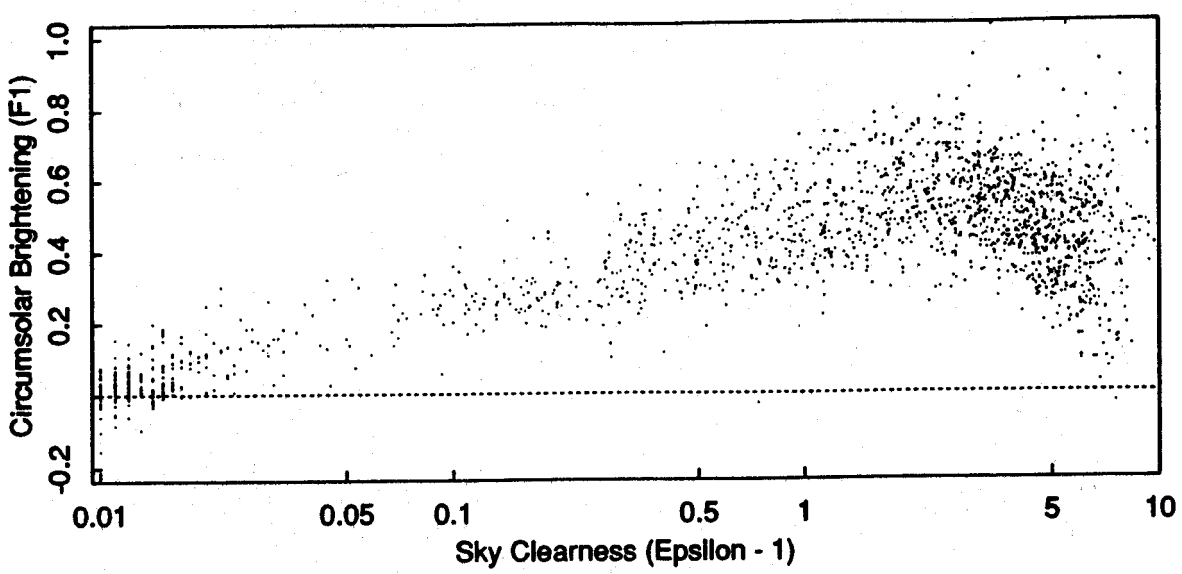

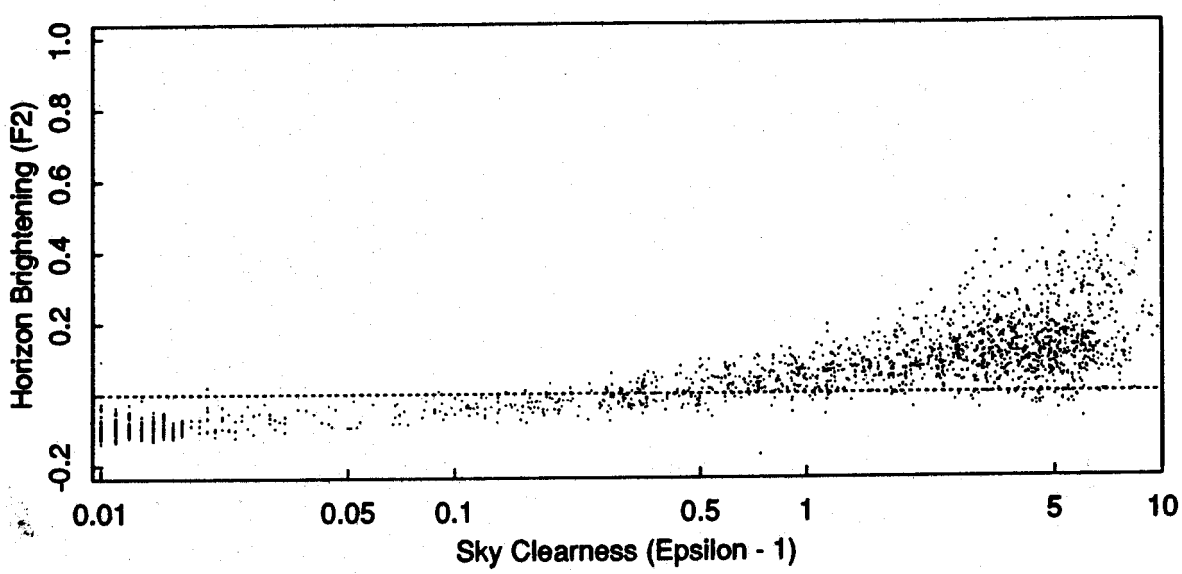

Figure 17: Same as Figure 12 but all SNLA sites

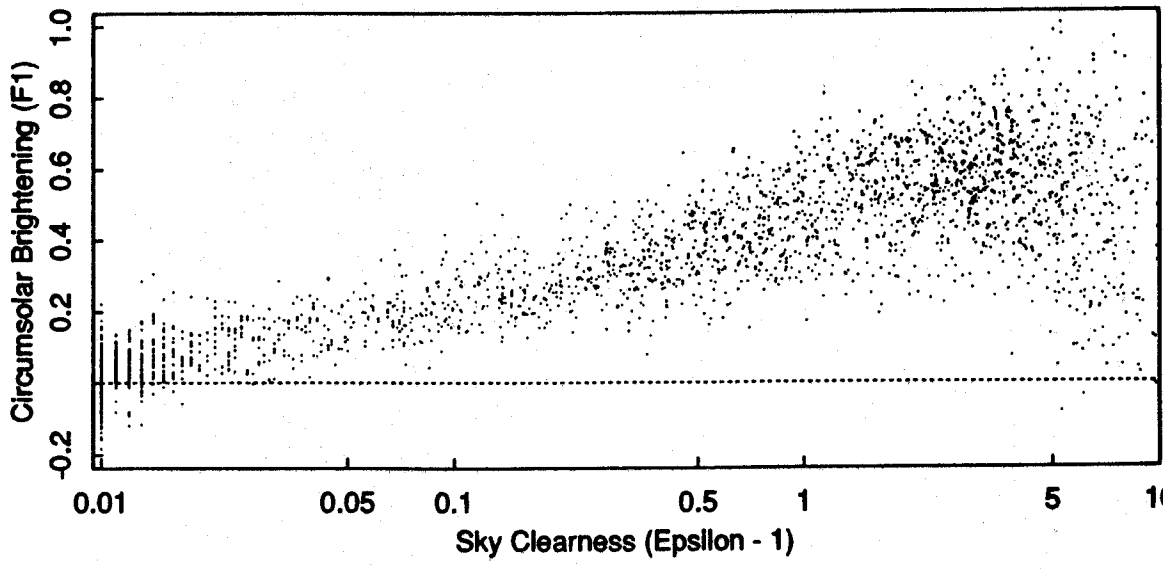

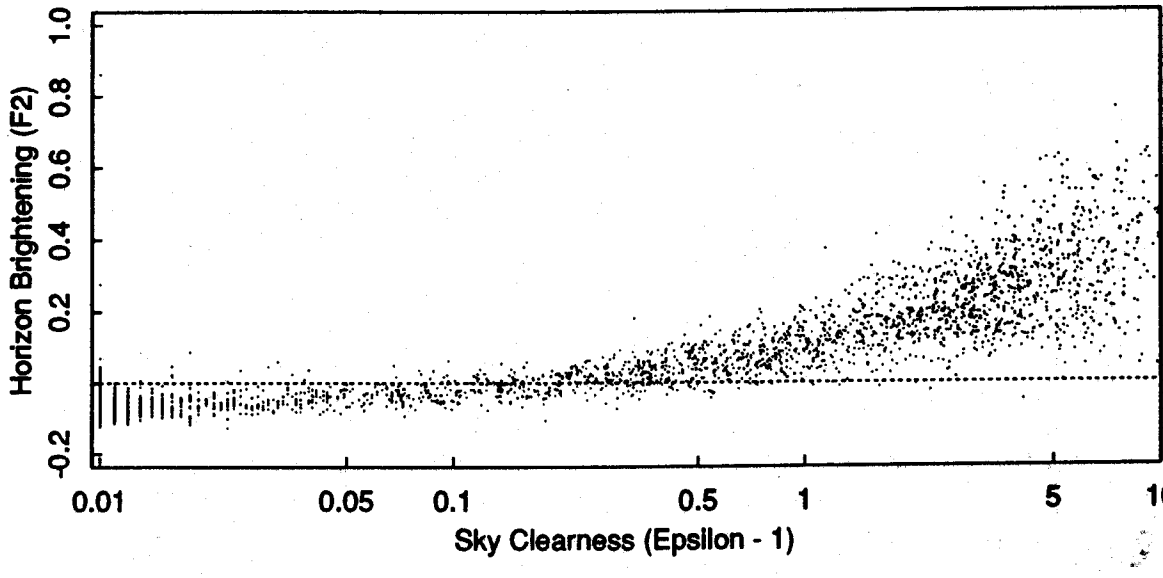

Figure 18: Same as Figure 12 but Albany, NY SEMRTS

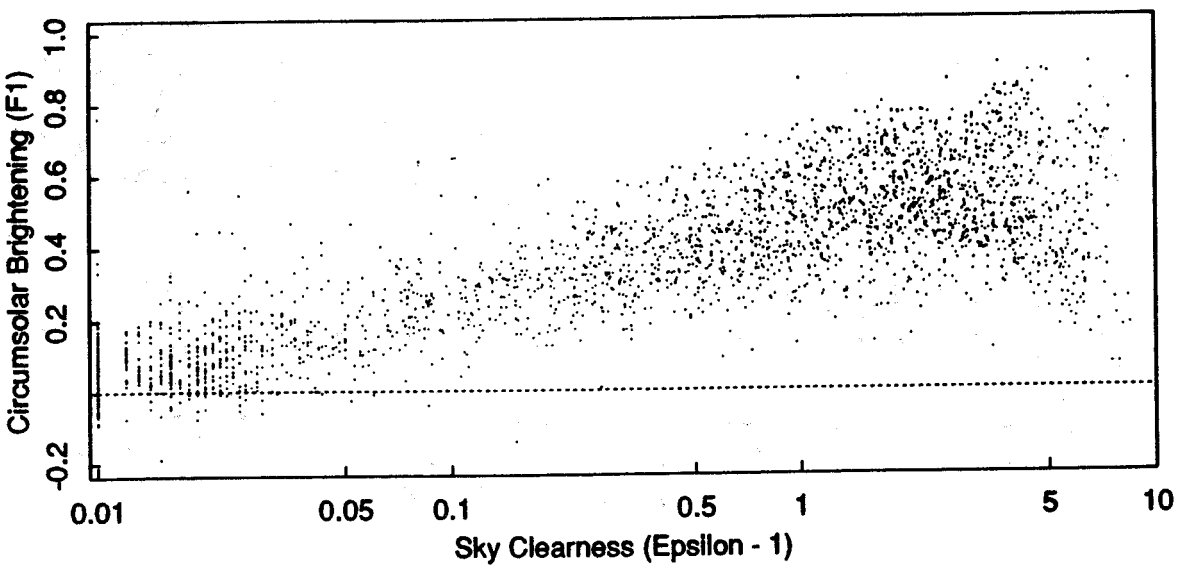

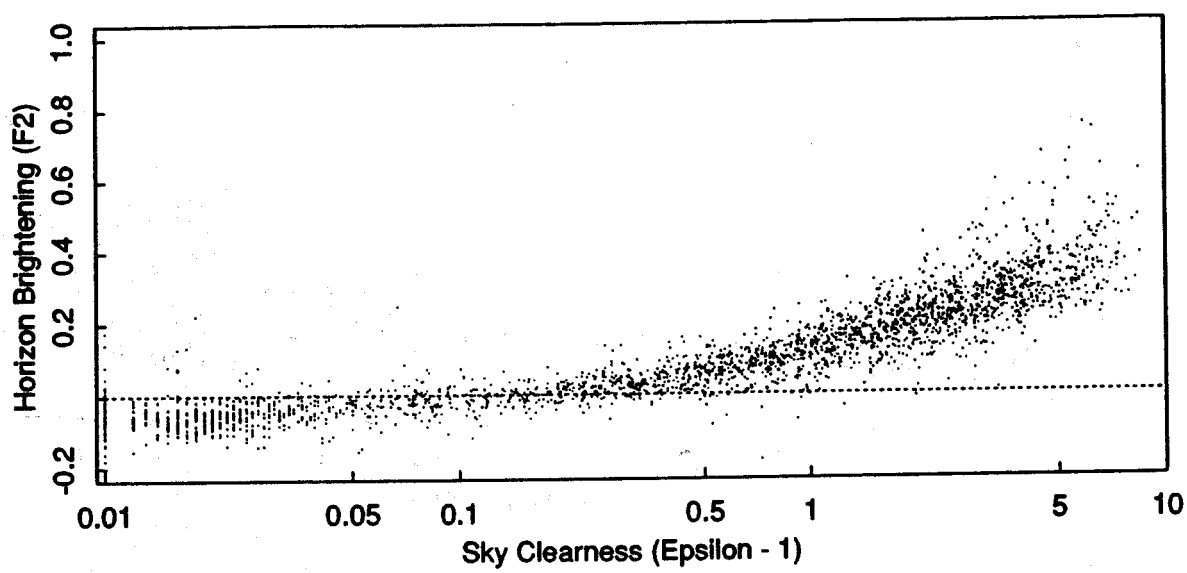

Figure 19: Same as Figure 12 but Trappes and Carpentras.

Table 1 : Selected interval for the parameter

Interval Number	Low Bound	High Bound
1	1	1.065
2	1.065	1.230
3	1.230	1.500
4	1.500	1.950
5	1.950	2.800
6	2.800	4.500
7	4.500	6.200
8	6.200	--

Table 2 : Model Coefficients Derived for Phoenix, AZ

e bin #	Upper Limit	Cases (%)	f11	f12	f13	f21	f22	f23
1	1.065	5.07	-0.003	0.728	-0.097	-0.075	0.142	-0.043
2	1.230	3.80	0.279	0.354	-0.176	0.030	-0.055	-0.054
3	1.500	5.52	0.469	0.168	-0.246	0.048	-0.042	-0.057
4	1.950	6.53	0.856	-0.519	-0.340	0.176	-0.380	-0.031
5	2.800	10.53	0.941	-0.625	-0.391	0.188	-0.360	-0.049
6	4.500	24.98	1.056	-1.134	-0.410	0.281	-0.794	-0.065
7	6.200	23.65	0.901	-2.139	-0.269	0.118	-0.665	0.046
8	---	19.91	0.107	0.481	0.143	-0.111	-0.137	0.234

F1 = F11(e) + F12(e)*^ + F13(e)*Z Note: Pheonix
F2 = F21(e) + F22(e)*^ + F23(e)*Z

Table 3 : Model Coefficients Derived for El Monte, CA

e bin #	Upper Limit	Cases (%)	f11	f12	f13	f21	f22	f23
1	1.065	14.65	0.027	0.701	-0.119	-0.058	0.107	-0.060
2	1.230	4.59	0.181	0.671	-0.178	-0.079	0.194	-0.035
3	1.500	8.79	0.476	0.407	-0.288	0.054	-0.032	-0.055
4	1.950	11.38	0.875	-0.218	-0.403	0.187	-0.309	-0.061
5	2.800	16.64	1.166	-1.014	-0.454	0.211	-0.410	-0.044
6	4.500	24.10	1.143	-2.064	-0.291	0.097	-0.319	0.053
7	6.200	11.25	1.094	-2.632	-0.259	0.029	-0.422	0.147
8	---	8.59	0.155	1.723	0.163	-0.131	-0.019	0.277

F1 = F11(e) + F12(e)*^ + F13(e)*Z Note: El Monte
F2 = F21(e) + F22(e)*^ + F23(e)*Z

Table 4 : Model Coefficients Derived for Osage, KS

e bin #	Upper Limit	Cases (%)	f11	f12	f13	f21	f22	f23
1	1.065	36.84	-0.353	1.474	0.057	-0.175	0.312	0.009
2	1.230	6.94	0.363	0.218	-0.212	0.019	-0.034	-0.059
3	1.500	5.98	-0.031	1.262	-0.084	-0.082	0.231	-0.017
4	1.950	10.05	0.691	0.039	-0.295	0.091	-0.131	-0.035
5	2.800	13.40	1.182	-1.350	-0.321	0.408	-0.985	-0.088
6	4.500	20.81	0.764	0.019	-0.203	0.217	-0.294	-0.103
7	6.200	5.02	0.219	1.412	0.244	0.471	-2.988	0.034
8	---	0.96	3.578	22.231	-10.745	2.426	4.892	-5.687

F1 = F11(e) + F12(e)*^ + F13(e)*Z Note: Osage
F2 = F21(e) + F22(e)*^ + F23(e)*Z

Table 5 : Model Coefficients Derived for Albuquerque, NM

e bin #	Upper Limit	Cases (%)	f11	f12	f13	f21	f22	f23
1	1.065	13.89	0.034	0.501	-0.094	-0.063	0.106	-0.044
2	1.230	7.22	0.229	0.467	-0.156	-0.005	-0.019	-0.023
3	1.500	7.44	0.486	0.241	-0.253	0.053	-0.064	-0.022
4	1.950	8.21	0.874	-0.393	-0.397	0.181	-0.327	-0.037
5	2.800	10.23	1.193	-1.296	-0.501	0.281	-0.656	-0.045
6	4.500	16.96	1.056	-1.758	-0.374	0.226	-0.759	0.034
7	6.200	18.76	0.901	-4.783	-0.109	0.063	-0.970	0.196
8	---	17.29	0.851	-7.055	-0.053	0.060	-2.833	0.330

F1 = F11(e) + F12(e)*^ + F13(e)*Z Note: Albuquerque
F2 = F21(e) + F22(e)*^ + F23(e)*Z

Table 6 : Model Coefficients Derived for Cape Canaveral, FLA

e bin #	Upper Limit	Cases (%)	f11	f12	f13	f21	f22	f23
1	1.065	12.89	0.075	0.533	-0.124	-0.067	0.042	-0.020
2	1.230	6.90	0.295	0.497	-0.218	-0.008	0.003	-0.029
3	1.500	9.98	0.514	0.081	-0.261	0.075	-0.160	-0.029
4	1.950	10.34	0.747	-0.329	-0.325	0.181	-0.416	-0.030
5	2.800	17.24	0.901	-0.883	-0.297	0.178	-0.489	0.008
6	4.500	20.33	0.591	-0.044	-0.116	0.235	-0.999	0.098
7	6.200	11.62	0.537	-2.402	0.320	0.169	-1.971	0.310
8	---	10.71	-0.805	4.546	1.072	-0.258	-0.950	0.753

F1 = F11(e) + F12(e)*^ + F13(e)*Z Note: Cape Canaveral
F2 = F21(e) + F22(e)*^ + F23(e)*Z

Table 8 : Model Coefficients Derived for all SNLA sites

e bin #	Upper Limit	Cases (%)	f11	f12	f13	f21	f22	f23
1	1.065	13.60	-0.196	1.084	-0.006	-0.114	0.180	-0.019
2	1.230	5.60	0.236	0.519	-0.180	-0.011	0.020	-0.038
3	1.500	7.52	0.454	0.321	-0.255	0.072	-0.098	-0.046
4	1.950	8.87	0.866	-0.381	-0.375	0.203	-0.403	-0.049
5	2.800	13.17	1.026	-0.711	-0.426	0.273	-0.602	-0.061
6	4.500	21.45	0.978	-0.986	-0.350	0.280	-0.915	-0.024
7	6.200	16.06	0.748	-0.913	-0.236	0.173	-1.045	0.065
8	---	13.73	0.318	-0.757	0.103	0.062	-1.698	0.236

F1 = F11(e) + F12(e)*^ + F13(e)*Z Note: Sandia Composite
F2 = F21(e) + F22(e)*^ + F23(e)*Z

Table 7 : Model Coefficients Derived for Albany, NY

e bin #	Upper Limit	Cases (%)	f11	f12	f13	f21	f22	f23
1	1.065	37.27	0.012	0.554	-0.076	-0.052	0.084	-0.029
2	1.230	7.71	0.267	0.437	-0.194	0.016	0.022	-0.036
3	1.500	7.49	0.420	0.336	-0.237	0.074	-0.052	-0.032
4	1.950	7.99	0.638	-0.001	-0.281	0.138	-0.189	-0.012
5	2.800	9.77	1.019	-1.027	-0.342	0.271	-0.628	0.014
6	4.500	13.43	1.149	-1.940	-0.331	0.322	-1.097	0.080
7	6.200	7.66	1.434	-3.994	-0.492	0.453	-2.376	0.117
8	---	8.69	1.007	-2.292	-0.482	0.390	-3.368	0.229

F1 = F11(e) + F12(e)*^ + F13(e)*Z Note: Albany SEMRTS
F2 = F21(e) + F22(e)*^ + F23(e)*Z

Table 9 : Model Coefficients Derived for all USA sites

e bin #	Upper Limit	Cases (%)	f11	f12	f13	f21	f22	f23
1	1.065	28.77	-0.034	0.671	-0.059	-0.059	0.086	-0.028
2	1.230	6.95	0.255	0.474	-0.191	0.018	-0.014	-0.033
3	1.500	7.50	0.427	0.349	-0.245	0.093	-0.121	-0.039
4	1.950	8.30	0.756	-0.213	-0.328	0.175	-0.304	-0.027
5	2.800	10.99	1.020	-0.857	-0.385	0.280	-0.638	-0.019
6	4.500	16.31	1.050	-1.344	-0.348	0.280	-0.893	0.037
7	6.200	10.68	0.974	-1.507	-0.370	0.154	-0.568	0.109
8	---	10.50	0.744	-1.817	-0.256	0.246	-2.618	0.230

F1 = F11(e) + F12(e)*^ + F13(e)*Z Note: USA Composite
F2 = F21(e) + F22(e)*^ + F23(e)*Z

Table 10: Model Coefficients Derived for French sites

e bin #	Upper Limit	Cases (%)	f11	f12	f13	f21	f22	f23
1	1.065	30.30	0.013	0.764	-0.100	-0.058	0.127	-0.023
2	1.230	8.70	0.095	0.920	-0.152	-0.000	0.051	-0.020
3	1.500	8.96	0.464	0.421	-0.280	0.064	-0.051	-0.002
4	1.950	10.64	0.759	-0.009	-0.373	0.201	-0.382	0.010
5	2.800	13.27	0.976	-0.400	-0.436	0.271	-0.638	0.051
6	4.500	16.03	1.176	-1.254	-0.462	0.295	-0.975	0.129
7	6.200	7.62	1.106	-1.563	-0.398	0.301	-1.442	0.212
8	---	4.48	0.934	-1.501	-0.271	0.420	-2.917	0.249

F1 = F11(e) + F12(e)*^ + F13(e)*Z
F2 = F21(e) + F22(e)*^ + F23(e)*Z

Note: Trappes and Carpentras

Table 11: Model Coefficients Derived for all sites

e bin #	Upper Limit	Cases (%)	f11	f12	f13	f21	f22	f23
1	1.065	29.38	-0.018	0.705	-0.071	-0.058	0.102	-0.026
2	1.230	7.65	0.191	0.645	-0.171	0.012	0.009	-0.027
3	1.500	8.08	0.440	0.378	-0.256	0.087	-0.104	-0.025
4	1.950	9.23	0.756	-0.121	-0.346	0.179	-0.321	-0.008
5	2.800	11.90	0.996	-0.645	-0.405	0.260	-0.590	0.017
6	4.500	16.20	1.098	-1.290	-0.393	0.269	-0.832	0.075
7	6.200	9.46	0.973	-1.135	-0.378	0.124	-0.258	0.149
8	---	8.10	0.689	-0.412	-0.273	0.199	-1.675	0.237

F1 = F11(e) + F12(e)*^ + F13(e)*Z
F2 = F21(e) + F22(e)*^ + F23(e)*Z

Note: All Sites Composite

Table 12: Model Validation Summary

MODEL	PEREZ								HAY	ISO	KLU
Coefficients	Pho	E.Mte	Os	Albu	C.Can	C_1	Alby	C_2	-	-	-
LOCATION	Five Surface Composite RMS Error (W/Sq.m)										
Phoenix, AZ	13	15	64	15	20	13	18	15	20	34	34
El Monte, CA	15	13	48	17	17	14	18	15	23	45	49
Osage, Ks	17	16	13	20	18	15	20	18	28	46	51
Albuquerque, NM	13	14	50	12	15	13	16	13	20	33	34
C. Canaveral, Fl	14	17	36	14	12	14	16	14	23	34	45
Composite 1	14	15	51	16	17	14	17	15	22	38	41
Albany, NY	17	16	42	16	17	16	13	14	24	36	30
Composite 2	16	16	45	16	17	15	14	14	23	36	33

Table 13: Summary of Cross-validation for SNL and French sites.

MODEL	SITE TESTED	COEFF. SET	S 45	N 90	E 90	S 90	W 90	COMPOSITE
			Mean Bias Error (W/sq.m)					
Isotropic	T & C	-	-31.0	19.0	-11.0	-25.0	-8.0	21.0
Hay	T & C	-	-19.0	3.0	-11.0	-16.0	-8.0	13.0
Klucher	T & C	-	-12.0	33.0	8.0	-5.0	11.0	17.0
Perez	T & C	T & C	-3.0	6.0	-1.0	-0.0	2.0	3.0
Perez	T & C	USA + T&C	-7.0	3.0	-5.0	-5.0	-1.0	5.0
Perez	T & C	USA	-10.0	2.0	-7.0	-8.0	-3.0	7.0
Isotropic	USA	-	-17.0	18.0	-5.0	-12.0	-5.0	11.0
Hay	USA	-	-6.0	0.0	-8.0	-6.0	-6.0	6.0
Klucher	USA	-	1.0	32.0	13.0	8.0	15.0	17.0
Perez	USA	T & C	7.0	5.0	3.0	9.0	5.0	6.0
Perez	USA	USA + T&C	3.0	2.0	-1.0	4.0	2.0	3.0
Perez	USA	USA	1.0	1.0	-3.0	1.0	0.0	2.2
			Root Mean Square Error (W/Sq.m)					
Isotropic	T & C	-	46.0	33.0	44.0	45.0	42.0	43.0
Hay	T & C	-	28.0	24.0	31.0	29.0	29.0	28.0
Klucher	T & C	-	23.0	49.0	39.0	27.0	39.0	37.0
Perez	T & C	T & C	14.0	12.0	17.0	16.0	17.0	15.0
Perez	T & C	USA + T&C	16.0	12.0	18.0	17.0	16.0	16.0
Perez	T & C	USA	18.0	11.0	19.0	18.0	17.0	17.0
Isotropic	USA	-	30.0	32.0	42.0	33.0	44.0	37.0
Hay	USA	-	17.0	24.0	28.0	21.0	27.0	24.0
Klucher	USA	-	15.0	48.0	41.0	26.0	42.0	36.0
Perez	USA	T & C	15.0	12.0	17.0	19.0	19.0	17.0
Perez	USA	USA + T&C	13.0	11.0	16.0	16.0	17.0	15.0
Perez	USA	USA	12.0	11.0	17.0	15.0	17.0	15.0

Table 14: Effect of Horizon Shields Reflectivity on Model Performance

MODEL	SITE TESTED	COEFF. SET	S 45	N 90	E 90	S 90	W 90	COMPOSITE
			Mean Bias Error (W/sq.m)					
Isotropic	Albuq. 1	-	-30.0	8.7	1.6	-38.5	-7.2	22.4
Hay	Albuq. 1	-	-2.3	-4.4	-0.7	-7.8	-6.5	5.0
Klucher	Albuq. 1	-	-6.2	17.1	11.9	-18.1	3.8	12.7
Perez	Albuq. 1	Albuq. 1	0.2	1.1	3.5	-3.8	-2.1	2.5
Perez	Albuq. 1	Albuq. 2	-6.2	3.1	3.5	-11.1	-3.2	6.3
Isotropic	Albuq. 2	-	-31.7	16.5	1.5	-37.0	-4.0	23.1
Hay	Albuq. 2	-	1.6	-2.6	-2.4	-1.5	-4.1	2.6
Klucher	Albuq. 2	-	0.9	29.4	17.4	-10.0	12.7	16.9
Perez	Albuq. 2	Albuq. 1	7.8	0.4	1.7	5.9	-2.2	4.5
Perez	Albuq. 2	Albuq. 2	0.6	3.0	1.0	-2.1	-3.0	2.2
			Root Mean Square Error (W/Sq.m)					
Isotropic	Albuq. 1	-	40.1	19.7	17.5	50.4	22.0	32.7
Hay	Albuq. 1	-	15.9	19.8	18.5	19.2	18.5	18.4
Klucher	Albuq. 1	-	14.9	27.5	20.9	26.0	18.4	22.0
Perez	Albuq. 1	Albuq. 1	9.8	6.4	12.0	11.7	9.6	10.1
Perez	Albuq. 1	Albuq. 2	13.1	7.9	11.6	18.4	10.1	12.7
Isotropic	Albuq. 2	-	42.7	27.9	25.5	48.7	26.3	35.5
Hay	Albuq. 2	-	19.6	23.4	22.3	19.4	22.2	21.4
Klucher	Albuq. 2	-	14.1	41.9	41.9	19.0	27.5	28.4
Perez	Albuq. 2	Albuq. 1	16.9	8.3	14.9	16.6	13.7	14.4
Perez	Albuq. 2	Albuq. 2	11.6	8.6	12.3	12.3	11.5	11.3

NOTE: Albuq.1: 11/5/86 to 12/31/86 ("No Honeycomb")
Albuq. 2: 1/3/87 to 2/241/87 ("With Honeycomb")

APPENDIX A: CROSS-VALIDATION RESULTS

This appendix contains validation statistical summaries for each of the 100 cross-validation tests performed. These summaries include, for each orientation and slope studied, the root mean square and mean bias errors resulting from using the Perez and the three reference models: Isotropic, Hay and Klucher. Tables also include mean global and diffuse values on each surface and number of events analyzed. Surfaces are referred to by numbers as follows:

38: South 45° (43° for Albany)
30: North Vertical
32: East Vertical
34: South Vertical
36: West Vertical
39: South 33°
40: South 53°

The table below is provided to help locating tests in this appendix.

COEFFICIENTS	Albu	ElMt	Osag	CCan	SNLA	Phoe	USA	T&C	ALL	Alba
VALIDATION DATA SET	Page Number									
Phoenix	A2	A2	A3	A3	A4	A4	A5	A5	A6	A6
El Monte	A7	A7	A8	A8	A9	A9	A10	A10	A11	A11
Osage	A12	A12	A13	A13	A14	A14	A15	A15	A16	A16
Albuquerque	A17	A17	A18	A18	A19	A19	A20	A20	A21	A21
Cape Canaveral	A22	A22	A23	A23	A24	A24	A25	A25	A26	A26
All SNLA	A27	A27	A28	A28	A29	A29	A30	A30	A31	A31
Albany SEMRTS	A32	A32	A33	A33	A34	A34	A35	A35	A36	A36
All USA	A37	A37	A38	A38	A39	A39	A40	A40	A41	A41
Trappes-Carpent.	A42	A42	A43	A43	A44	A44	A45	A45	A46	A46
All Sites	A47	A47	A48	A48	A49	A49	A50	A50	A51	A51

-----f12.po-----
Tue Jan 26 16:26:10 EST 1988

#/Code	Cases	Avg-G	Avg-D	--ISO-- RMS	MBE	-PEREZ- RMS	MBE	--HAY-- RMS	MBE	-KLUCH- RMS	MBE
1/ 38	1577	529	118	29	-12	14	3	15	4	19	10
2/ 30	1577	60	46	26	16	13	7	21	-7	43	33
3/ 32	1577	245	74	42	-12	17	-3	25	-9	36	12
4/ 34	1577	313	76	34	-14	15	-2	18	-4	26	10
5/ 36	1577	248	67	38	-5	16	4	21	-3	37	19
Composite error				34	12	15	4	20	6	34	19

Site: Phoenix Coefficients: ALBUQUERQUE

-----f12.pl-----
Tue Jan 26 16:24:50 EST 1988

#/Code	Cases	Avg-G	Avg-D	--ISO-- RMS	MBE	-PEREZ- RMS	MBE	--HAY-- RMS	MBE	-KLUCH- RMS	MBE
1/ 38	1577	529	118	29	-12	14	8	15	4	19	10
2/ 30	1577	60	46	26	16	13	-2	21	-7	43	33
3/ 32	1577	245	74	42	-12	16	-3	25	-9	36	12
4/ 34	1577	313	76	34	-14	14	1	18	-4	26	10
5/ 36	1577	248	67	38	-5	17	4	21	-3	37	19
Composite error				34	12	15	4	20	6	34	19

Site: Phoenix Coefficients: EL MONTE

-----f12.pk-----
Tue Jan 26 16:25:25 EST 1988

#/Code	Cases	Avg-G	Avg-D	--ISO-- RMS	MBE	-PEREZ- RMS	MBE	--HAY-- RMS	MBE	-KLUCH- RMS	MBE
1/ 38	1577	529	118	29	-12	54	-6	15	4	19	10
2/ 30	1577	60	46	26	16	59	-24	21	-7	43	33
3/ 32	1577	245	74	42	-12	67	-20	25	-9	36	12
4/ 34	1577	313	76	34	-14	72	-20	18	-4	26	10
5/ 36	1577	248	67	38	-5	67	-15	21	-3	37	19
Composite error				34	12	64	18	20	6	34	19

Site: Phoenix Coefficients: OSAGE

-----f12.pf-----
Tue Jan 26 16:26:53 EST 1988

#/Code	Cases	Avg-G	Avg-D	--ISO-- RMS	MBE	-PEREZ- RMS	MBE	--HAY-- RMS	MBE	-KLUCH- RMS	MBE
1/ 38	1577	529	118	29	-12	21	13	15	4	19	10
2/ 30	1577	60	46	26	16	12	6	21	-7	43	33
3/ 32	1577	245	74	42	-12	20	5	25	-9	36	12
4/ 34	1577	313	76	34	-14	21	9	18	-4	26	10
5/ 36	1577	248	67	38	-5	23	11	21	-3	37	19
Composite error				34	12	20	9	20	6	34	19

Site: Phoenix Coefficients: CAPE CANAVERAL

-----f12.psn1-----
Tue Jan 26 16:27:25 EST 1988

#/Code	Cases	Avg-G	Avg-D	--ISO-- RMS	MBE	-PEREZ- RMS	MBE	--HAY-- RMS	MBE	-KLUCH- RMS	MBE
1/ 38	1577	529	118	29	-12	13	6	15	4	19	10
2/ 30	1577	60	46	26	16	10	1	21	-7	43	33
3/ 32	1577	245	74	42	-12	14	-3	25	-9	36	12
4/ 34	1577	313	76	34	-14	13	-0	18	-4	26	10
5/ 36	1577	248	67	38	-5	15	3	21	-3	37	19
Composite error				34	12	13	3	20	6	34	19

Site: Phoenix Coefficients: SANDIA COMPOSITE

-----f12.pp-----
Tue Jan 26 16:24:17 EST 1988

#/Code	Cases	Avg-G	Avg-D	--ISO-- RMS	MBE	-PEREZ- RMS	MBE	--HAY-- RMS	MBE	-KLUCH- RMS	MBE
1/ 38	1577	529	118	29	-12	12	4	15	4	19	10
2/ 30	1577	60	46	26	16	10	0	21	-7	43	33
3/ 32	1577	245	74	42	-12	15	-5	25	-9	36	12
4/ 34	1577	313	76	34	-14	13	-3	18	-4	26	10
5/ 36	1577	248	67	38	-5	14	1	21	-3	37	19
Composite error				34	12	13	3	20	6	34	19

Site: Phoenix Coefficients: Pk mix

-----f12.pusa-----
Tue Jan 26 16:28:43 EST 1988

#/Code	Cases	Avg-G	Avg-D	--ISO-- RMS	MBE	-PEREZ- RMS	MBE	--HAY-- RMS	MBE	-KLUCH- RMS	MBE
1/ 38	1577	529	118	29	-12	16	10	15	4	19	10
2/ 30	1577	60	46	26	16	13	6	21	-7	43	33
3/ 32	1577	245	74	42	-12	14	3	25	-9	36	12
4/ 34	1577	313	76	34	-14	14	6	18	-4	26	10
5/ 36	1577	248	67	38	-5	17	10	21	-3	37	19
Composite error				34	12	15	8	20	6	34	19

Site: Phoenix Coefficients: USA COMPOSITE

-----f12.ptc-----
Tue Jan 26 16:29:22 EST 1988

#/Code	Cases	Avg-G	Avg-D	--ISO-- RMS	MBE	-PEREZ- RMS	MBE	--HAY-- RMS	MBE	-KLUCH- RMS	MBE
1/ 38	1577	529	118	29	-12	24	20	15	4	19	10
2/ 30	1577	60	46	26	16	17	12	21	-7	43	33
3/ 32	1577	245	74	42	-12	19	12	25	-9	36	12
4/ 34	1577	313	76	34	-14	22	17	18	-4	26	10
5/ 36	1577	248	67	38	-5	25	19	21	-3	37	19
Composite error				34	12	22	16	20	6	34	19

Site: Phoenix Coefficients: FRENCH COMPOSITE

-----f12.pall-----
Tue Jan 26 16:29:53 EST 1988

#/Code	Cases	Avg-G	Avg-D	--ISO-- RMS	MBE	-PEREZ- RMS	MBE	--HAY-- RMS	MBE	-KLUCH- RMS	MBE
1/ 38	1577	529	118	29	-12	19	14	15	4	19	10
2/ 30	1577	60	46	26	16	14	8	21	-7	43	33
3/ 32	1577	245	74	42	-12	15	6	25	-9	36	12
4/ 34	1577	313	76	34	-14	16	10	18	-4	26	10
5/ 36	1577	248	67	38	-5	20	13	21	-3	37	19
Composite error				34	12	17	11	20	6	34	19

Site: Phoenix Coefficients: ALL SITES COMPOSITE

-----f12.palb-----
Tue Jan 26 16:28:02 EST 1988

#/Code	Cases	Avg-G	Avg-D	--ISO-- RMS	MBE	-PEREZ- RMS	MBE	--HAY-- RMS	MBE	-KLUCH- RMS	MBE
1/ 38	1577	529	118	29	-12	19	14	15	4	19	10
2/ 30	1577	60	46	26	16	16	11	21	-7	43	33
3/ 32	1577	245	74	42	-12	16	8	25	-9	36	12
4/ 34	1577	313	76	34	-14	17	10	18	-4	26	10
5/ 36	1577	248	67	38	-5	21	15	21	-3	37	19
Composite error				34	12	18	12	20	6	34	19

Site: Phoenix Coefficients: Albany

-----f12.lo-----
Tue Jan 26 16:32:01 EST 1988

#/Code	Cases	Avg-G	Avg-D	--ISO-- RMS	MBE	-PEREZ- RMS	MBE	--HAY-- RMS	MBE	-KLUCH- RMS	MBE
1/ 38	1502	472	159	36	-19	16	-3	16	-5	18	3
2/ 30	1502	59	53	42	29	15	10	24	6	64	48
3/ 32	1502	202	83	49	-1	20	1	27	-4	52	23
4/ 34	1502	278	93	40	-11	16	-3	19	-4	38	14
5/ 36	1502	195	84	55	-2	19	1	28	-4	57	23
Composite error				45	16	17	5	23	5	49	27

Site: EL MONTE Coefficients: ALBUQUERQUE

-----f12.ll-----
Tue Jan 26 16:31:05 EST 1988

#/Code	Cases	Avg-G	Avg-D	--ISO-- RMS	MBE	-PEREZ- RMS	MBE	--HAY-- RMS	MBE	-KLUCH- RMS	MBE
1/ 38	1502	472	159	36	-19	12	1	16	-5	18	3
2/ 30	1502	59	53	42	29	10	2	24	6	64	48
3/ 32	1502	202	83	49	-1	16	-0	27	-4	52	23
4/ 34	1502	278	93	40	-11	13	-1	19	-4	38	14
5/ 36	1502	195	84	55	-2	16	-1	28	-4	57	23
Composite error				45	16	13	1	23	5	49	27

Site: EL MONTE Coefficients: EL MONTE

-----f12.lk-----
Tue Jan 26 16:31:33 EST 1988

#/Code	Cases	Avg-G	Avg-D	--ISO-- RMS	MBE	-PEREZ- RMS	MBE	--HAY-- RMS	MBE	-KLUCH- RMS	MBE
1/ 38	1502	472	159	36	-19	43	-5	16	-5	18	3
2/ 30	1502	59	53	42	29	43	-10	24	6	64	48
3/ 32	1502	202	83	49	-1	50	-10	27	-4	52	23
4/ 34	1502	278	93	40	-11	55	-11	19	-4	38	14
5/ 36	1502	195	84	55	-2	48	-9	28	-4	57	23
Composite error				45	16	48	9	23	5	49	27

Site: EL MONTE Coefficients: OSAGE

-----f12.lf-----
Tue Jan 26 16:32:28 EST 1988

#/Code	Cases	Avg-G	Avg-D	--ISO-- RMS	MBE	-PEREZ- RMS	MBE	--HAY-- RMS	MBE	-KLUCH- RMS	MBE
1/ 38	1502	472	159	36	-19	15	2	16	-5	18	3
2/ 30	1502	59	53	42	29	13	8	24	6	64	48
3/ 32	1502	202	83	49	-1	20	5	27	-4	52	23
4/ 34	1502	278	93	40	-11	16	3	19	-4	38	14
5/ 36	1502	195	84	55	-2	20	3	28	-4	57	23
Composite error				45	16	17	5	23	5	49	27

Site: EL MONTE Coefficients: CAPE CANAVERAL

-----f12.lsnl-----
Tue Jan 26 16:32:57 EST 1988

#/Code	Cases	Avg-G	Avg-D	--ISO-- RMS	MBE	-PEREZ- RMS	MBE	--HAY-- RMS	MBE	-KLUCH- RMS	MBE
1/ 38	1502	472	159	36	-19	13	-1	16	-5	18	3
2/ 30	1502	59	53	42	29	11	4	24	6	64	48
3/ 32	1502	202	83	49	-1	16	-0	27	-4	52	23
4/ 34	1502	278	93	40	-11	14	-2	19	-4	38	14
5/ 36	1502	195	84	55	-2	16	-1	28	-4	57	23
Composite error				45	16	14	2	23	5	49	27

Site: EL MONTE Coefficients: SANDIA COMPOSITE

-----f12.lp-----
Tue Jan 26 16:30:33 EST 1988

#/Code	Cases	Avg-G	Avg-D	--ISO-- RMS	MBE	-PEREZ- RMS	MBE	--HAY-- RMS	MBE	-KLUCH- RMS	MBE
1/ 38	1502	472	159	36	-19	14	-2	16	-5	18	3
2/ 30	1502	59	53	42	29	11	4	24	6	64	48
3/ 32	1502	202	83	49	-1	18	-2	27	-4	52	23
4/ 34	1502	278	93	40	-11	15	-4	19	-4	38	14
5/ 36	1502	195	84	55	-2	17	-2	28	-4	57	23
Composite error				45	16	15	3	23	5	49	27

Site: EL MONTE Coefficients: PHOENIX

-----f12.lusa-----
Tue Jan 26 16:33:52 EST 1988

#/Code	Cases	Avg-G	Avg-D	--ISO-- RMS	MBE	-PEREZ- RMS	MBE	--HAY-- RMS	MBE	-KLUCH- RMS	MBE
1/ 38	1502	472	159	36	-19	14	4	16	-5	18	3
2/ 30	1502	59	53	42	29	15	10	24	6	64	48
3/ 32	1502	202	83	49	-1	17	6	27	-4	52	23
4/ 34	1502	278	93	40	-11	14	4	19	-4	38	14
5/ 36	1502	195	84	55	-2	17	5	28	-4	57	23
Composite error				45	16	15	6	23	5	49	27

Site: EL MONTE Coefficients: USA COMPOSITE

-----f12.ltc-----
Tue Jan 26 16:34:19 EST 1988

#/Code	Cases	Avg-G	Avg-D	--ISO-- RMS	MBE	-PEREZ- RMS	MBE	--HAY-- RMS	MBE	-KLUCH- RMS	MBE
1/ 38	1502	472	159	36	-19	18	12	16	-5	18	3
2/ 30	1502	59	53	42	29	19	14	24	6	64	48
3/ 32	1502	202	83	49	-1	21	13	27	-4	52	23
4/ 34	1502	278	93	40	-11	19	13	19	-4	38	14
5/ 36	1502	195	84	55	-2	20	11	28	-4	57	23
Composite error				45	16	19	13	23	5	49	27

Site: EL MONTE Coefficients: FRENCH COMPOSITE

-----f12.lall-----
Tue Jan 26 16:34:47 EST 1988

#/Code	Cases	Avg-G	Avg-D	--ISO-- RMS	MBE	-PEREZ- RMS	MBE	--HAY-- RMS	MBE	-KLUCH- RMS	MBE
1/ 38	1502	472	159	36	-19	15	7	16	-5	18	3
2/ 30	1502	59	53	42	29	16	12	24	6	64	48
3/ 32	1502	202	83	49	-1	18	9	27	-4	52	23
4/ 34	1502	278	93	40	-11	15	8	19	-4	38	14
5/ 36	1502	195	84	55	-2	18	8	28	-4	57	23
Composite error				45	16	16	9	23	5	49	27

Site: EL MONTE Coefficients: ALL SITES COMPOSITE

-----f12.lalb-----
Tue Jan 26 16:33:25 EST 1988

#/Code	Cases	Avg-G	Avg-D	--ISO-- RMS	MBE	-PEREZ- RMS	MBE	--HAY-- RMS	MBE	-KLUCH- RMS	MBE
1/ 38	1502	472	159	36	-19	15	7	16	-5	18	3
2/ 30	1502	59	53	42	29	18	14	24	6	64	48
3/ 32	1502	202	83	49	-1	19	10	27	-4	52	23
4/ 34	1502	278	93	40	-11	16	8	19	-4	38	14
5/ 36	1502	195	84	55	-2	19	10	28	-4	57	23
Composite error				45	16	18	10	23	5	49	27

Site: EL MONTE Coefficients: ALBANY

-----f12.ko-----
Tue Jan 26 16:35:28 EST 1988

#/Code	Cases	Avg-G	Avg-D	--ISO-- RMS	MBE	-PEREZ- RMS	MBE	--HAY-- RMS	MBE	-KLUCH- RMS	MBE
1/ 38	418	408	183	34	-12	17	-1	20	-4	21	5
2/ 30	418	66	64	47	36	16	9	29	13	68	53
3/ 32	418	124	85	50	15	27	2	37	1	60	34
4/ 34	418	202	96	28	4	13	3	19	3	35	24
5/ 36	418	241	107	62	-7	22	-3	31	0	57	20
Composite error				46	19	20	5	28	6	51	32

Site: OSAGE Coefficients: ALBUQUERQUE

-----f12.kl-----
Tue Jan 26 16:35:08 EST 1988

#/Code	Cases	Avg-G	Avg-D	--ISO-- RMS	MBE	-PEREZ- RMS	MBE	--HAY-- RMS	MBE	-KLUCH- RMS	MBE
1/ 38	418	408	183	34	-12	15	0	20	-4	21	5
2/ 30	418	66	64	47	36	11	1	29	13	68	53
3/ 32	418	124	85	50	15	24	-3	37	1	60	34
4/ 34	418	202	96	28	4	11	1	19	3	35	24
5/ 36	418	241	107	62	-7	17	-4	31	0	57	20
Composite error				46	19	16	2	28	6	51	32

Site: OSAGE Coefficients: EL MONTE

-----f12.kk-----
Tue Jan 26 16:35:18 EST 1988

#/Code	Cases	Avg-G	Avg-D	--ISO-- RMS	MBE	-PEREZ- RMS	MBE	--HAY-- RMS	MBE	-KLUCH- RMS	MBE
1/ 38	418	408	183	34	-12	13	0	20	-4	21	5
2/ 30	418	66	64	47	36	10	-0	29	13	68	53
3/ 32	418	124	85	50	15	16	-2	37	1	60	34
4/ 34	418	202	96	28	4	10	1	19	3	35	24
5/ 36	418	241	107	62	-7	16	0	31	0	57	20
Composite error				46	19	13	1	28	6	51	32

Site: OSAGE Coefficients: OSAGE

-----f12.kf-----
Tue Jan 26 16:35:38 EST 1988

#/Code	Cases	Avg-G	Avg-D	--ISO-- RMS	MBE	-PEREZ- RMS	MBE	--HAY-- RMS	MBE	-KLUCH- RMS	MBE
1/ 38	418	408	183	34	-12	16	-1	20	-4	21	5
2/ 30	418	66	64	47	36	14	7	29	13	68	53
3/ 32	418	124	85	50	15	26	1	37	1	60	34
4/ 34	418	202	96	28	4	13	3	19	3	35	24
5/ 36	418	241	107	62	-7	19	-1	31	0	57	20
Composite error				46	19	18	3	28	6	51	32

Site: OSAGE Coefficients: CAPE CANAVERAL

-----f12.ksnl-----
Tue Jan 26 16:35:47 EST 1988

#/Code	Cases	Avg-G	Avg-D	--ISO-- RMS	MBE	-PEREZ- RMS	MBE	--HAY-- RMS	MBE	-KLUCH- RMS	MBE
1/ 38	418	408	183	34	-12	15	-1	20	-4	21	5
2/ 30	418	66	64	47	36	11	3	29	13	68	53
3/ 32	418	124	85	50	15	20	-1	37	1	60	34
4/ 34	418	202	96	28	4	11	1	19	3	35	24
5/ 36	418	241	107	62	-7	18	-4	31	0	57	20
Composite error				46	19	15	2	28	6	51	32

Site: OSAGE Coefficients: SANDIA COMPOSITE

-----f12.kp-----
Tue Jan 26 16:34:58 EST 1988

#/Code	Cases	Avg-G	Avg-D	--ISO-- RMS	MBE	-PEREZ- RMS	MBE	--HAY-- RMS	MBE	-KLUCH- RMS	MBE
1/ 38	418	408	183	34	-12	16	-1	20	-4	21	5
2/ 30	418	66	64	47	36	11	4	29	13	68	53
3/ 32	418	124	85	50	15	24	-1	37	1	60	34
4/ 34	418	202	96	28	4	11	1	19	3	35	24
5/ 36	418	241	107	62	-7	19	-4	31	0	57	20
Composite error				46	19	17	3	28	6	51	32

Site: OSAGE Coefficients: Phoenix

-----f12.kusa-----
Tue Jan 26 16:36:06 EST 1988

#/Code	Cases	Avg-G	Avg-D	--ISO-- RMS	MBE	-PEREZ- RMS	MBE	--HAY-- RMS	MBE	-KLUCH- RMS	MBE
1/ 38	418	408	183	34	-12	16	3	20	-4	21	5
2/ 30	418	66	64	47	36	15	10	29	13	68	53
3/ 32	418	124	85	50	15	24	5	37	1	60	34
4/ 34	418	202	96	28	4	14	7	19	3	35	24
5/ 36	418	241	107	62	-7	18	3	31	0	57	20
Composite error				46	19	18	6	28	6	51	32

Site: OSAGE Coefficients: USA COMPOSITE

-----f12.ktc-----
Tue Jan 26 16:36:16 EST 1988

#/Code	Cases	Avg-G	Avg-D	--ISO-- RMS	MBE	-PEREZ- RMS	MBE	--HAY-- RMS	MBE	-KLUCH- RMS	MBE
1/ 38	418	408	183	34	-12	18	10	20	-4	21	5
2/ 30	418	66	64	47	36	18	12	29	13	68	53
3/ 32	418	124	85	50	15	25	10	37	1	60	34
4/ 34	418	202	96	28	4	19	14	19	3	35	24
5/ 36	418	241	107	62	-7	20	8	31	0	57	20
Composite error				46	19	20	11	28	6	51	32

Site: OSAGE Coefficients: FRENCH COMPOSITE

-----f12.kall-----
Tue Jan 26 16:36:25 EST 1988

#/Code	Cases	Avg-G	Avg-D	--ISO-- RMS	MBE	-PEREZ- RMS	MBE	--HAY-- RMS	MBE	-KLUCH- RMS	MBE
1/ 38	418	408	183	34	-12	16	6	20	-4	21	5
2/ 30	418	66	64	47	36	16	11	29	13	68	53
3/ 32	418	124	85	50	15	24	7	37	1	60	34
4/ 34	418	202	96	28	4	16	10	19	3	35	24
5/ 36	418	241	107	62	-7	18	5	31	0	57	20
Composite error				46	19	18	8	28	6	51	32

Site: OSAGE Coefficients: ALL SITES COMPOSITE

-----f12.kalb-----
Tue Jan 26 16:35:57 EST 1988

#/Code	Cases	Avg-G	Avg-D	--ISO-- RMS	MBE	-PEREZ- RMS	MBE	--HAY-- RMS	MBE	-KLUCH- RMS	MBE
1/ 38	418	408	183	34	-12	17	6	20	-4	21	5
2/ 30	418	66	64	47	36	19	13	29	13	68	53
3/ 32	418	124	85	50	15	26	8	37	1	60	34
4/ 34	418	202	96	28	4	17	11	19	3	35	24
5/ 36	418	241	107	62	-7	19	6	31	0	57	20
Composite error				46	19	20	9	28	6	51	32

Site: OSAGE Coefficients: ALBANY

-----f12.oo-----
Tue Jan 26 16:38:35 EST 1988

#/Code	Cases	Avg-G	Avg-D	--ISO-- RMS	MBE	-PEREZ- RMS	MBE	--HAY-- RMS	MBE	-KLUCH- RMS	MBE
1/ 38	1828	535	122	31	-17	11	0	15	-3	14	2
2/ 30	1828	57	46	29	16	10	1	23	-4	45	30
3/ 32	1828	217	61	35	1	13	2	22	-2	39	19
4/ 34	1828	328	78	36	-16	13	-2	18	-6	26	4
5/ 36	1828	226	69	35	-7	13	-2	21	-6	35	12
Composite error				33	13	12	2	20	4	34	17

Site: ALBUQUERQUE Coefficients: ALBUQUERQUE

-----f12.ol-----
Tue Jan 26 16:37:31 EST 1988

#/Code	Cases	Avg-G	Avg-D	--ISO-- RMS	MBE	-PEREZ- RMS	MBE	--HAY-- RMS	MBE	-KLUCH- RMS	MBE
1/ 38	1828	535	122	31	-17	12	1	15	-3	14	2
2/ 30	1828	57	46	29	16	14	-5	23	-4	45	30
3/ 32	1828	217	61	35	1	16	-0	22	-2	39	19
4/ 34	1828	328	78	36	-16	14	-3	18	-6	26	4
5/ 36	1828	226	69	35	-7	16	-4	21	-6	35	12
Composite error				33	13	14	3	20	4	34	17

Site: ALBUQUERQUE Coefficients: EL MONTE

-----f12.ok-----
Tue Jan 26 16:38:03 EST 1988

#/Code	Cases	Avg-G	Avg-D	--ISO-- RMS	MBE	-PEREZ- RMS	MBE	--HAY-- RMS	MBE	-KLUCH- RMS	MBE
1/ 38	1828	535	122	31	-17	42	-11	15	-3	14	2
2/ 30	1828	57	46	29	16	47	-17	23	-4	45	30
3/ 32	1828	217	61	35	1	50	-13	22	-2	39	19
4/ 34	1828	328	78	36	-16	56	-19	18	-6	26	4
5/ 36	1828	226	69	35	-7	52	-16	21	-6	35	12
Composite error				33	13	50	15	20	4	34	17

Site: ALBUQUERQUE Coefficients: OSAGE

-----f12.of-----
Tue Jan 26 16:39:07 EST 1988

#/Code	Cases	Avg-G	Avg-D	--ISO-- RMS	MBE	-PEREZ- RMS	MBE	--HAY-- RMS	MBE	-KLUCH- RMS	MBE
1/ 38	1828	535	122	31	-17	15	4	15	-3	14	2
2/ 30	1828	57	46	29	16	11	3	23	-4	45	30
3/ 32	1828	217	61	35	1	18	6	22	-2	39	19
4/ 34	1828	328	78	36	-16	16	3	18	-6	26	4
5/ 36	1828	226	69	35	-7	16	3	21	-6	35	12
Composite error				33	13	15	4	20	4	34	17

Site: ALBUQUERQUE Coefficients: CAPE CANAVERAL

-----f12.osnl-----
Tue Jan 26 16:39:39 EST 1988

#/Code	Cases	Avg-G	Avg-D	--ISO-- RMS	MBE	-PEREZ- RMS	MBE	--HAY-- RMS	MBE	-KLUCH- RMS	MBE
1/ 38	1828	535	122	31	-17	12	1	15	-3	14	2
2/ 30	1828	57	46	29	16	10	-1	23	-4	45	30
3/ 32	1828	217	61	35	1	14	1	22	-2	39	19
4/ 34	1828	328	78	36	-16	13	-3	18	-6	26	4
5/ 36	1828	226	69	35	-7	14	-2	21	-6	35	12
Composite error				33	13	13	2	20	4	34	17

Site: ALBUQUERQUE Coefficients: SANDIA COMPOSITE

-----f12.op-----
Tue Jan 26 16:36:59 EST 1988

#/Code	Cases	Avg-G	Avg-D	--ISO-- RMS	MBE	-PEREZ- RMS	MBE	--HAY-- RMS	MBE	-KLUCH- RMS	MBE
1/ 38	1828	535	122	31	-17	12	-2	15	-3	14	2
2/ 30	1828	57	46	29	16	11	-2	23	-4	45	30
3/ 32	1828	217	61	35	1	14	-1	22	-2	39	19
4/ 34	1828	328	78	36	-16	15	-5	18	-6	26	4
5/ 36	1828	226	69	35	-7	14	-4	21	-6	35	12
Composite error				33	13	13	3	20	4	34	17

Site: ALBUQUERQUE Coefficients: PHOENIX

-----f12.ousa-----
Tue Jan 26 16:40:55 EST 1988

#/Code	Cases	Avg-G	Avg-D	--ISO-- RMS	MBE	-PEREZ- RMS	MBE	--HAY-- RMS	MBE	-KLUCH- RMS	MBE
1/ 38	1828	535	122	31	-17	13	4	15	-3	14	2
2/ 30	1828	57	46	29	16	11	3	23	-4	45	30
3/ 32	1828	217	61	35	1	15	6	22	-2	39	19
4/ 34	1828	328	78	36	-16	13	1	18	-6	26	4
5/ 36	1828	226	69	35	-7	14	2	21	-6	35	12
Composite error				33	13	13	4	20	4	34	17

Site: Albuquerque Coefficients: USA COMPOSITE

-----f12.otc-----
Tue Jan 26 16:41:32 EST 1988

#/Code	Cases	Avg-G	Avg-D	--ISO-- RMS	MBE	-PEREZ- RMS	MBE	--HAY-- RMS	MBE	-KLUCH- RMS	MBE
1/ 38	1828	535	122	31	-17	17	11	15	-3	14	2
2/ 30	1828	57	46	29	16	13	7	23	-4	45	30
3/ 32	1828	217	61	35	1	19	12	22	-2	39	19
4/ 34	1828	328	78	36	-16	17	10	18	-6	26	4
5/ 36	1828	226	69	35	-7	17	9	21	-6	35	12
Composite error				33	13	17	10	20	4	34	17

Site: Albuquerque Coefficients: FRENCH COMPOSITE

-----f12.oall-----
Tue Jan 26 16:42:05 EST 1988

#/Code	Cases	Avg-G	Avg-D	--ISO-- RMS	MBE	-PEREZ- RMS	MBE	--HAY-- RMS	MBE	-KLUCH- RMS	MBE
1/ 38	1828	535	122	31	-17	14	6	15	-3	14	2
2/ 30	1828	57	46	29	16	12	4	23	-4	45	30
3/ 32	1828	217	61	35	1	16	7	22	-2	39	19
4/ 34	1828	328	78	36	-16	14	4	18	-6	26	4
5/ 36	1828	226	69	35	-7	14	4	21	-6	35	12
Composite error				33	13	14	5	20	4	34	17

Site: ALBUQUERQUE Coefficients: ALL SITES COMPOSITE

-----f12.oalb-----
Tue Jan 26 16:40:13 EST 1988

#/Code	Cases	Avg-G	Avg-D	--ISO-- RMS	MBE	-PEREZ- RMS	MBE	--HAY-- RMS	MBE	-KLUCH- RMS	MBE
1/ 38	1828	535	122	31	-17	15	8	15	-3	14	2
2/ 30	1828	57	46	29	16	13	7	23	-4	45	30
3/ 32	1828	217	61	35	1	18	10	22	-2	39	19
4/ 34	1828	328	78	36	-16	15	6	18	-6	26	4
5/ 36	1828	226	69	35	-7	16	6	21	-6	35	12
Composite error				33	13	16	8	20	4	34	17

Site: ALBUQUERQUE Coefficients: ALBANY

-----f12.fo-----
Tue Jan 26 16:42:51 EST 1988

#/Code	Cases	Avg-G	Avg-D	--ISO-- RMS	--ISO-- MBE	-PEREZ- RMS	-PEREZ- MBE	--HAY-- RMS	--HAY-- MBE	-KLUCH- RMS	-KLUCH- MBE
1/ 38	551	398	152	20	-1	13	4	13	-1	21	13
2/ 30	551	84	69	39	20	14	-2	30	-3	59	40
3/ 32	551	259	99	60	-10	28	-8	39	-11	58	17
4/ 34	551	150	85	22	3	11	-5	21	-9	36	24
5/ 36	551	173	86	46	3	18	2	26	-2	53	29
Composite error				40	10	18	5	27	7	48	26

Site: CAPE CANAVERAL Coefficients: ALBUQUERQUE

-----f12.fl-----
Tue Jan 26 16:42:29 EST 1988

#/Code	Cases	Avg-G	Avg-D	--ISO-- RMS	--ISO-- MBE	-PEREZ- RMS	-PEREZ- MBE	--HAY-- RMS	--HAY-- MBE	-KLUCH- RMS	-KLUCH- MBE
1/ 38	551	398	152	20	-1	12	3	13	-1	21	13
2/ 30	551	84	69	39	20	20	-11	30	-3	59	40
3/ 32	551	259	99	60	-10	25	-9	39	-11	58	17
4/ 34	551	150	85	22	3	16	-11	21	-9	36	24
5/ 36	551	173	86	46	3	18	-1	26	-2	53	29
Composite error				40	10	19	8	27	7	48	26

Site: CAPE CANAVERAL Coefficients: EL MONTE

-----f12.fk-----
Tue Jan 26 16:42:41 EST 1988

#/Code	Cases	Avg-G	Avg-D	--ISO-- RMS	MBE	-PEREZ- RMS	MBE	--HAY-- RMS	MBE	-KLUCH- RMS	MBE
1/ 38	551	398	152	20	-1	33	2	13	-1	21	13
2/ 30	551	84	69	39	20	36	-15	30	-3	59	40
3/ 32	551	259	99	60	-10	49	-12	39	-11	58	17
4/ 34	551	150	85	22	3	36	-14	21	-9	36	24
5/ 36	551	173	86	46	3	39	-1	26	-2	53	29
Composite error				40	10	39	11	27	7	48	26

Site: CAPE CANAVERAL Coefficients: OSAGE

-----f12.ff-----
Tue Jan 26 16:43:02 EST 1988

#/Code	Cases	Avg-G	Avg-D	--ISO-- RMS	MBE	-PEREZ- RMS	MBE	--HAY-- RMS	MBE	-KLUCH- RMS	MBE
1/ 38	551	398	152	20	-1	12	4	13	-1	21	13
2/ 30	551	84	69	39	20	13	-3	30	-3	59	40
3/ 32	551	259	99	60	-10	24	-5	39	-11	58	17
4/ 34	551	150	85	22	3	11	-6	21	-9	36	24
5/ 36	551	173	86	46	3	14	4	26	-2	53	29
Composite error				40	10	16	4	27	7	48	26

Site: CAPE CANAVERAL Coefficients: CAPE CANAVERAL

-----f12.fsn1-----
Tue Jan 26 16:43:12 EST 1988

#/Code	Cases	Avg-G	Avg-D	--ISO-- RMS	MBE	-PEREZ- RMS	MBE	--HAY-- RMS	MBE	-KLUCH- RMS	MBE
1/ 38	551	398	152	20	-1	13	4	13	-1	21	13
2/ 30	551	84	69	39	20	16	-7	30	-3	59	40
3/ 32	551	259	99	60	-10	25	-9	39	-11	58	17
4/ 34	551	150	85	22	3	13	-8	21	-9	36	24
5/ 36	551	173	86	46	3	16	1	26	-2	53	29
Composite error				40	10	17	6	27	7	48	26

Site: CAPE CANAVERAL Coefficients: SANDIA COMPOSITE

-----f12.fp-----
Tue Jan 26 16:42:17 EST 1988

#/Code	Cases	Avg-G	Avg-D	--ISO-- RMS	MBE	-PEREZ- RMS	MBE	--HAY-- RMS	MBE	-KLUCH- RMS	MBE
1/ 38	551	398	152	20	-1	12	3	13	-1	21	13
2/ 30	551	84	69	39	20	16	-7	30	-3	59	40
3/ 32	551	259	99	60	-10	27	-10	39	-11	58	17
4/ 34	551	150	85	22	3	14	-9	21	-9	36	24
5/ 36	551	173	86	46	3	15	-0	26	-2	53	29
Composite error				40	10	18	7	27	7	48	26

Site: CAPE CANAVERAL Coefficients: PHOENIX

-----f12.fusa-----
Tue Jan 26 16:43:34 EST 1988

#/Code	Cases	Avg-G	Avg-D	--ISO-- RMS	MBE	-PEREZ- RMS	MBE	--HAY-- RMS	MBE	-KLUCH- RMS	MBE
1/ 38	551	398	152	20	-1	15	8	13	-1	21	13
2/ 30	551	84	69	39	20	15	-2	30	-3	59	40
3/ 32	551	259	99	60	-10	23	-2	39	-11	58	17
4/ 34	551	150	85	22	3	10	-3	21	-9	36	24
5/ 36	551	173	86	46	3	17	6	26	-2	53	29
Composite error				40	10	17	5	27	7	48	26

Site: CAPE CANAVERAL Coefficients: USA COMPOSITE

-----f12.ftc-----
Tue Jan 26 16:43:44 EST 1988

#/Code	Cases	Avg-G	Avg-D	--ISO-- RMS	MBE	-PEREZ- RMS	MBE	--HAY-- RMS	MBE	-KLUCH- RMS	MBE
1/ 38	551	398	152	20	-1	20	14	13	-1	21	13
2/ 30	551	84	69	39	20	15	2	30	-3	59	40
3/ 32	551	259	99	60	-10	22	5	39	-11	58	17
4/ 34	551	150	85	22	3	12	3	21	-9	36	24
5/ 36	551	173	86	46	3	23	13	26	-2	53	29
Composite error				40	10	19	9	27	7	48	26

Site: CAPE CANAVERAL Coefficients: FRENCH COMPOSITE

-----f12.fall-----
Tue Jan 26 16:43:55 EST 1988

#/Code	Cases	Avg-G	Avg-D	--ISO-- RMS	MBE	-PEREZ- RMS	MBE	--HAY-- RMS	MBE	-KLUCH- RMS	MBE
1/ 38	551	398	152	20	-1	17	10	13	-1	21	13
2/ 30	551	84	69	39	20	15	-0	30	-3	59	40
3/ 32	551	259	99	60	-10	23	0	39	-11	58	17
4/ 34	551	150	85	22	3	10	-0	21	-9	36	24
5/ 36	551	173	86	46	3	19	9	26	-2	53	29
Composite error				40	10	17	6	27	7	48	26

Site: CAPE CANAVERAL Coefficients: ALL SITES COMPOSITE

-----f12.falb-----
Tue Jan 26 16:43:23 EST 1988

#/Code	Cases	Avg-G	Avg-D	--ISO-- RMS	MBE	-PEREZ- RMS	MBE	--HAY-- RMS	MBE	-KLUCH- RMS	MBE
1/ 38	551	398	152	20	-1	17	11	13	-1	21	13
2/ 30	551	84	69	39	20	15	2	30	-3	59	40
3/ 32	551	259	99	60	-10	23	3	39	-11	58	17
4/ 34	551	150	85	22	3	10	1	21	-9	36	24
5/ 36	551	173	86	46	3	19	10	26	-2	53	29
Composite error				40	10	18	7	27	7	48	26

Site: CAPE CANAVERAL Coefficients: ALBANY

-----f12.snlo-----
Tue Jan 26 16:50:42 EST 1988

#/Code	Cases	Avg-G	Avg-D	--ISO-- RMS	MBE	-PEREZ- RMS	MBE	--HAY-- RMS	MBE	-KLUCH- RMS	MBE
1/ 38	5876	495	138	31	-14	14	1	16	-1	18	6
2/ 30	5876	62	51	34	21	13	5	24	-1	53	38
3/ 32	5876	218	75	44	-3	19	-0	27	-5	46	19
4/ 34	5876	285	83	35	-11	14	-2	19	-5	31	12
5/ 36	5876	220	76	45	-4	17	1	25	-4	46	19
Composite error				38	13	16	3	22	4	41	22

Site: SANDIA COMPOSITE Coefficients: ALBUQUERQUE

-----f12.snll-----
Tue Jan 26 16:47:19 EST 1988

#/Code	Cases	Avg-G	Avg-D	--ISO-- RMS	MBE	-PEREZ- RMS	MBE	--HAY-- RMS	MBE	-KLUCH- RMS	MBE
1/ 38	5876	495	138	31	-14	13	3	16	-1	18	6
2/ 30	5876	62	51	34	21	13	-3	24	-1	53	38
3/ 32	5876	218	75	44	-3	18	-2	27	-5	46	19
4/ 34	5876	285	83	35	-11	14	-2	19	-5	31	12
5/ 36	5876	220	76	45	-4	17	-1	25	-4	46	19
Composite error				38	13	15	2	22	4	41	22

Site: SANDIA COMPOSITE Coefficients: EL MONTE

-----f12.snlk-----
Tue Jan 26 16:49:00 EST 1988

#/Code	Cases	Avg-G	Avg-D	--ISO-- RMS	MBE	-PEREZ- RMS	MBE	--HAY-- RMS	MBE	-KLUCH- RMS	MBE
1/ 38	5876	495	138	31	-14	44	-6	16	-1	18	6
2/ 30	5876	62	51	34	21	47	-16	24	-1	53	38
3/ 32	5876	218	75	44	-3	54	-13	27	-5	46	19
4/ 34	5876	285	83	35	-11	57	-15	19	-5	31	12
5/ 36	5876	220	76	45	-4	53	-12	25	-4	46	19
Composite error				38	13	51	13	22	4	41	22

Site: SANDIA COMPOSITE Coefficients: OSAGE

-----f12.snlf-----
Tue Jan 26 16:52:24 EST 1988

#/Code	Cases	Avg-G	Avg-D	--ISO-- RMS	MBE	-PEREZ- RMS	MBE	--HAY-- RMS	MBE	-KLUCH- RMS	MBE
1/ 38	5876	495	138	31	-14	17	6	16	-1	18	6
2/ 30	5876	62	51	34	21	12	5	24	-1	53	38
3/ 32	5876	218	75	44	-3	20	4	27	-5	46	19
4/ 34	5876	285	83	35	-11	17	4	19	-5	31	12
5/ 36	5876	220	76	45	-4	19	5	25	-4	46	19
Composite error				38	13	17	5	22	4	41	22

Site: SANDIA COMPOSITE Coefficients: CAPE CANAVERAL

-----f12.snlsnl-----
Tue Jan 26 16:54:05 EST 1988

#/Code	Cases	Avg-G	Avg-D	--ISO-- RMS	MBE	-PEREZ- RMS	MBE	--HAY-- RMS	MBE	-KLUCH- RMS	MBE
1/ 38	5876	495	138	31	-14	13	2	16	-1	18	6
2/ 30	5876	62	51	34	21	11	1	24	-1	53	38
3/ 32	5876	218	75	44	-3	17	-1	27	-5	46	19
4/ 34	5876	285	83	35	-11	13	-2	19	-5	31	12
5/ 36	5876	220	76	45	-4	15	0	25	-4	46	19
Composite error				38	13	14	1	22	4	41	22

Site: SANDIA COMPOSITE Coefficients: SANDIA COMPOSITE

-----f12.snlp-----
Tue Jan 26 16:45:37 EST 1988

#/Code	Cases	Avg-G	Avg-D	--ISO-- RMS	MBE	-PEREZ- RMS	MBE	--HAY-- RMS	MBE	-KLUCH- RMS	MBE
1/ 38	5876	495	138	31	-14	13	-0	16	-1	18	6
2/ 30	5876	62	51	34	21	11	0	24	-1	53	38
3/ 32	5876	218	75	44	-3	17	-3	27	-5	46	19
4/ 34	5876	285	83	35	-11	14	-4	19	-5	31	12
5/ 36	5876	220	76	45	-4	15	-2	25	-4	46	19
Composite error				38	13	14	2	22	4	41	22

Site: SANDIA COMPOSITE Coefficients: Phoenix

-----f12.snlusa-----
Tue Jan 26 16:57:28 EST 1988

#/Code	Cases	Avg-G	Avg-D	--ISO-- RMS	MBE	-PEREZ- RMS	MBE	--HAY-- RMS	MBE	-KLUCH- RMS	MBE
1/ 38	5876	495	138	31	-14	14	6	16	-1	18	6
2/ 30	5876	62	51	34	21	13	6	24	-1	53	38
3/ 32	5876	218	75	44	-3	17	4	27	-5	46	19
4/ 34	5876	285	83	35	-11	13	3	19	-5	31	12
5/ 36	5876	220	76	45	-4	16	5	25	-4	46	19
Composite error				38	13	15	5	22	4	41	22

Site: SANDIA COMPOSITE Coefficients: USA COMPOSITE

-----f12.snltc-----
Tue Jan 26 16:59:12 EST 1988

#/Code	Cases	Avg-G	Avg-D	--ISO-- RMS	MBE	-PEREZ- RMS	MBE	--HAY-- RMS	MBE	-KLUCH- RMS	MBE
1/ 38	5876	495	138	31	-14	20	14	16	-1	18	6
2/ 30	5876	62	51	34	21	16	10	24	-1	53	38
3/ 32	5876	218	75	44	-3	20	11	27	-5	46	19
4/ 34	5876	285	83	35	-11	19	12	19	-5	31	12
5/ 36	5876	220	76	45	-4	21	13	25	-4	46	19
Composite error				38	13	19	12	22	4	41	22

Site: SANDIA COMPOSITE Coefficients: FRENCH COMPOSITE

-----f12.snlall-----
Tue Jan 26 17:00:55 EST 1988

#/Code	Cases	Avg-G	Avg-D	--ISO-- RMS	MBE	-PEREZ- RMS	MBE	--HAY-- RMS	MBE	-KLUCH- RMS	MBE
1/ 38	5876	495	138	31	-14	16	9	16	-1	18	6
2/ 30	5876	62	51	34	21	14	7	24	-1	53	38
3/ 32	5876	218	75	44	-3	18	7	27	-5	46	19
4/ 34	5876	285	83	35	-11	15	6	19	-5	31	12
5/ 36	5876	220	76	45	-4	17	8	25	-4	46	19
Composite error				38	13	16	8	22	4	41	22

Site: SANDIA COMPOSITE Coefficients: ALL SITES COMPOSITE

-----f12.snlalb-----
Tue Jan 26 16:55:47 EST 1988

#/Code	Cases	Avg-G	Avg-D	--ISO-- RMS	MBE	-PEREZ- RMS	MBE	--HAY-- RMS	MBE	-KLUCH- RMS	MBE
1/ 38	5876	495	138	31	-14	17	9	16	-1	18	6
2/ 30	5876	62	51	34	21	16	10	24	-1	53	38
3/ 32	5876	218	75	44	-3	19	9	27	-5	46	19
4/ 34	5876	285	83	35	-11	16	8	19	-5	31	12
5/ 36	5876	220	76	45	-4	19	10	25	-4	46	19
Composite error				38	13	17	9	22	4	41	22

Site: SANDIA COMPOSITE Coefficients: ALBANY

-----f12.albo-----
Tue Jan 26 17:16:24 EST 1988

#/Code	Cases	Avg-G	Avg-D	--ISO-- RMS	MBE	-PEREZ- RMS	MBE	--HAY-- RMS	MBE	-KLUCH- RMS	MBE
1/ 38	10865	384	160	28	-18	13	-6	17	-8	13	-2
2/ 39	10865	379	157	36	-23	17	-9	22	-12	16	-6
3/ 40	10865	358	145	38	-21	17	-7	22	-10	17	-3
4/ 30	10865	65	61	29	16	10	-3	24	1	45	29
5/ 32	10865	161	84	40	-7	20	-10	27	-10	37	10
6/ 34	10865	221	90	32	-13	16	-5	22	-6	23	5
7/ 36	10865	160	82	42	-5	20	-7	28	-7	40	12
Composite error				36	16	16	7	24	8	30	13

Site: ALBANY Coefficients: ALBUQUERQUE

-----f12.albl-----
Tue Jan 26 17:08:40 EST 1988

#/Code	Cases	Avg-G	Avg-D	--ISO-- RMS	MBE	-PEREZ- RMS	MBE	--HAY-- RMS	MBE	-KLUCH- RMS	MBE
1/ 38	10865	384	160	28	-18	12	-4	17	-8	13	-2
2/ 39	10865	379	157	36	-23	15	-7	22	-12	16	-6
3/ 40	10865	358	145	38	-21	15	-5	22	-10	17	-3
4/ 30	10865	65	61	29	16	14	-9	24	1	45	29
5/ 32	10865	161	84	40	-7	20	-13	27	-10	37	10
6/ 34	10865	221	90	32	-13	18	-4	22	-6	23	5
7/ 36	10865	160	82	42	-5	19	-9	28	-7	40	12
Composite error				36	16	16	8	24	8	30	13

Site: ALBANY Coefficients: EL MONTE

-----f12.albk-----
Tue Jan 26 17:12:32 EST 1988

#/Code	Cases	Avg-G	Avg-D	--ISO-- RMS	MBE	-PEREZ- RMS	MBE	--HAY-- RMS	MBE	-KLUCH- RMS	MBE
1/ 38	10865	384	160	28	-18	29	-8	17	-8	13	-2
2/ 39	10865	379	157	36	-23	37	-13	22	-12	16	-6
3/ 40	10865	358	145	38	-21	41	-11	22	-10	17	-3
4/ 30	10865	65	61	29	16	42	-19	24	1	45	29
5/ 32	10865	161	84	40	-7	49	-21	27	-10	37	10
6/ 34	10865	221	90	32	-13	47	-13	22	-6	23	5
7/ 36	10865	160	82	42	-5	46	-18	28	-7	40	12
Composite error				36	16	42	15	24	8	30	13

Site: ALBANY Coefficients: OSAGE

-----f12.albf-----
Tue Jan 26 17:20:17 EST 1988

#/Code	Cases	Avg-G	Avg-D	--ISO-- RMS	MBE	-PEREZ- RMS	MBE	--HAY-- RMS	MBE	-KLUCH- RMS	MBE
1/ 38	10865	384	160	28	-18	14	-3	17	-8	13	-2
2/ 39	10865	379	157	36	-23	17	-6	22	-12	16	-6
3/ 40	10865	358	145	38	-21	17	-3	22	-10	17	-3
4/ 30	10865	65	61	29	16	10	-3	24	1	45	29
5/ 32	10865	161	84	40	-7	17	-8	27	-10	37	10
6/ 34	10865	221	90	32	-13	20	-1	22	-6	23	5
7/ 36	10865	160	82	42	-5	19	-5	28	-7	40	12
Composite error				36	16	17	5	24	8	30	13

Site: ALBANY Coefficients: CAPE CANAVERAL

-----f12.albsnl-----
Tue Jan 26 17:24:09 EST 1988

#/Code	Cases	Avg-G	Avg-D	--ISO-- RMS	MBE	-PEREZ- RMS	MBE	--HAY-- RMS	MBE	-KLUCH- RMS	MBE
1/ 38	10865	384	160	28	-18	12	-5	17	-8	13	-2
2/ 39	10865	379	157	36	-23	15	-8	22	-12	16	-6
3/ 40	10865	358	145	38	-21	16	-5	22	-10	17	-3
4/ 30	10865	65	61	29	16	11	-7	24	1	45	29
5/ 32	10865	161	84	40	-7	19	-12	27	-10	37	10
6/ 34	10865	221	90	32	-13	17	-4	22	-6	23	5
7/ 36	10865	160	82	42	-5	19	-9	28	-7	40	12
Composite error				36	16	16	7	24	8	30	13

Site: ALBANY Coefficients: SANDIA COMPOSITE

-----f12.albp-----
Tue Jan 26 17:04:48 EST 1988

#/Code	Cases	Avg-G	Avg-D	--ISO-- RMS	MBE	-PEREZ- RMS	MBE	--HAY-- RMS	MBE	-KLUCH- RMS	MBE
1/ 38	10865	384	160	28	-18	12	-6	17	-8	13	-2
2/ 39	10865	379	157	36	-23	16	-9	22	-12	16	-6
3/ 40	10865	358	145	38	-21	17	-7	22	-10	17	-3
4/ 30	10865	65	61	29	16	11	-6	24	1	45	29
5/ 32	10865	161	84	40	-7	20	-13	27	-10	37	10
6/ 34	10865	221	90	32	-13	17	-6	22	-6	23	5
7/ 36	10865	160	82	42	-5	20	-9	28	-7	40	12
Composite error				36	16	17	8	24	8	30	13

Site: ALBANY Coefficients: PHOENIX

-----f12.albusa-----
Tue Jan 26 17:31:55 EST 1988

#/Code	Cases	Avg-G	Avg-D	--ISO-- RMS	MBE	-PEREZ- RMS	MBE	--HAY-- RMS	MBE	-KLUCH- RMS	MBE
1/ 38	10865	384	160	28	-18	10	-2	17	-8	13	-2
2/ 39	10865	379	157	36	-23	13	-4	22	-12	16	-6
3/ 40	10865	358	145	38	-21	13	-2	22	-10	17	-3
4/ 30	10865	65	61	29	16	9	-2	24	1	45	29
5/ 32	10865	161	84	40	-7	16	-7	27	-10	37	10
6/ 34	10865	221	90	32	-13	16	0	22	-6	23	5
7/ 36	10865	160	82	42	-5	17	-4	28	-7	40	12
Composite error				36	16	14	4	24	8	30	13

Site: ALBANY Coefficients: USA COMPOSITE

-----f12.albtc-----
Tue Jan 26 17:35:47 EST 1988

#/Code	Cases	Avg-G	Avg-D	--ISO-- RMS	MBE	-PEREZ- RMS	MBE	--HAY-- RMS	MBE	-KLUCH- RMS	MBE
1/ 38	10865	384	160	28	-18	12	3	17	-8	13	-2
2/ 39	10865	379	157	36	-23	12	2	22	-12	16	-6
3/ 40	10865	358	145	38	-21	15	6	22	-10	17	-3
4/ 30	10865	65	61	29	16	9	1	24	1	45	29
5/ 32	10865	161	84	40	-7	14	-2	27	-10	37	10
6/ 34	10865	221	90	32	-13	20	8	22	-6	23	5
7/ 36	10865	160	82	42	-5	17	2	28	-7	40	12
Composite error				36	16	15	4	24	8	30	13

Site: ALBANY Coefficients: FRENCH COMPOSITE

-----f12.alball-----
Tue Jan 26 17:39:39 EST 1988

#/Code	Cases	Avg-G	Avg-D	--ISO-- RMS	MBE	-PEREZ- RMS	MBE	--HAY-- RMS	MBE	-KLUCH- RMS	MBE
1/ 38	10865	384	160	28	-18	10	0	17	-8	13	-2
2/ 39	10865	379	157	36	-23	12	-2	22	-12	16	-6
3/ 40	10865	358	145	38	-21	13	1	22	-10	17	-3
4/ 30	10865	65	61	29	16	9	-0	24	1	45	29
5/ 32	10865	161	84	40	-7	15	-5	27	-10	37	10
6/ 34	10865	221	90	32	-13	17	3	22	-6	23	5
7/ 36	10865	160	82	42	-5	16	-2	28	-7	40	12
Composite error				36	16	13	2	24	8	30	13

Site: ALBANY Coefficients: ALL SITES COMPOSITE

-----f12.albalb-----
Tue Jan 26 17:28:01 EST 1988

#/Code	Cases	Avg-G	Avg-D	--ISO-- RMS	MBE	-PEREZ- RMS	MBE	--HAY-- RMS	MBE	-KLUCH- RMS	MBE
1/ 38	10865	384	160	28	-18	10	-0	17	-8	13	-2
2/ 39	10865	379	157	36	-23	12	-2	22	-12	16	-6
3/ 40	10865	358	145	38	-21	13	1	22	-10	17	-3
4/ 30	10865	65	61	29	16	9	1	24	1	45	29
5/ 32	10865	161	84	40	-7	14	-4	27	-10	37	10
6/ 34	10865	221	90	32	-13	16	3	22	-6	23	5
7/ 36	10865	160	82	42	-5	16	-0	28	-7	40	12
Composite error				36	16	13	2	24	8	30	13

Site: ALBANY Coefficients: ALBANY

-----f12.usao-----
Tue Jan 26 18:01:49 EST 1988

#/Code	Cases	Avg-G	Avg-D	--ISO-- RMS	MBE	-PEREZ- RMS	MBE	--HAY-- RMS	MBE	-KLUCH- RMS	MBE
1/ 38	16741	423	152	30	-17	13	-4	17	-6	15	1
2/ 39	10865	379	157	36	-23	17	-9	22	-12	16	-6
3/ 40	10865	358	145	38	-21	17	-7	22	-10	17	-3
4/ 30	16741	64	58	31	18	11	0	24	0	48	32
5/ 32	16741	181	81	42	-6	19	-7	27	-8	41	13
6/ 34	16741	244	88	33	-12	16	-4	21	-6	26	7
7/ 36	16741	181	80	43	-5	19	-4	27	-6	42	15
Composite error				36	15	16	5	23	7	33	15

Site: USA COMPOSITE Coefficients: ALBUQUERQUE

-----f12.usal-----
Tue Jan 26 17:50:45 EST 1988

#/Code	Cases	Avg-G	Avg-D	--ISO-- RMS	MBE	-PEREZ- RMS	MBE	--HAY-- RMS	MBE	-KLUCH- RMS	MBE
1/ 38	16741	423	152	30	-17	12	-1	17	-6	15	1
2/ 39	10865	379	157	36	-23	15	-7	22	-12	16	-6
3/ 40	10865	358	145	38	-21	15	-5	22	-10	17	-3
4/ 30	16741	64	58	31	18	13	-7	24	0	48	32
5/ 32	16741	181	81	42	-6	19	-9	27	-8	41	13
6/ 34	16741	244	88	33	-12	16	-3	21	-6	26	7
7/ 36	16741	181	80	43	-5	18	-6	27	-6	42	15
Composite error				36	15	16	6	23	7	33	15

Site: USA COMPOSITE Coefficients: EL MONTE

-----f12.usak-----
Tue Jan 26 17:56:17 EST 1988

#/Code	Cases	Avg-G	Avg-D	--ISO-- RMS	MBE	-PEREZ- RMS	MBE	--HAY-- RMS	MBE	-KLUCH- RMS	MBE
1/ 38	16741	423	152	30	-17	35	-8	17	-6	15	1
2/ 39	10865	379	157	36	-23	37	-13	22	-12	16	-6
3/ 40	10865	358	145	38	-21	41	-11	22	-10	17	-3
4/ 30	16741	64	58	31	18	44	-18	24	0	48	32
5/ 32	16741	181	81	42	-6	51	-19	27	-8	41	13
6/ 34	16741	244	88	33	-12	51	-14	21	-6	26	7
7/ 36	16741	181	80	43	-5	49	-16	27	-6	42	15
Composite error				36	15	45	15	23	7	33	15

Site: USA COMPOSITE Coefficients: OSAGE

-----f12.usaf-----
Tue Jan 26 18:07:22 EST 1988

#/Code	Cases	Avg-G	Avg-D	--ISO-- RMS	MBE	-PEREZ- RMS	MBE	--HAY-- RMS	MBE	-KLUCH- RMS	MBE
1/ 38	16741	423	152	30	-17	15	-0	17	-6	15	1
2/ 39	10865	379	157	36	-23	17	-6	22	-12	16	-6
3/ 40	10865	358	145	38	-21	17	-3	22	-10	17	-3
4/ 30	16741	64	58	31	18	11	-0	24	0	48	32
5/ 32	16741	181	81	42	-6	18	-4	27	-8	41	13
6/ 34	16741	244	88	33	-12	19	1	21	-6	26	7
7/ 36	16741	181	80	43	-5	19	-1	27	-6	42	15
Composite error				36	15	17	3	23	7	33	15

Site: USA COMPOSITE Coefficients: CAPE CANAVERAL

-----f12.usasnl-----
Tue Jan 26 18:12:54 EST 1988

#/Code	Cases	Avg-G	Avg-D	--ISO-- RMS	MBE	-PEREZ- RMS	MBE	--HAY-- RMS	MBE	-KLUCH- RMS	MBE
1/ 38	16741	423	152	30	-17	12	-2	17	-6	15	1
2/ 39	10865	379	157	36	-23	15	-8	22	-12	16	-6
3/ 40	10865	358	145	38	-21	16	-5	22	-10	17	-3
4/ 30	16741	64	58	31	18	11	-4	24	0	48	32
5/ 32	16741	181	81	42	-6	18	-8	27	-8	41	13
6/ 34	16741	244	88	33	-12	16	-4	21	-6	26	7
7/ 36	16741	181	80	43	-5	18	-6	27	-6	42	15
Composite error				36	15	15	5	23	7	33	15

Site: USA COMPOSITE Coefficients: SANDIA COMPOSITE

-----f12.usap-----
Tue Jan 26 17:45:12 EST 1988

#/Code	Cases	Avg-G	Avg-D	--ISO-- RMS	MBE	-PEREZ- RMS	MBE	--HAY-- RMS	MBE	-KLUCH- RMS	MBE
1/ 38	16741	423	152	30	-17	13	-4	17	-6	15	1
2/ 39	10865	379	157	36	-23	16	-9	22	-12	16	-6
3/ 40	10865	358	145	38	-21	17	-7	22	-10	17	-3
4/ 30	16741	64	58	31	18	11	-4	24	0	48	32
5/ 32	16741	181	81	42	-6	19	-9	27	-8	41	13
6/ 34	16741	244	88	33	-12	16	-5	21	-6	26	7
7/ 36	16741	181	80	43	-5	18	-7	27	-6	42	15
Composite error				36	15	16	7	23	7	33	15

Site: USA COMPOSITE Coefficients: PHOENIX

-----f12.usausa-----
Tue Jan 26 18:23:59 EST 1988

#/Code	Cases	Avg-G	Avg-D	--ISO-- RMS	MBE	-PEREZ- RMS	MBE	--HAY-- RMS	MBE	-KLUCH- RMS	MBE
1/ 38	16741	423	152	30	-17	12	1	17	-6	15	1
2/ 39	10865	379	157	36	-23	13	-4	22	-12	16	-6
3/ 40	10865	358	145	38	-21	13	-2	22	-10	17	-3
4/ 30	16741	64	58	31	18	11	1	24	0	48	32
5/ 32	16741	181	81	42	-6	16	-3	27	-8	41	13
6/ 34	16741	244	88	33	-12	15	1	21	-6	26	7
7/ 36	16741	181	80	43	-5	17	-0	27	-6	42	15
Composite error				36	15	14	2	23	7	33	15

Site: USA COMPOSITE Coefficients: USA COMPOSITE

-----f12.usatc-----
Tue Jan 26 18:29:31 EST 1988

#/Code	Cases	Avg-G	Avg-D	--ISO-- RMS	MBE	-PEREZ- RMS	MBE	--HAY-- RMS	MBE	-KLUCH- RMS	MBE
1/ 38	16741	423	152	30	-17	15	7	17	-6	15	1
2/ 39	10865	379	157	36	-23	12	2	22	-12	16	-6
3/ 40	10865	358	145	38	-21	15	6	22	-10	17	-3
4/ 30	16741	64	58	31	18	12	5	24	0	48	32
5/ 32	16741	181	81	42	-6	16	3	27	-8	41	13
6/ 34	16741	244	88	33	-12	20	10	21	-6	26	7
7/ 36	16741	181	80	43	-5	18	5	27	-6	42	15
Composite error				36	15	16	6	23	7	33	15

Site: USA COMPOSITE Coefficients: FRENCH COMPOSITE

-----f12.usaall-----
Tue Jan 26 18:35:03 EST 1988

#/Code	Cases	Avg-G	Avg-D	--ISO-- RMS	MBE	-PEREZ- RMS	MBE	--HAY-- RMS	MBE	-KLUCH- RMS	MBE
1/ 38	16741	423	152	30	-17	13	3	17	-6	15	1
2/ 39	10865	379	157	36	-23	12	-2	22	-12	16	-6
3/ 40	10865	358	145	38	-21	13	1	22	-10	17	-3
4/ 30	16741	64	58	31	18	11	2	24	0	48	32
5/ 32	16741	181	81	42	-6	16	-1	27	-8	41	13
6/ 34	16741	244	88	33	-12	16	4	21	-6	26	7
7/ 36	16741	181	80	43	-5	17	2	27	-6	42	15
Composite error				36	15	14	3	23	7	33	15

Site: USA COMPOSITE Coefficients: ALL SITES COMPOSITE

-----f12.usaalb-----
Tue Jan 26 18:18:26 EST 1988

#/Code	Cases	Avg-G	Avg-D	--ISO-- RMS	MBE	-PEREZ- RMS	MBE	--HAY-- RMS	MBE	-KLUCH- RMS	MBE
1/ 38	16741	423	152	30	-17	13	3	17	-6	15	1
2/ 39	10865	379	157	36	-23	12	-2	22	-12	16	-6
3/ 40	10865	358	145	38	-21	13	1	22	-10	17	-3
4/ 30	16741	64	58	31	18	12	4	24	0	48	32
5/ 32	16741	181	81	42	-6	16	1	27	-8	41	13
6/ 34	16741	244	88	33	-12	16	5	21	-6	26	7
7/ 36	16741	181	80	43	-5	17	3	27	-6	42	15
Composite error				36	15	14	3	23	7	33	15

Site: USA COMPOSITE Coefficients: ALBANY

-----f12.tco-----
Tue Jan 26 18:47:42 EST 1988

#/Code	Cases	Avg-G	Avg-D	--ISO-- RMS	--ISO-- MBE	-PEREZ- RMS	-PEREZ- MBE	--HAY-- RMS	--HAY-- MBE	-KLUCH- RMS	-KLUCH- MBE
1/ 38	11222	379	164	46	-31	23	-15	28	-19	23	-12
2/ 30	11222	64	59	33	19	12	1	24	3	49	33
3/ 32	11222	171	88	44	-11	21	-11	31	-11	39	8
4/ 34	11222	234	103	45	-25	23	-14	29	-16	27	-5
5/ 36	11222	169	86	42	-8	18	-7	29	-8	39	11
Composite error				43	21	20	11	28	13	37	17

Site: FRENCH COMPOSITE Coefficients: ALBUQUERQUE

-----f12.tcl-----
Tue Jan 26 18:41:23 EST 1988

#/Code	Cases	Avg-G	Avg-D	--ISO-- RMS	--ISO-- MBE	-PEREZ- RMS	-PEREZ- MBE	--HAY-- RMS	--HAY-- MBE	-KLUCH- RMS	-KLUCH- MBE
1/ 38	11222	379	164	46	-31	19	-12	28	-19	23	-12
2/ 30	11222	64	59	33	19	13	-5	24	3	49	33
3/ 32	11222	171	88	44	-11	23	-12	31	-11	39	8
4/ 34	11222	234	103	45	-25	21	-12	29	-16	27	-5
5/ 36	11222	169	86	42	-8	20	-9	29	-8	39	11
Composite error				43	21	20	11	28	13	37	17

Site: FRENCH COMPOSITE Coefficients: EL MONTE

-----f12.tck-----
Tue Jan 26 18:44:32 EST 1988

#/Code	Cases	Avg-G	Avg-D	--ISO-- RMS	MBE	-PEREZ- RMS	MBE	--HAY-- RMS	MBE	-KLUCH- RMS	MBE
1/ 38	11222	379	164	46	-31	33	-14	28	-19	23	-12
2/ 30	11222	64	59	33	19	32	-11	24	3	49	33
3/ 32	11222	171	88	44	-11	41	-16	31	-11	39	8
4/ 34	11222	234	103	45	-25	41	-16	29	-16	27	-5
5/ 36	11222	169	86	42	-8	39	-12	29	-8	39	11
Composite error				43	21	37	14	28	13	37	17

Site: FRENCH COMPOSITE Coefficients: OSAGE

-----f12.tcf-----
Tue Jan 26 18:50:52 EST 1988

#/Code	Cases	Avg-G	Avg-D	--ISO-- RMS	MBE	-PEREZ- RMS	MBE	--HAY-- RMS	MBE	-KLUCH- RMS	MBE
1/ 38	11222	379	164	46	-31	21	-12	28	-19	23	-12
2/ 30	11222	64	59	33	19	11	-0	24	3	49	33
3/ 32	11222	171	88	44	-11	22	-9	31	-11	39	8
4/ 34	11222	234	103	45	-25	22	-10	29	-16	27	-5
5/ 36	11222	169	86	42	-8	19	-5	29	-8	39	11
Composite error				43	21	19	8	28	13	37	17

Site: FRENCH CONDOSITE Coefficients: CAPE CANAVERAL

-----f12.tcsnl-----
Tue Jan 26 18:54:02 EST 1988

#/Code	Cases	Avg-G	Avg-D	--ISO-- RMS	MBE	-PEREZ- RMS	MBE	--HAY-- RMS	MBE	-KLUCH- RMS	MBE
1/ 38	11222	379	164	46	-31	21	-13	28	-19	23	-12
2/ 30	11222	64	59	33	19	11	-3	24	3	49	33
3/ 32	11222	171	88	44	-11	22	-12	31	-11	39	8
4/ 34	11222	234	103	45	-25	22	-13	29	-16	27	-5
5/ 36	11222	169	86	42	-8	18	-8	29	-8	39	11
Composite error				43	21	19	11	28	13	37	17

Site: FRENCH COMPOSITE Coefficients: SANDIA COMPOSITE

-----f12.tcp-----
Tue Jan 26 18:38:13 EST 1988

#/Code	Cases	Avg-G	Avg-D	--ISO-- RMS	MBE	-PEREZ- RMS	MBE	--HAY-- RMS	MBE	-KLUCH- RMS	MBE
1/ 38	11222	379	164	46	-31	22	-15	28	-19	23	-12
2/ 30	11222	64	59	33	19	12	-3	24	3	49	33
3/ 32	11222	171	88	44	-11	23	-13	31	-11	39	8
4/ 34	11222	234	103	45	-25	24	-15	29	-16	27	-5
5/ 36	11222	169	86	42	-8	19	-9	29	-8	39	11
Composite error				43	21	20	12	28	13	37	17

Site: FRENCH COMPOSITE Coefficients: PHOENIX

-----f12.tcusa-----
Tue Jan 26 19:00:22 EST 1988

#/Code	Cases	Avg-G	Avg-D	--ISO-- RMS	MBE	-PEREZ- RMS	MBE	--HAY-- RMS	MBE	-KLUCH- RMS	MBE
1/ 38	11222	379	164	46	-31	18	-10	28	-19	23	-12
2/ 30	11222	64	59	33	19	11	2	24	3	49	33
3/ 32	11222	171	88	44	-11	19	-7	31	-11	39	8
4/ 34	11222	234	103	45	-25	18	-8	29	-16	27	-5
5/ 36	11222	169	86	42	-8	17	-3	29	-8	39	11
Composite error				43	21	17	7	28	13	37	17

Site: FRENCH COMPOSITE Coefficients: USA COMPOSITE

-----f12.tctc-----
Tue Jan 26 19:03:32 EST 1988

#/Code	Cases	Avg-G	Avg-D	--ISO-- RMS	MBE	-PEREZ- RMS	MBE	--HAY-- RMS	MBE	-KLUCH- RMS	MBE
1/ 38	11222	379	164	46	-31	14	-3	28	-19	23	-12
2/ 30	11222	64	59	33	19	12	5	24	3	49	33
3/ 32	11222	171	88	44	-11	17	-1	31	-11	39	8
4/ 34	11222	234	103	45	-25	16	-0	29	-16	27	-5
5/ 36	11222	169	86	42	-8	17	2	29	-8	39	11
Composite error				43	21	15	3	28	13	37	17

Site: FRENCH COMPOSITE Coefficients: FRENCH COMPOSITE

-----f12.tcall-----
Tue Jan 26 19:06:43 EST 1988

#/Code	Cases	Avg-G	Avg-D	--ISO-- RMS	MBE	-PEREZ- RMS	MBE	--HAY-- RMS	MBE	-KLUCH- RMS	MBE
1/ 38	11222	379	164	46	-31	16	-7	28	-19	23	-12
2/ 30	11222	64	59	33	19	12	3	24	3	49	33
3/ 32	11222	171	88	44	-11	18	-4	31	-11	39	8
4/ 34	11222	234	103	45	-25	17	-5	29	-16	27	-5
5/ 36	11222	169	86	42	-8	16	-1	29	-8	39	11
Composite error				43	21	16	5	28	13	37	17

Site: FRENCH COMPOSITE Coefficients: ALL SITES COMPOSITE

-----f12.tcalb-----
Tue Jan 26 18:57:12 EST 1988

#/Code	Cases	Avg-G	Avg-D	--ISO-- RMS	MBE	-PEREZ- RMS	MBE	--HAY-- RMS	MBE	-KLUCH- RMS	MBE
1/ 38	11222	379	164	46	-31	17	-8	28	-19	23	-12
2/ 30	11222	64	59	33	19	13	5	24	3	49	33
3/ 32	11222	171	88	44	-11	18	-4	31	-11	39	8
4/ 34	11222	234	103	45	-25	17	-5	29	-16	27	-5
5/ 36	11222	169	86	42	-8	16	0	29	-8	39	11
Composite error				43	21	16	5	28	13	37	17

Site: FRENCH COMPOSITE Coefficients: ALBANY

-----f12.allo-----
Tue Jan 26 19:41:52 EST 1988

#/Code	Cases	Avg-G	Avg-D	--ISO-- RMS	MBE	-PEREZ- RMS	MBE	--HAY-- RMS	MBE	-KLUCH- RMS	MBE
1/ 38	16741	423	152	30	-17	13	-4	17	-6	15	1
2/ 30	27963	64	58	32	18	11	1	24	1	48	33
3/ 32	27963	177	84	43	-8	20	-8	29	-9	40	11
4/ 34	27963	240	94	38	-17	19	-8	25	-10	27	2
5/ 36	27963	176	82	43	-6	19	-5	28	-7	41	13
6/ 39	10885	378	156	36	-23	17	-9	22	-12	16	-6
7/ 40	10865	358	145	38	-21	17	-7	22	-10	17	-3
Composite error				38	15	17	6	25	8	35	16

Site: ALL SITES COMPOSITE Coefficients: ALBUQUERQUE

-----f12.alll-----
Tue Jan 26 19:24:18 EST 1988

#/Code	Cases	Avg-G	Avg-D	--ISO-- RMS	MBE	-PEREZ- RMS	MBE	--HAY-- RMS	MBE	-KLUCH- RMS	MBE
1/ 38	16741	423	152	30	-17	12	-1	17	-6	15	1
2/ 30	27963	64	58	32	18	13	-6	24	1	48	33
3/ 32	27963	177	84	43	-8	21	-10	29	-9	40	11
4/ 34	27963	240	94	38	-17	18	-7	25	-10	27	2
5/ 36	27963	176	82	43	-6	19	-7	28	-7	41	13
6/ 39	10885	378	156	36	-23	15	-7	22	-12	16	-6
7/ 40	10865	358	145	38	-21	15	-5	22	-10	17	-3
Composite error				38	15	17	7	25	8	35	16

Site: ALL SITES COMPOSITE Coefficients: EL MONTE

-----f12.allk-----
Tue Jan 26 19:33:05 EST 1988

#/Code	Cases	Avg-G	Avg-D	--ISO-- RMS	MBE	-PEREZ- RMS	MBE	--HAY-- RMS	MBE	-KLUCH- RMS	MBE
1/ 38	16741	423	152	30	-17	35	-8	17	-6	15	1
2/ 30	27963	64	58	32	18	40	-15	24	1	48	33
3/ 32	27963	177	84	43	-8	47	-17	29	-9	40	11
4/ 34	27963	240	94	38	-17	47	-14	25	-10	27	2
5/ 36	27963	176	82	43	-6	45	-14	28	-7	41	13
6/ 39	10885	378	156	36	-23	37	-13	22	-12	16	-6
7/ 40	10865	358	145	38	-21	41	-11	22	-10	17	-3
Composite error				38	15	43	14	25	8	35	16

Site: ALL SITES COMPOSITE Coefficients: OSAGE

-----f12.allf-----
Tue Jan 26 19:50:40 EST 1988

#/Code	Cases	Avg-G	Avg-D	--ISO-- RMS	MBE	-PEREZ- RMS	MBE	--HAY-- RMS	MBE	-KLUCH- RMS	MBE
1/ 38	16741	423	152	30	-17	15	-0	17	-6	15	1
2/ 30	27963	64	58	32	18	11	-0	24	1	48	33
3/ 32	27963	177	84	43	-8	20	-6	29	-9	40	11
4/ 34	27963	240	94	38	-17	20	-4	25	-10	27	2
5/ 36	27963	176	82	43	-6	19	-3	28	-7	41	13
6/ 39	10885	378	156	36	-23	17	-6	22	-12	16	-6
7/ 40	10865	358	145	38	-21	17	-3	22	-10	17	-3
Composite error				38	15	17	4	25	8	35	16

Site: ALL SITES COMPOSITE Coefficients: CAPE CANAVERAL

-----f12.allsnl-----
Tue Jan 26 19:59:27 EST 1988

#/Code	Cases	Avg-G	Avg-D	--ISO-- RMS	MBE	-PEREZ- RMS	MBE	--HAY-- RMS	MBE	-KLUCH- RMS	MBE
1/ 38	16741	423	152	30	-17	12	-2	17	-6	15	1
2/ 30	27963	64	58	32	18	11	-4	24	1	48	33
3/ 32	27963	177	84	43	-8	20	-10	29	-9	40	11
4/ 34	27963	240	94	38	-17	18	-7	25	-10	27	2
5/ 36	27963	176	82	43	-6	18	-7	28	-7	41	13
6/ 39	10885	378	156	36	-23	15	-8	22	-12	16	-6
7/ 40	10865	358	145	38	-21	16	-5	22	-10	17	-3
Composite error				38	15	17	7	25	8	35	16

Site: ALL SITES COMPOSITE Coefficients: SANDIA COMPOSITE

-----f12.allp-----
Tue Jan 26 19:15:30 EST 1988

#/Code	Cases	Avg-G	Avg-D	--ISO-- RMS	MBE	-PEREZ- RMS	MBE	--HAY-- RMS	MBE	-KLUCH- RMS	MBE
1/ 38	16741	423	152	30	-17	13	-4	17	-6	15	1
2/ 30	27963	64	58	32	18	12	-4	24	1	48	33
3/ 32	27963	177	84	43	-8	21	-11	29	-9	40	11
4/ 34	27963	240	94	38	-17	19	-9	25	-10	27	2
5/ 36	27963	176	82	43	-6	19	-8	28	-7	41	13
6/ 39	10885	378	156	36	-23	16	-9	22	-12	16	-6
7/ 40	10865	358	145	38	-21	17	-7	22	-10	17	-3
Composite error				38	15	17	8	25	8	35	16

Site: ALL SITES COMPOSITE Coefficients: PHOENIX

-----f12.allusa-----
Tue Jan 26 20:17:02 EST 1988

#/Code	Cases	Avg-G	Avg-D	--ISO-- RMS	MBE	-PEREZ- RMS	MBE	--HAY-- RMS	MBE	-KLUCH- RMS	MBE
1/ 38	16741	423	152	30	-17	12	1	17	-6	15	1
2/ 30	27963	64	58	32	18	11	1	24	1	48	33
3/ 32	27963	177	84	43	-8	17	-5	29	-9	40	11
4/ 34	27963	240	94	38	-17	16	-2	25	-10	27	2
5/ 36	27963	176	82	43	-6	17	-1	28	-7	41	13
6/ 39	10885	378	156	36	-23	13	-4	22	-12	16	-6
7/ 40	10865	358	145	38	-21	13	-2	22	-10	17	-3
Composite error				38	15	15	3	25	8	35	16

Site: ALL SITES COMPOSITE Coefficients: USA COMPOSITE

-----f12.alltc-----
Tue Jan 26 20:25:57 EST 1988

#/Code	Cases	Avg-G	Avg-D	--ISO-- RMS	MBE	-PEREZ- RMS	MBE	--HAY-- RMS	MBE	-KLUCH- RMS	MBE
1/ 38	16741	423	152	30	-17	15	7	17	-6	15	1
2/ 30	27963	64	58	32	18	12	5	24	1	48	33
3/ 32	27963	177	84	43	-8	17	1	29	-9	40	11
4/ 34	27963	240	94	38	-17	18	6	25	-10	27	2
5/ 36	27963	176	82	43	-6	18	4	28	-7	41	13
6/ 39	10885	378	156	36	-23	12	2	22	-12	16	-6
7/ 40	10865	358	145	38	-21	15	6	22	-10	17	-3
Composite error				38	15	16	5	25	8	35	16

Site: ALL SITES COMPOSITE Coefficients: FRENCH COMPOSITE

-----f12.allall-----
Tue Jan 26 20:34:45 EST 1988

#/Code	Cases	Avg-G	Avg-D	--ISO-- RMS	MBE	-PEREZ- RMS	MBE	--HAY-- RMS	MBE	-KLUCH- RMS	MBE
1/ 38	16741	423	152	30	-17	13	3	17	-6	15	1
2/ 30	27963	64	58	32	18	11	3	24	1	48	33
3/ 32	27963	177	84	43	-8	17	-2	29	-9	40	11
4/ 34	27963	240	94	38	-17	16	1	25	-10	27	2
5/ 36	27963	176	82	43	-6	17	1	28	-7	41	13
6/ 39	10885	378	156	36	-23	12	-2	22	-12	16	-6
7/ 40	10865	358	145	38	-21	13	1	22	-10	17	-3
Composite error				38	15	15	2	25	8	35	16

Site: ALL SITES COMPOSITE Coefficients: ALL SITES COMPOSITE

-----f12.allalb-----
Tue Jan 26 20:08:15 EST 1988

#/Code	Cases	Avg-G	Avg-D	--ISO-- RMS	MBE	-PEREZ- RMS	MBE	--HAY-- RMS	MBE	-KLUCH- RMS	MBE
1/ 38	16741	423	152	30	-17	13	3	17	-6	15	1
2/ 30	27963	64	58	32	18	12	5	24	1	48	33
3/ 32	27963	177	84	43	-8	17	-1	29	-9	40	11
4/ 34	27963	240	94	38	-17	16	1	25	-10	27	2
5/ 36	27963	176	82	43	-6	17	2	28	-7	41	13
6/ 39	10885	378	156	36	-23	12	-2	22	-12	16	-6
7/ 40	10865	358	145	38	-21	13	1	22	-10	17	-3
Composite error				38	15	15	3	25	8	35	16

Site: ALL SITES COMPOSITE Coefficients: ALBANY

APPENDIX B: COMPLEMENTARY RESULTS

This appendix presents the results of the analysis of data recorded at the Cape Canaveral site between 7/17/87 and 11/15/87. This had to be delayed because of still pending data acquisition/processing questions at reporting time. These were addressed and answered satisfactorily.

Results presented include a cross-validation of data sets and models derived respectively from (1) the pre-7/17 Cape Canaveral data set - FSE.A -, (2) the post-7/17 Cape Canaveral data set - FSE.B -, (3) the complete Cape Canaveral data set - FSE.ALL - and, (3) the SNLA data set as defined in the main report.

Validation summaries are presented on pages B-2 to B-5. Presentation format is identical to that of appendix A. Results are further summarized in the table below which includes composite root mean square errors for each test performed.

MODEL Coefficients	FSE-B	FSE-A	PEREZ FSE-ALL	PEREZ SNLA	HAY -	ISO -	KLU -
TEST DATA SET	S45, S, N, W Composite RMS Error (W/Sq.m)						
FSE-B	13	14	13	15	23	34	45
FSE-A	14	13	13	14	23	34	37
FSE-ALL	13	14	13	14	23	34	41
SNLA	16	16	16	13	23	38	41

These complementary results are consistent with those presented in the main report and therefore further validate the conclusions and recommendations of this study.

-----f12.ab-----
Wed Feb 3 11:23:24 EST 1988

#/Code	Cases	Avg-G	Avg-D	--ISO-- RMS	MBE	-PEREZ- RMS	MBE	--HAY-- RMS	MBE	-KLUCH- RMS	MBE
1/ 38	539	445	150	31	-15	14	1	17	-6	17	3
2/ 30	539	64	60	33	19	12	0	25	-2	51	37
3/ 32	539	224	91	54	-12	22	-4	36	-14	49	12
4/ 34	539	232	92	30	-13	13	-5	22	-12	25	8
5/ 36	539	167	77	40	2	16	5	26	-1	45	26
Composite error				39	14	16	4	26	9	40	21

Site: FSE.A Coefficients: FSE.B

-----f12.aa-----
Wed Feb 3 11:23:35 EST 1988

#/Code	Cases	Avg-G	Avg-D	--ISO-- RMS	MBE	-PEREZ- RMS	MBE	--HAY-- RMS	MBE	-KLUCH- RMS	MBE
1/ 38	539	445	150	31	-15	13	3	17	-6	17	3
2/ 30	539	64	60	33	19	13	-2	25	-2	51	37
3/ 32	539	224	91	54	-12	20	-4	36	-14	49	12
4/ 34	539	232	92	30	-13	11	-4	22	-12	25	8
5/ 36	539	167	77	40	2	15	4	26	-1	45	26
Composite error				39	14	15	3	26	9	40	21

Site: FSE.A Coefficients: FSE.A

-----f12.asnl-----
Wed Feb 3 11:23:56 EST 1988

#/Code	Cases	Avg-G	Avg-D	--ISO-- RMS	MBE	-PEREZ- RMS	MBE	--HAY-- RMS	MBE	-KLUCH- RMS	MBE
1/ 38	539	445	150	31	-15	14	0	17	-6	17	3
2/ 30	539	64	60	33	19	13	-4	25	-2	51	37
3/ 32	539	224	91	54	-12	24	-8	36	-14	49	12
4/ 34	539	232	92	30	-13	14	-7	22	-12	25	8
5/ 36	539	167	77	40	2	15	1	26	-1	45	26
Composite error				39	14	16	5	26	9	40	21

Site: FSE.A Coefficients: SANDIA COMPOSITE

-----f12.af-----
Wed Feb 3 11:23:45 EST 1988

#/Code	Cases	Avg-G	Avg-D	--ISO-- RMS	MBE	-PEREZ- RMS	MBE	--HAY-- RMS	MBE	-KLUCH- RMS	MBE
1/ 38	539	445	150	31	-15	14	2	17	-6	17	3
2/ 30	539	64	60	33	19	12	-1	25	-2	51	37
3/ 32	539	224	91	54	-12	21	-4	36	-14	49	12
4/ 34	539	232	92	30	-13	12	-4	22	-12	25	8
5/ 36	539	167	77	40	2	15	4	26	-1	45	26
Composite error				39	14	15	3	26	9	40	21

Site: FSE.A Coefficients: FSE.ALL

-----f12.bb-----
Wed Feb 3 11:22:41 EST 1988

#/Code	Cases	Avg-G	Avg-D	--ISO-- RMS	MBE	-PEREZ- RMS	MBE	--HAY-- RMS	MBE	-KLUCH- RMS	MBE
1/ 38	551	398	152	20	-1	12	4	13	-1	21	13
2/ 30	551	84	69	39	20	13	-3	30	-3	59	40
3/ 32	551	259	99	60	-10	24	-5	39	-11	58	17
4/ 34	551	150	85	22	3	11	-6	21	-9	36	24
5/ 36	551	173	86	46	3	14	4	26	-2	53	29
Composite error				40	10	16	4	27	7	48	26

Site: FSE.B Coefficients: FSE.B

-----f12.ba-----
Wed Feb 3 11:22:52 EST 1988

#/Code	Cases	Avg-G	Avg-D	--ISO-- RMS	MBE	-PEREZ- RMS	MBE	--HAY-- RMS	MBE	-KLUCH- RMS	MBE
1/ 38	551	398	152	20	-1	14	6	13	-1	21	13
2/ 30	551	84	69	39	20	15	-5	30	-3	59	40
3/ 32	551	259	99	60	-10	22	-4	39	-11	58	17
4/ 34	551	150	85	22	3	12	-6	21	-9	36	24
5/ 36	551	173	86	46	3	16	3	26	-2	53	29
Composite error				40	10	16	5	27	7	48	26

Site: FSE.B Coefficients: FSE.A

-----f12.bsnl-----
Wed Feb 3 11:23:14 EST 1988

#/Code	Cases	Avg-G	Avg-D	--ISO-- RMS	MBE	-PEREZ- RMS	MBE	--HAY-- RMS	MBE	-KLUCH- RMS	MBE
1/ 38	551	398	152	20	-1	13	4	13	-1	21	13
2/ 30	551	84	69	39	20	16	-7	30	-3	59	40
3/ 32	551	259	99	60	-10	25	-8	39	-11	58	17
4/ 34	551	150	85	22	3	13	-8	21	-9	36	24
5/ 36	551	173	86	46	3	16	1	26	-2	53	29
Composite error				40	10	17	6	27	7	48	26

Site: FSE.B Coefficients: SANDIA COMPOSITE

-----f12.bf-----
Wed Feb 3 11:23:03 EST 1988

#/Code	Cases	Avg-G	Avg-D	--ISO-- RMS	MBE	-PEREZ- RMS	MBE	--HAY-- RMS	MBE	-KLUCH- RMS	MBE
1/ 38	551	398	152	20	-1	13	5	13	-1	21	13
2/ 30	551	84	69	39	20	14	-3	30	-3	59	40
3/ 32	551	259	99	60	-10	23	-4	39	-11	58	17
4/ 34	551	150	85	22	3	11	-5	21	-9	36	24
5/ 36	551	173	86	46	3	15	3	26	-2	53	29
Composite error				40	10	16	4	27	7	48	26

Site: FSE.B Coefficients: FSE.ALL

-----f12.fb-----
Wed Feb 3 11:24:15 EST 1988

#/Code	Cases	Avg-G	Avg-D	--ISO-- RMS	MBE	-PEREZ- RMS	MBE	--HAY-- RMS	MBE	-KLUCH- RMS	MBE
1/ 38	1090	421	151	26	-8	13	2	15	-3	19	8
2/ 30	1090	74	64	36	20	13	-1	28	-3	55	39
3/ 32	1090	242	95	57	-11	23	-5	37	-12	54	14
4/ 34	1090	191	88	26	-4	12	-5	22	-11	31	16
5/ 36	1090	170	81	43	3	15	4	26	-1	49	28
Composite error				40	11	16	4	27	8	44	24

Site: FSE.ALL Coefficients: FSE.B

-----f12.fa-----
Wed Feb 3 11:24:35 EST 1988

#/Code	Cases	Avg-G	Avg-D	--ISO-- RMS	MBE	-PEREZ- RMS	MBE	--HAY-- RMS	MBE	-KLUCH- RMS	MBE
1/ 38	1090	421	151	26	-8	14	5	15	-3	19	8
2/ 30	1090	74	64	36	20	14	-3	28	-3	55	39
3/ 32	1090	242	95	57	-11	21	-4	37	-12	54	14
4/ 34	1090	191	88	26	-4	12	-5	22	-11	31	16
5/ 36	1090	170	81	43	3	16	3	26	-1	49	28
Composite error				40	11	16	4	27	8	44	24

Site: FSE.ALL Coefficients: FSE.A

-----f12.fsnl-----
Wed Feb 3 11:25:14 EST 1988

#/Code	Cases	Avg-G	Avg-D	--ISO-- RMS	--ISO-- MBE	-PEREZ- RMS	-PEREZ- MBE	--HAY-- RMS	--HAY-- MBE	-KLUCH- RMS	-KLUCH- MBE
1/ 38	1090	421	151	26	-8	13	2	15	-3	19	8
2/ 30	1090	74	64	36	20	14	-5	28	-3	55	39
3/ 32	1090	242	95	57	-11	25	-8	37	-12	54	14
4/ 34	1090	191	88	26	-4	13	-8	22	-11	31	16
5/ 36	1090	170	81	43	3	15	1	26	-1	49	28
Composite error				40	11	17	6	27	8	44	24

Site: FSE.ALL Coefficients: SANDIA COMPOSITE

-----f12.ff-----
Wed Feb 3 11:24:54 EST 1988

#/Code	Cases	Avg-G	Avg-D	--ISO-- RMS	--ISO-- MBE	-PEREZ- RMS	-PEREZ- MBE	--HAY-- RMS	--HAY-- MBE	-KLUCH- RMS	-KLUCH- MBE
1/ 38	1090	421	151	26	-8	13	4	15	-3	19	8
2/ 30	1090	74	64	36	20	13	-2	28	-3	55	39
3/ 32	1090	242	95	57	-11	22	-4	37	-12	54	14
4/ 34	1090	191	88	26	-4	11	-5	22	-11	31	16
5/ 36	1090	170	81	43	3	15	4	26	-1	49	28
Composite error				40	11	15	4	27	8	44	24

Site: FSE.ALL Coefficients: FSE.ALL

-----f12.snlb-----
Wed Feb 3 11:27:04 EST 1988

#/Code	Cases	Avg-G	Avg-D	--ISO-- RMS	MBE	-PEREZ- RMS	MBE	--HAY-- RMS	MBE	-KLUCH- RMS	MBE
1/ 38	6415	491	139	31	-15	16	5	16	-2	18	6
2/ 30	6415	62	52	34	21	12	5	24	-1	53	38
3/ 32	6415	219	77	45	-4	20	3	28	-6	46	19
4/ 34	6415	281	84	34	-11	17	3	19	-6	31	11
5/ 36	6415	216	76	44	-4	19	5	25	-4	46	20
Composite error				38	13	17	4	23	4	41	22

Site: SANDIA COMPOSITE Coefficients: FSE.B

-----f12.snla-----
Wed Feb 3 11:28:53 EST 1988

#/Code	Cases	Avg-G	Avg-D	--ISO-- RMS	MBE	-PEREZ- RMS	MBE	--HAY-- RMS	MBE	-KLUCH- RMS	MBE
1/ 38	6415	491	139	31	-15	16	7	16	-2	18	6
2/ 30	6415	62	52	34	21	13	3	24	-1	53	38
3/ 32	6415	219	77	45	-4	18	3	28	-6	46	19
4/ 34	6415	281	84	34	-11	15	3	19	-6	31	11
5/ 36	6415	216	76	44	-4	18	4	25	-4	46	20
Composite error				38	13	16	4	23	4	41	22

Site: SANDIA COMPOSITE Coefficients: FSE.A

-----f12.snlsnl-----
Wed Feb 3 11:32:35 EST 1988

#/Code	Cases	Avg-G	Avg-D	--ISO-- RMS	MBE	-PEREZ- RMS	MBE	--HAY-- RMS	MBE	-KLUCH- RMS	MBE
1/ 38	6415	491	139	31	-15	13	2	16	-2	18	6
2/ 30	6415	62	52	34	21	11	1	24	-1	53	38
3/ 32	6415	219	77	45	-4	17	-2	28	-6	46	19
4/ 34	6415	281	84	34	-11	13	-2	19	-6	31	11
5/ 36	6415	216	76	44	-4	15	0	25	-4	46	20
Composite error				38	13	14	2	23	4	41	22

Site: SANDIA COMPOSITE Coefficients: SANDIA COMPOSITE

-----f12.snlf-----
Wed Feb 3 11:30:44 EST 1988

#/Code	Cases	Avg-G	Avg-D	--ISO-- RMS	MBE	-PEREZ- RMS	MBE	--HAY-- RMS	MBE	-KLUCH- RMS	MBE
1/ 38	6415	491	139	31	-15	16	6	16	-2	18	6
2/ 30	6415	62	52	34	21	12	4	24	-1	53	38
3/ 32	6415	219	77	45	-4	19	3	28	-6	46	19
4/ 34	6415	281	84	34	-11	16	3	19	-6	31	11
5/ 36	6415	216	76	44	-4	18	5	25	-4	46	20
Composite error				38	13	16	4	23	4	41	22

Site: SANDIA COMPOSITE Coefficients: FSE.ALL

APPENDIX C: RELATED PUBLICATIONS AND REPORTS

Richard Perez

Atmospheric Sciences Research Center

Intermediate Report

to SANDIA National Laboratories

Selection of Sites for the experimental generation of Perez Model's coefficients

I. Selection Process

The site selection process is based on the following facts and findings.

a) Five sites were to be selected among a total of ten potential sites where SNL currently operates experimental photovoltaic installations.

b) Existing literature on solar climatic regionalization of the United States was reviewed and methods relevancy to the project were evaluated.

c) Climatic/geographic factors potentially relevant to the model's configuration/performance were identified and used to complement existing regionalization methods.

A) Possible sites

These include ten locations where SNL is involved in PV system testing. These locations are: (1) Washington, DC; (2) Osage, Kansas; (3) Dallas, Texas; (4) Phoenix, Arizona; (5) Hesperia, California; (6) Molokai Island, Hawaii; (7) San Diego, California; (8) Sacramento, California; (9) Cape Canaveral, Florida; and, (10) Albuquerque, New Mexico.

In addition to these sites, other National Laboratories were suggested as possible locations if environmentally justified.

B) Literature Review/Assessment

Three scientific abstract data bases were searched to scan the available literature in the field of solar climatic regionalization. These include: (1) Meteorological Abstracts; (2) Engineering Index Compendex; and, (3) Science Citation Index.

Review of literature indicate that there exists two main approaches to the generation of solar regions in a given area. The first and most historic method identifies solar regions based on their yearly global energy yield [1] or on the yield of the direct and/or diffuse components [2,3]. In this case region boundaries are represented by energy isopleths. The second approach identifies regions by similarities in temporal variations and average, maximum and minimum yield of the global component [4,5,6,7,8]. Temporal/spatial variations are studied on the scale of a month [4,5,6,8] or a day [7]. The regionalization methods used for this second approach range from sophisticated statistical techniques such as principal component [5,7,8] or harmonic analysis [4] to classifications according to yearly energy yield amplitude and phase [6].

It will be noted that other regionalization techniques which include solar radiation as only a partial input (along with heating, cooling degree days, and other meteorological and social parameters relevant to building design, e.g. [4]) have not been included in this analysis.

The following table indicates for each of the eight references cited the type of data used as input, the criteria used for region mapping and the assessed relevancy of each method to this project's concern.

Table 1

Ref.#	Type of Input Data	Classification/Mapping Method/Criteria	Assessed Relevancy to Project
1	WMO average global yearly yield	Worldwide regionalization based on yearly isopleths	Total yearly energy yield includes physical characterization of importance to the model. However, this criteria alone is very incomplete.
2	U.S. winter and summer monthly yield of global direct and diffuse radiation. (based on U.S. old radiation network data)	Maps of winter and summer global direct and diffuse isopleths	Diffuse and direct radiation yearly and seasonal yields are of direct relevancy to the model's performance since they give a more accurate estimation of average turbidity and cloudiness level than global radiation only.
3	U.S. monthly and yearly yield of global direct and diffuse radiation (based on SOLMET and ERSATZ data bases)	Monthly and yearly maps of global direct and diffuse isopleths	Same as above

4	U.S. monthly ave. of global radiation based on 222 NWS-SOLMET Station over 25 yr period	Fourrier analysis. Regionalization based on phase/amplitude of harmonics	Mean monthly global radiation temporal variance structures are probably more indicative of periodical synoptic climatological phenomena than of the quality of radiation received at the earth surface. The relevance of this study of the project may be considered marginal.
5	Same as above	Q-mode principal components analysis. Regionalization based on minimization of euclidian distances in space of components	Same comment as above. The proposed maps include 14 distinct regions in a small area of the SW U.S. and four regions within the Florida peninsula alone, while including the northern Pacific coast, the northern Rockies, most of the Great Plains, the Great Lakes, the Appalachian and North Atlantic regions in one category.

6	Yearly radiation curve for 1000 locations world-wide Source: WMO	Worldwide systematic classification based on yearly solar energy curve amplitude, maximum, minimum and phase	Same comment as above. However, the simpler and more pragmatic approach used here yields an incomplete but seemingly acceptable regionalization of the conterminous United States.
7	Daily totals of global radiation covering a period of 5 years at 60 sites	P-mode principal components analysis of stations covariance matrix, regionalization process based on similar clustering technique as Ref. #5	Although this is also a method which focuses on temporal variance structures, the use of daily input data rather than monthly averages greatly increases the relevancy of this method to the project. Indeed long term series do yield indirect information on cloudiness type and turbidity levels.
8	Monthly totals for eleven California sites (NWS). 22 years of data	P-mode principal component analysis of covariance matrix	Same as 5. Regionalization covers California only.

Based on the argumentation developed in Table 1 it was decided to select both the SERI insolation atlas (Diffuse/Direct maps), [3], and Willmott's classification, [7], as a basis for the present selection.

C) Other relevant climatic inputs

These exist four physical regional characteristics, which probably have an impact on the model's configuration and performance and which are only indirectly, if at all, accounted for by looking at direct or diffuse yield maps or at regionalizations based on time/space variability.

These factors are: (1) the site's altitude; (2) the regional albedo; (3) the site's air quality (particulate content); and, (4) the site's moisture content.

The altitude of the site may influence the level of horizon brightening during clear days since the proportion of scattered radiation (both single and multiple) originating from the top of the atmosphere decreases with altitude while that coming from high zenith angles augments.

The albedo of the surrounding region is also a factor which may influence the level of horizon brightening observed during clear days. Indeed much of this brightening effect is caused by scattered radiation reflected from the ground (retroscattering).

Pollution and moisture levels may strongly affect the intensity of forward-scattered radiation for both clear and intermediate skies.

It is of prime importance to assess if the effect of these factors may be fully explained using the existing model's sky condition parameterization method, or if this has to be expanded to include sites' altitude, albedo, pollution and/or moisture levels.

II. Proposed Sites

Based on the previous arguments and constaints the sites selected for the first

measurement phase are the following:

1) Albuquerque, NM
2) Phoenix, AZ
3) Pasadena, CA
4) Osage, KS
5) Cape Canaveral, FL

The first three sites are located in the same Wilmott's region (region 4) and the two first exhibit a similar direct/diffuse split. However, they greatly differ in terms of altitude (Albuquerque vs. Phoenix) and pollution/moisture levels (Pasadena vs. Phoenix/Albuquerque).

Osage, Kansas is located in Wilmott's northern great plains region (region 5) and is a key location to assess the extent of the validity of coefficients developed in SW U.S.

Cape Canaveral is a low albedo, high moisture content, high turbidity area and should offer maximum contrast with SW coefficients. This is located in Wilmott's region 10.

The U.S. map shown in Figure 5 superimposes the Wilmott's partition with the direct irradiance yearly yield, the main albedo regions (based on three types of dominant vegetation: forest, prairie, desert), and three altitude regions (0 to 500 m, 500 to 1500 m and 1500 m+) of the United States. Both the selected and other potential sites have been reported on this map which should summarize the main aspects of the present selection process.

References

1. Werner, J., (1982): Solartechnik in Verschiedenen Klimazonen der Welt. Sonnenenergie & Warmepumpe.

2. Solar Energy Climatic Analysis - SANDIA National Laboratories, Report #RS-3141/20654.

3. Solar Radiation Energy Resource Atlas of the United States. Solar Energy Institute Publication #SERI/SP-642-1037 (1981).

4. Balling, R.C., (1983): Harmonic Analysis of Monthly Insolation Levels in the United States. Solar Energy, 31, 3.

5. Balling, R.C. and M.J. Vojtesak, (1983): Solar climates of the United States Based on Long-term Monthly Averaged Daily Insolation Values. Solar Energy, 31, 3.

6. Terjung, W.H., (1940): A Global Classification of Solar Radiation. Solar Energy, 13.

7. Willmott, C.J. and M.T. Vernon, (1980): Solar Climates of the Conterminous United States: A Preliminary Investigation. Solar Energy, 24.

8. Granger, O.E., (1980): Climatology of Global Solar Radiation in California and Interpolation Technique Based on Orthogonal Functions. Solar Energy, 24.

9. Anderson, B., W.L. Carroll and M.R. Martin, (1985): Aggregation of U.S. Population Centers Using Climate Parameters Related to Building Energy Use. Proc. ASHRAE annual meeting, Waikiki, Hawaii.

Richard Perez
Atmospheric Sciences Research Center

Intermediate
Report to SANDIA National Laboratories

Performance Improvement and Structural Simplification of Perez Diffuse Irradiance Model

I. Introduction

Two major areas of simplification and performance improvement were investigated during this work period. The first area involved model mathematical and/or geometrical/structure modifications, while the second involved statistical modifications in the use and representation of the model's brightness coefficients.

At each step of the modification process, the performance of the model was monitored through dependent tests against three months of hourly data from Trappes, France.

II. Original model

In the original configuration, diffuse irradiance, Dc, on a sloping surface of tilts is obtained from the horizontal diffuse as:

$$Dc = Dh\left\{\frac{(1+\cos s)/2 + a(F_1-1) + b(F_2-1)}{1 + c(F_1-1) + d(F_2-1)}\right\} \qquad (1)$$

where a and b are the solid angles occupied by the circumsolar region and the horizon band multiplied by the cosine of their respective mean incidence on the slope, while c and d are the equivalent of a and b for the horizontal plane.

The brightness coefficients F_1 and F_2 represent respectively the radiance enhancements within the circumsular and the horizon zones with respect to the main portion of the sky hemisphere.

These are discrete functions of the insolation conditions parameterized by the solar altitude, Dh, and the quantity ε defined by,

$$\varepsilon = \left\{ \frac{Dh + I}{Dh} \right\} ,$$

where I is the normal direct irradiance.

Currently F_1 and F_2 are available under the form of 5 x 6 x 8 matrices defined by preselected intervals for each of the three insolation conditions descriptors (5 intervals for z, 6 for Dh and 8 for ε).

The performance of this model is shown in Table 1 where the statistical results of a dependent test against three months of hourly data in Trappes, France, are presented. These include the root mean square (RMS) and mean bias errors computed for a 45^{o} tilt south facing plane and four vertical planes facing respectively north, east, south and west.

Table 1

Orientation	45°South	90°North	90°East	90°South	90°West
RMSE Perez ($KJm^{-2}h^{-1}$)	61.5	52.4	99.3	58.5	81.3
MBE Perez ($KJm^{-2}h^{-1}$)	5.4	21.3	-14.4	11.3	39.7
RMSE iso ($KJm^{-2}h^{-1}$)	102.9	145.5	215.8	87.9	164.1
MBE iso ($KJm^{-2}h^{-1}$)	-55.4	88.2	-27.6	-21.5	8.8
RMSE Hay ($KJm^{-2}h^{-1}$)	79.2	103.0	162.2	82.9	112.4
MBE Hay ($KJm^{-2}h^{-1}$)	-36.5	39.9	-31.3	-23.0	8.2
RMSE Klucher ($K\,m^{-2}h^{-1}$)	63.5	206.1	198.0	66.1	175.5
MBE Klucher ($K\,m^{-2}h^{-1}$)	-3.2	138.0	37.4	35.0	76.7

III. Mathematical and structural model modifications

A. Use of reduced brightness coefficients

The most important step toward model simplification was taken by rewriting its governing equation and by changing the definition of the brightness coefficients.

Equation (1) may be written as

$$Dc = Dh\left\{\frac{D^{i}c + D^{c}c + D^{h}c}{Dh^{i} + Dh^{c} + Dh^{h}}\right\} \qquad (2)$$

where the subcripts c and h correspond to the sloping surface and the horizon respectively, while the superscripts i, c and h correspond to the respective energy contributions of the main portion of the sky (isotropic), the circumsolar region and the horizon band. Noting that

$Dh = 1 + D^{c}h + D^{h}h$, (2) may be written as ,

$$Dc = Dh\left\{\frac{D^{i}c}{Dh} + \frac{D^{c}c}{Dh} + \frac{D^{h}c}{Dh}\right\} \qquad (3)$$

which may in turn be written as ,

$$Dc = Dh\left\{\frac{D^{i}c}{Dh} + \frac{D^{c}c\ D^{c}h}{Dh\ Dh^{c}} + \frac{D^{h}c\ D^{h}h}{Dh\ Dh^{h}}\right\}, \qquad (4)$$

Noting that $Dc^c/Dh^c = a/c$ and that $D^hc/D^hh = b/d$, and defining D^ch/Dh as f_1 and Dh^h/Dh as f_2, equation (4) becomes

$$Dc = Dh\left\{\frac{D^ic + f_1\, a/c + f_2\, b/d}{1}\right\} \qquad (5)$$

Finally, noting that $D^ic = (1 + \cos s)(Dh - D^ch - D^hh)/2$, equation (5) becomes,

$$Dc = Dh\left\{0.5(1 + \cos s)(1 - f_1 - f_2) + f_1\, a/c + f_2\, b/d\right\} \qquad (6)$$

This is the new model governing equation using "reduced" brightness coefficients f_1 and f_2. It will be noted that the new equation is linear with respect to the reduced coefficients, which was not the case for the original equation. As before, the new reduced coefficients will be obtained for a given site, by least square fitting of experimental data. This process is now greatly simplified and much less computer time consuming, due to the linear character of equation (6). The relationships between the new reduced coefficients and the original ones are the following:

$$f_1 = \left\{\frac{c(F_1 - 1)}{1 + c(F_{1-1}) + d(F2-1)}\right\} \qquad (7)$$

$$f_2 = \left\{\frac{c(F_2 - 1)}{1 + c(F_{1-1}) + d(F2-1)}\right\} \qquad (8)$$

Conceptually, these reduced brightness coefficients may be described as the respective contributions of the circumsolar and the horizon band region on the horizontal.

Table 2 shows the compared performance of the original model and the new equation based on three months of testing against Trappes data.

Table 2

Orientation	45°South	90°North	90°East	90°South	90°West
Original Equation					
RMSE	61.5	52.4	99.3	58.5	81.3
MBE	5.4	21.3	-14.4	11.3	39.7
New Equation					
RMSE	59.8	52.9	97.0	57.9	81.6
MBE	1.0	22.7	-15.7	7.4	39.8

No performance loss but rather a slight improvement may be observed with this new, much simpler version of the model. Much of the gain may be attributed to the simplification of the least square fitting process, which had originally relied on a series of approximations.

B. Allowance for negative coefficients

Both equations (2) and (6) assume that the brightness or reduced brightness coefficients cannot be negative. This decision was originally made for physical reasons, since negative coefficient would actually mean negative radiance (originating from the sensing point) in the considered sky hemisphere zone. However, given its structural configuration, the model cannot account for cases when the top of the atmosphere is the brightest region, as can be observed during overcast events. One possibility would be to add a third anisotropic zone in the model making it more complex and difficult to use. The other possibility is to allow for negative f_2 or F_2 coefficients as needed to simulate the effect of a bright atmosphere top on sloping surfaces.

The new formulation (equation (6)), with allowance for negative coefficients has been established for and tested against three months of Trappes data. Statistical results are shown in Table III along with the original model's performance characteristics.

Table 3

Orientation	45°South	90°North	90°East	90°South	90°West
Original Equation					
RMSE	61.5	52.4	99.3	58.5	81.3
MBE	5.4	21.3	-14.4	11.3	39.7
New equation + allowance for <o coef.					
RMSE	58.2	46.4	95.7	51.2	76.3
MBE	-8.0	12.4	-26.7	-5.2	28.7

The gain in performance is now substantial for all surfaces notably the vertical south surface and vertical north surface.

In summary, the two steps taken to modify the model's mathematical/structural formulation resulted in increased simplicity of use along with a small but noticable overall performance improvement.

C. Other structural changes

Two levels of structural implification were investigated. These include:

1) Simple model with ponctual circumsolar region and infinitesimally narrow horizon band: In this configuration all circumsolar energy is assumed to originate from a point centered on the sun's position while the horizon band energy originates from an arc of great circle at the base of the atmosphere. The latter has therefore no effect on the horizontal plane. Equation (6) becomes:

$$Dc = Dh \quad 0.5(1+\cos S)(1-f_1)+f_1 \cos \theta c/\cos \theta h + f_2 \sin s \qquad (9)$$

Coefficients for this new formulation have been established, allowing for negative values, and the resulting model was tested against the same three month data file from Trappes. Results are presented in Table 4 and compared to the performance of both the model described in Section II.B and the original model.

Table 4

Orientation	45°South	90°North	90°East	90°South	90°West
Original Equation (Section I)					
RMSE	61.5	52.4	99.3	58.5	81.3
MBE	5.4	21.3	-14.4	11.3	39.7
New Equation (Section III.B)					
RMSE	58.2	46.4	95.7	51.2	76.3
MBE	-8.0	12.4	-26.7	-5.2	28.7
Simplified Equation (Section III.C1)					
RMSE	56.1	54.8	118.9	52.8	80.4
MBE	-0.5	19.2	-52.9	19.8	6.4
Simplified Equation (Section III.C2)					
RMSE	58.2	44.9	95.6	50.6	74.6
MBE	-8.0	12.7	-27.0	-3.7	28.3

Although this simple configuration works well for the south facing slope, there is a noticable performance setback for other orientations, which indicates that the model must retain an extended circumsolar region. Tests proved that 15° half-angle gave the best overall results.

2) Simple model with infinitesimally narrow horizon band: In this configuration, the extended circumsolar region is maintained, however, the horizon band is set as in the previous section. The governing equation is:

$$Dc = Dh \; 0.5(1+\cos S)(1-f_1) + f_1 \, a/b + f_2 \sin s \qquad (10)$$

The arc of great circle horizon band configuration has the advantage of rendering the equation continuous with s for low values of s, which was not the case in the original configuration.

Test results are shown in Table 4. Overall performance is equivalent if not slightly better than the III.B configuration.

Because of the simplicity of equation (10) and the good performance of this configuration, it is suggested to use this as a base model in future

work.

In order to confirm the facts presented in this section, the same tests have been performed on three months from Carpentras, France, a site climatically different from Trappes. Results are presented in Table 5 for the original model, the simplified version (II.B) and the simplified version with narrow horizon band (III.C2). Also, for comparative purposes, this table includes the performance evaluation of the isotropic, Hay and Klucher models.

Table 5

Orientation	45°South	90°North	90°East	90°South	90°West
Isotropic Model					
RMSE	112.3	145.3	175.3	68.6	170.3
MBE	-71.2	82.0	-53.7	-17.4	-29.5
Hay Model					
RMSE	81.8	100.6	129.5	97.3	102.6
MBE	-57.4	-5.7	-76.0	-47.5	-31.9
Klucher Model					
RMSE	58.5	222.4	158.7	92.2	170.8
MBE	-11.4	157.4	43.3	61.9	71.3
Perez Original					
RMSE	40.2	50.9	58.8	70.8	65.1
MBE	-6.6	27.6	-17.9	12.6	16.2
Perez Simplified (VersionIII.B)					
RMSE	40.8	47.1	56.8	67.0	62.6
MBE	-12.6	25.3	-24.6	9.4	11.7
Perez Simplified (VersionIII.C2)					
RMSE	40.1	47.3	57.2	66.3	61.7
MBE	-10.0	25.3	-25.2	7.8	11.2

IV. Statistical modifications

In this section we investigate the use of analytic functions rather than matrices (of brightness coefficients) to express anistropy changes with insolation conditions. As before, functions of z, Dh and ε are esta-

blished through least square fitting but in this case the coefficients of the analytical functions rather than their actual values for different insolation conditions are obtained. This investigation was rendered manageable computer-time-wise due to the use of the model's simpler formulation described in section III.B.

Nine such functions were tried and tested against the same three months of data from Trappes. These functions are described in Table 6. The choice of each function's projection on ε, Dh and z axes was based on visual inspection of the variation of brightness coefficients F_1 and F_2 with insolation.

Test results are presented in Table 7. Performance is compared to the base case model which in this case was the model described in section III.B.

As can be expected, the performance of analytical functions-based models improves with the number of coefficients allowed. However, the improvement from the eight coefficients function #1 to the 36-coefficients function #9 is small when compared to the increase in equation complexity. Also, it can be noted that none of the analytic functions used showed an overall performance superior to the matrix-based model.

In addition, it can be said that whereas an analytical function-based model is easier to manipulate for hand-performed calculations (at least for simple functions such as #1 and 2), a matrix based model constitute a more economic approach for computer-based applications. (3 "IF" statements for the matrix-based model as opposed to 8 sums, 12 multiplications and 4 function calls for the simplest analytical function studied.)

V. Conclusions and future work

At the conclusion of this working period, the following points can be

Table 6

Selected formulations of F_1 and F_2 experimental analytical functions

Function #	Projection on z axis @ ε, Dh = cst	Projection on Dh axis @ z, ε = cst	Projection on ε axis @ z, Dh = cst
1	$az + b$	$cDh + d$	$e\ln(\varepsilon) + f$
2	$az + b$	$cDh + d$	$e\,\varepsilon^{1/2} + f$
3	$az + b$	$cDh + d$	$e\varepsilon^3 + F\varepsilon^2 + g\varepsilon + h$
4	$az + b$	$cDh + d$	$e\varepsilon + F\varepsilon^{1/2} + f\varepsilon^{1/3} + h$
5	$az + b$	$cDh + d$	$e\varepsilon^{1/2} + F\varepsilon^{1/3} + g\varepsilon^{1/4} + h$
6	$az + b$	$cDh + d$	$e\varepsilon + F\varepsilon^{1/2} + g\ln(\varepsilon) + h$
7	$az + b$	$cDh^2 + dDh + e$	$F\varepsilon^3 + g\varepsilon^2 + h\varepsilon + i$
8	$az^2 + bz + c$	$cDH + e$	$F\varepsilon^3 + g\varepsilon^2 + h\varepsilon + i$
9	$az^2 + bz + c$	$cDh^2 + dDh + e$	$F\varepsilon^3 + g\varepsilon^2 + h\varepsilon + i$

Functions' Equation

1 $\alpha_1 zDh\ \ln(\varepsilon) + \alpha_2 zDh + \alpha_3 z\ln(\varepsilon) + \alpha L_1 z + \alpha_5 Dh\ln(\varepsilon) + \alpha_6 Dh + \alpha_7 \ln(\varepsilon) + \alpha_8$

2 $\alpha_1\ zDh\alpha^{1/2} + \alpha_2 zDh + \alpha_3 z\varepsilon^{1/2} + \alpha_4 z + \alpha_5 Dh\ln(\varepsilon) + \alpha_6 Dh + \alpha_7 \varepsilon^{1/2} + \alpha_8$

3 $\alpha_1\ zDh\varepsilon^3 + \alpha_2 zDh\varepsilon^2 + \ldots\ldots\ldots\ldots\ldots + \alpha_{16}$

4 $\alpha_1\ zDh\varepsilon + \alpha_2\ zDh197^{1/2} + \ldots\ldots\ldots\ldots\ldots + \alpha_{16}$

5 $\alpha_1\ zDh\varepsilon^{1/2} + \alpha_2\ zDh\varepsilon^{1/3} + \ldots\ldots\ldots\ldots\ldots + \alpha_{16}$

6 $\alpha_1\ zDh\varepsilon + \alpha_2\ zDh\varepsilon^{1/2} + \ldots\ldots\ldots\ldots\ldots + \alpha_{16}$

7 $\alpha_1\ zDh^2\varepsilon^3 + \alpha_2\ zDh^2\varepsilon^2 + \ldots\ldots\ldots\ldots\ldots + \alpha_{24}$

8 $\alpha_1\ z^2Dh^2\varepsilon^3 + \alpha_2\ z^2Dh\varepsilon^2 + \ldots\ldots\ldots\ldots\ldots + \alpha_{24}$

9 $\alpha_1\ z^2Dh^2\varepsilon^3 + \alpha_2\ z^2Dh^2\varepsilon^2 + \ldots\ldots\ldots\ldots\ldots + \alpha_{36}$

Table 7

Surface Orientation	45°South	90°North	90°East	90°South	90°West
Base case (III.B)					
RMSE ($kJm^{-2}h^{-1}$)	58.2	46.4	95.7	51.2	76.3
MBE (")	-8.0	12.4	-26.7	-5.2	28.7
Function 1					
RMSE (")	66.7	45.2	102.1	54.3	77.5
MBE (")	-7.8	13.3	-25.6	-4.5	30.7
Function 2					
RMSE (")	67.3	45.3	102.6	54.9	77.9
MBE (")	-7.7	13.4	-25.2	-4.4	30.6
Function 3					
RMSE (")	62.3	43.8	99.2	52.5	77.2
MBE (")	-8.3	13.0	-24.3	-5.2	30.8
Function 4					
RMSE (")	63.6	45.2	101.1	53.1	77.3
MBE (")	-8.8	12.7	-27.0	-5.7	31.0
Function 5					
RMSE (")	63.6	45.5	101.0	53.1	77.1
MBE (")	-8.2	13.5	-26.7	-4.8	31.6
Function 6					
RMSE (")	63.6	44.8	102.2	53.0	77.6
MBE (")	-8.5	13.3	-27.6	-5.2	32.2
Function 7					
RMSE (")	60.0	44.3	98.0	51.0	78.0
MBE (")	-8.0	12.4	-24.0	-5.4	30.8
Function 8					
RMSE (")	60.0	44.3	98.0	51.0	78.0
MBE (")	-8.0	12.4	-24.0	-5.4	30.8
Function 9					
RMSE (")	60.0	47.0	94.7	51.5	78.0
MBE (")	-7.5	13.4	-26.3	-4.6	30.6

made:

- The simple model described in section III.C.2 will be the base model for future work.

- Analytical functions-based models do not reach the level of performance of matrix-based models if the complexity of the functions is kept to a reasonable level.

- Simple analytical functions-based models have been described. Their applications appear to be limited to hand-held applications such as, for example, preliminary calculations or estimates of departure from isotropic sky.

In the upcoming phase of model work the two following points will be investigated:

- Optimization of Dh, ε, z categories.

- Partial analytic approach for the estimation of F_1 and F_2 - notably with respect to the z dimension.

Solar Energy Vol. 36, No. 6, pp. 481–497, 1986
Printed in the U.S.A.

0038-092X/86 $3.00 + .00

AN ANISOTROPIC HOURLY DIFFUSE RADIATION MODEL FOR SLOPING SURFACES: DESCRIPTION, PERFORMANCE VALIDATION, SITE DEPENDENCY EVALUATION

R. PEREZ†, R. STEWART†, C. ARBOGAST, R. SEALS, J. SCOTT†
Atmospheric Sciences Research Center, State University of New York at Albany, 1400 Washington Avenue, Albany, New York 12222

(*Received* 31 *May* 1985; *accepted* 7 *November* 1985)

Abstract—A model is described to estimate hourly or higher frequency diffuse sky radiation impinging on plane surfaces of any orientation, once knowing this value on the horizontal. This model features a simple geometrical sky hemisphere description, allowing for the observed effects of forward-scattered and back-scattered radiation and a parameterization of insolation conditions based on available radiative quantities.

Model performance is studied through (1) long term independent tests performed against hourly ground-shielded tilted irradiance data from Trappes, France; Carpentras, France and San Antonio, Texas; (2) long term dependent tests performed against hourly data from the same stations plus Albany, New York; and (3) real time tests based on one-minute data from Albany, New York. Performance is assessed through comparison with three reference models: the isotropic, the Hay, and Klucher anisotropic models. Substantial performance improvement over the three reference models is found for all stations and all surface orientations. Additional performance improvements from independent to dependent testing can be explained logically on the basis of climate, altitude and latitude differences between stations.

1. INTRODUCTION

As solar energy system modeling became more refined over the last ten years, the requirements for input radiation parameters became more demanding. Both accurate radiation data bases and adequate models are in increasing need by the engineering community worldwide. The current undertaking of the International Energy Agency in this field[1] is an illustration of this specific interest.

Notably, the hourly modeling of the energy received by tilted planes, based on the knowledge of horizontal global radiation and normal incidence direct radiation, is of prime importance. The anisotropic nature of diffuse radiation has been the largest source of error associated with this computation. Many authors have pointed out the shortcomings of the classical isotropic assumption, e.g., [2, 3], and recent photovoltaic projects in the United States have demonstrated the need for better models in this area[4].

However, there exist today, several models which attempt to account for diffuse radiation anisotropy. The most successful have been observed to better the isotropic model in many instances, e.g., [5, 6, 7].

The model described and tested in this paper was developed as an attempt to improve systematically on the isotropic assumption for all weather conditions and all captor orientations, by using (1) a simple, realistic geometric representation of radiance distribution within the sky hemisphere; (2) a sky-condition description scheme making full use of the information already available to compute hourly irradiance on slopes, i.e., global horizontal, direct and/or diffuse, position of the sun; and (3) an experimentally-derived law governing the relationship between sky condition and radiance distribution. This model will be subsequently referred to as *Perez model.*

2. METHODS

2.1 *Description of the Perez model*

The model is composed of three distinct elements: (1) A geometrical representation of the sky dome, (2) A parametric representation of the insolation conditions, and (3) A statistical component linking the two.

2.1.1 *The geometrical framework.* This is represented in Fig. 1, where the sky hemisphere is divided into three zones. Radiance originating from each of these regions can be different, while remaining constant within a given zone. Such a configuration was decided upon in order to account for the two main zones of anisotropy observed in the

† Member ISES.

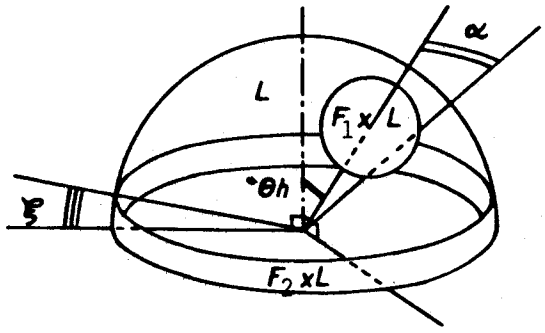

Fig. 1. Model geometrical representation of the sky hemisphere.

atmosphere: circumsolar brightening, due to forward scattering by aerosols, and horizon brightening due primarily to multiple Rayleigh scattering and retroscattering in clear atmospheres[10].

If the radiances originating from the main portion of the dome, the circumsolar, and the horizon zone are respectively equal to L, $F_1 \times L$, and $F_2 \times L$, the resulting horizontal diffuse irradiance Dh can be expressed as

$$Dh = \pi L\{1 + 2(1 - \cos\alpha)Xh(z)(F_1 - 1)\cos z' + 0.5(1 - \cos 2\xi)(F_2 - 1)\}, \quad (1)$$

where α is the half angle of the circular region centered on the sun's position and set at 15° for the model studied here. The parameter Xh is the fraction of this circular region which is seen by the horizontal, while the angle z' is equal to the solar zenith angle, z, if the circular region is totally visible, and equal to its average incidence angle if it is only partially visible. The angle ξ is the horizon band angular thickness, set at 6.5° for the presented model.

Equation (1) assumes that the circumsolar region is small enough so that all points within this region are seen under the same angle, z'.

Similarly the diffuse irradiance, Dc, received by a sloping plane is expressed as

$$Dc = \pi L\{0.5(1 + \cos s) + 2(1 - \cos\alpha)Xc(\theta)(F_1 - 1)\cos\theta' + 2\xi \sin\xi'(F_2 - 1)/\pi\}, \quad (2)$$

where s is the plane's tilt angle, while the angles θ and θ' and the parameter Xc are the equivalent of z, z', and Xh respectively, for the considered surface.

The last term of eqn (2) is a sinusoidal approximation of the horizon band contribution to the energy budget of the plane, where the angle ξ' is defined as

$$\xi' = s + \xi(\tfrac{1}{2} - s/\pi). \quad (3)$$

This approximation causes a minor deviation from the actual integrated value[11] and generates a slight discontinuity for $s = 0$; however, its effect is negligible when placed in the operating model context.

The combination of eqns (1) and (2) leads to the model's governing equation

$$Dc = Dh\{0.5(1 + \cos s) + a(\theta)(F_1 - 1) + b(s)(F_2 - 1)\}\{1 + c(z)(F_1 - 1) + d(F_2 - 1)\}^{-1}, \quad (4)$$

where

$$a(\theta) = 2(1 - \cos\alpha)Xc(\theta)\cos\theta', \quad (5)$$

$$b(s) = 2\xi \sin\xi'/\pi, \quad (6)$$

$$c(z) = 2(1 - \cos\alpha)Xh(z)\cos z', \quad (7)$$

$$d = (1 - \cos 2\xi)/2. \quad (8)$$

Equation (4) is identical to the isotropic equation for $F_1 = F_2 = 1$.

2.1.2 *The sky condition parameterization.* Considering that the calculation of irradiance on a slope at a given instant requires the knowledge of the normal incidence direct irradiance, the horizontal diffuse irradiance, and the solar position, it is logical to use that information to describe the type of sky condition existing at that instant. The three following variables are used for this purpose:

- z, solar zenith angle
- Dh, horizontal diffuse radiation
- $\varepsilon = (Dh + I)/Dh$, where I is the normal incidence direct.

It is assumed, at this stage of model development, that z, Dh and ϵ are independent quantities defining a 3-dimensional space. This space is divided into over 200 "sky condition categories," by defining intervals for each of the variables. These are presented in Table 1.

2.1.3 *The sky condition/model configuration relationship.* The only undefined terms in eqns (1) and (2) are the coefficients F_1 and F_2. These non-dimensional multiplicative factors set the radiance magnitude in the two anisotropic regions relatively to that in the main portion of the dome. The degree of anisotropy of the model is a function of these two terms only. The model can go from an isotropic configuration (F_1, $F_2 = 1$) to a configuration incorporating circumsolar and/or horizon brightening.

The magnitude of these coefficients is treated as a function of the three variables describing the sky conditions. At this stage of model development, these are not continuous functions, but matrices corresponding to the discrete partition of the sky condition space presented above.

These coefficients constitute the statistical/experimental part of the model. They are obtained through the analysis of hourly—or higher fre-

Table 1. Description of the ϵ, Dh and θh intervals depicting the sky conditions

Dh (KJ/min)			ε			z (degrees)	
Name of Interval	Lower Bound	Upper Bound	Name of Interval	Lower Bound	Upper Bound	Lower Bound	Upper Bound
A	0	3	A	1	1	0	35
B	3	6	B	1.003	1.03	35	45
C	6	10	C	1.03	1.1	45	55
D	10	15	D	1.1	1.5	55	65
E	15	20	E	1.5	2.5	65	90
F	20	--	F	2.5	5		
			G	5	9		
			H	9	--		

quency—data recorded with ground-shielded pyranometers of different slopes and orientations. In order not to bias the model in favor of a specific orientation, measurements are needed in the four cardinal directions. Also, as this type of model is used primarily for sun-facing captors, one or more sloping, south-facing or sun-tracking measurements are needed.

The analysis consists of optimizing F_1 and F_2 for each [θ, ϵ, Dh] interval by least square fitting of measured data.

2.2 *Data sets*

Data from Trappes and Carpentras, France[12]; San Antonio, Texas[13]; and Albany, New York [14] are used in this analysis. These sites represent four distinct solar environments with latitudes ranging from 30° to 48°N and climates ranging from semi-arid subtropical to temperate marine. Table 2 summarizes the geographical and climatological particularities of each station.

The selected sites had to meet the three criteria presented below:

(1) *Availability of high quality hourly measurements of horizontal global and direct and/or diffuse irradiance, as well as tilted global irradiance for four azimuths.* The type of instrumentation used and the level of quality control achieved at the two leading Meteorologie Nationale stations, and two of the U.S. Solar Energy Meteorological Research and Training Sites, ensures the data quality needed for a study of this nature. Table 3 summarizes the measurements performed and instrumentation used at each site.

Table 2. Description of selected sites

Station	Latitude	Longitude	Elevation	Climate Type
Albany, New York	42° 42'N	73° 50'W	94m	Humid Continental Temperate
San Antonio, Texas	29° 46'N	98° 49'W	253m	Semi-arid Sub tropical
Carpentras, France	44° 05'N	5° 03'E	99m	Mediterranean
Trappes, France	48° 46'N	2° 0'E	167m	Marine Temperate

Table 3. Type of measurements used from each site and instrumentation

Station(s)**	Measurements(s)	Instrument
T,C,A,S	Direct irradiance	Eppley NIPS
T,C,A,S	Global irradiance	Thermal pyranometers*
T,C	South, west, east and north vertical global irradiance	Thermal pyranometers*
S	South, west, east and north ground-shielded vertical global irradiance	Thermal pyranometers*
A	South, west, east and north ground-shielded vertical global irradiance	Li-Cor filtered radiometers
T,C	45° tilt, south facing global irradiance	Thermal pyranometers*
A,S	Latitude, latitude +10° and latitude -10° tilt south facing, ground shielded global irradiance	Thermal pyranometers*
T,C	North and south vertical reflected radiation. Sky shielded instruments.	Thermal pyranometers*

NOTES: * Both Kipp and Zonen CM5 and Eppley PSPs are used at the French stations. The American sites used only Eppley PSPs

** A: Albany; C: Carpentras; S: San Antonio; T: Trappes

(2) *Elimination of most assumptions regarding ground-reflected radiation.* In order to focus on sky radiance distribution, assumptions regarding directionality of ground-reflected radiation and albedo must be minimized.

Tilting pyranometers from the two American sites are equipped with artificial horizons (cylindrical black-painted shields for Albany, and planar black-painted shields for San Antonio). The two French stations provide independent records of ground reflected radiation measured with sky-shielded vertically mounted pyranometers facing north and south. Ground-reflected iradiance is removed from east and west vertical sensors by assuming that it is equal to the half sum of the north and south vertical reflected irradiances. Further, the ground component is removed from the 45° south facing sensor by assuming isotropy of the south-reflected component.

(3) *Availability of at least three seasonally representative months of hourly data.* This criteria allows notably for analysis of a given site under three typical solar geometry configuration.

Albany data includes the months of February, April, and June 1980, (out of the four years available), while San Antonio data includes December 1980, March, July, and December of 1981. Data from Trappes cover a 21-month period starting in April 1979, while Carpentras data cover a two-year period (Jan. 1979 to Dec. 1980).

In addition to the four hourly data bases described above, one-minute data from Albany, NY covering the months of February, April and June 1980 are used to study the model on a short time interval basis.

2.3 *Model testing, reference models*

The model's performance is observed from three different viewpoints: (1) dependent tests, (2) independent tests, and (3) real time performance.

2.3.1 *Dependent tests.* The enhancement matrices F_1 and F_2 are established for each station as explained earlier. The completed models are then tested against the data sets used for their establishment.

For each available sensor orientation, the mean bias error (MBE) and the root mean square error (RMSE), accumulated over the complete testing period at each station, are used to rate model performance.

The goal of these dependent tests is to evaluate the limits of the Perez model configuration ability to recreate existing conditions.

2.3.2 *Independent tests.* The Albany-established model is now tested against data from the three other sites. As above, MBE and RMSE cor-

responding to the complete testing period for each site are used to rate performance.

The question of site/climate dependency of the sky condition description method used is answered to a large extent by these tests.

2.3.3 *Real time tests.* Based on the Albany one-minute data set, the model's behavior is observed in real time for typical weather conditions, such as winter/summer clear days, winter/summer thin overcast days and winter/summer partly cloudy days.

2.3.4 *Reference models.* Three models are used as reference to provide an objective comparative basis to all the above tests. These are the following: (1) The isotropic (Liu and Jordan[15]) model, (2) The Hay model[6] and, (3) The Klucher model[7]. The latter models were selected as they had been found to operate generally better than the isotropic and several other models, e.g. [16].

The Klucher model is based on the Temps and Coulson[17] clear sky equation. This was designed to incorporate both the observed horizon and circumsolar brightening in the computation of energy impinging on slopes. The governing equation is

$$Dc = Dh(1 + \cos s)/2\{1 + F \sin^3(s/2)\} \times \{1 + F \cos^2 \theta \sin^3 z\}, \quad (11)$$

where F is used to parameterize the sky condition and is given by,

$$F = 1 - (Dh/Gh)^2, \quad (12)$$

where Gh is the horizontal global irradiance.

The Hay model incorporates only circumsolar brightening in its structure. As for Klucher's, the sky condition is depicted by one term expressing the amount of direct irradiance received at the earth surface. This clearness index term is given by,

$$K = I/I_o, \quad (13)$$

where I_o is the extraterrestrial radiation. The model's governing equation is,

$$Dc = Dh\{(K \cos \theta/\cos z) + (1 - K)(1 + \cos s)/2\}. \quad (14)$$

Both Klucher and Hay models return to an isotropic configuration in the absence of direct sunlight.

3. RESULTS

3.1 *Model's parameters establishment*

As an example of the complete analysis of each data set as described in Section 2.1.2, the variations of F_1 and F_2 with the two radiative quantities describing the sky conditions are plotted on Fig. 2(a) through 2(d) for the stations of Trappes, Carpentras, Albany and San Antonio, respectively, for solar zenith angles lying between 55° and 65°.

The scale on the Dh axis is linear, while that on the ϵ axis is logarithmic. No point was plotted if less than five hourly events were observed within a given [Dh, ϵ, z] category.

The most evident feature of these plots is their similarity: For four sets of independent data, the same type of pattern may be observed for F_1 and F_2. This includes the following:

- Increase in circumsolar brightening (F_1) with Dh for low ϵ values, (low direct radiation, bright atmosphere).
- Existence of both circumsolar and horizon brightening (F_1 and F_2) as ϵ increases, with increased relative horizon contribution when approaching very clear conditions (Low Dh, high ϵ). This is particularly visible on Fig. 3.
- Evidence of continuity between overcast and clear sky conditions indicating the persistence of a specific pattern for all intermediate cases (e.g., broken clouds).
- Tendency toward isotropic configuration for dark overcast atmospheres.

Disparities may also be noted between the four plots. The most interesting pertains to the relative importance of horizon brightening for clear atmospheres: this is maximum for the San Antonio, Texas station, and the Carpentras station, while horizon contribution is comparatively lower for Trappes and Albany. The effect of both climate/geography and instrumentation are discussed in the next section. However, it is interesting to note that (1) the station at the highest elevation exhibits the most brightening at the horizon; (2) the two driest stations, exhibiting the largest number of clear atmosphere events, also show the most pronounced horizon brightening—compare for example Figs. 4(a) (Trappes) and 4(b) (Carpentras) where the number of hourly events in each [Dh, ϵ] is reported for the studied solar zenith angle range; (3) the regions of San Antonio and Carpentras, due to their dry climate, have the least amount of green vegetation, and consequently the highest albedo.

3.2 *Model performance*

3.2.1 *Long-term tests.* Tables 4(a) through 4(d) summarize the overall results obtained by testing models against each complete data set. These show for Trappes, Carpentras, Albany and San Antonio respectively, (1) the average hourly energy, Gc, received by each sloping sensor; (2) the root mean square error obtained for each model in terms of percentage of the previous value; and (3) the mean bias error for each model, also in percent.

Each table contains tests results for the three reference models, the new model using Albany-derived parameters (i.e., independent test), and the new model using each station's derived parameters (i.e., dependent tests).

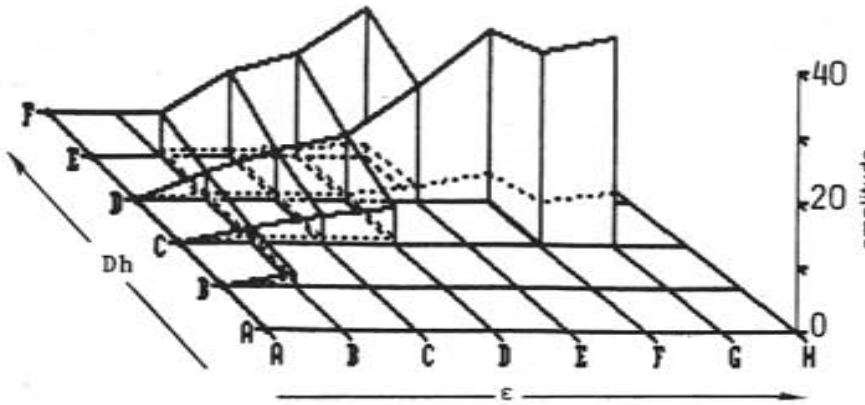

Figure 2a: Trappes, France

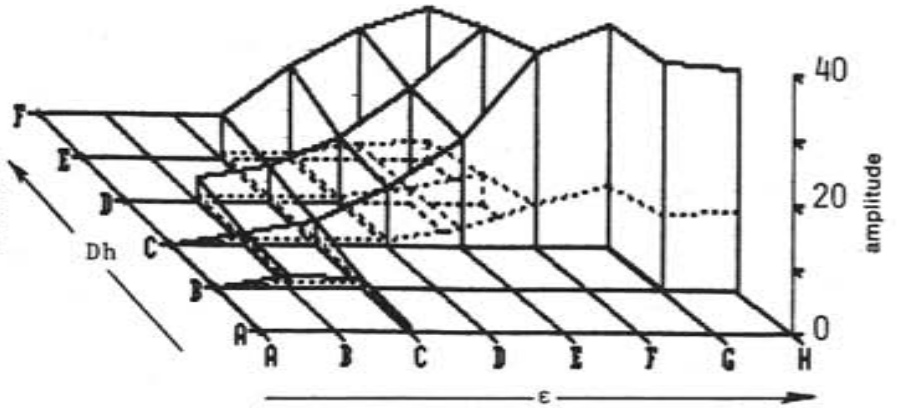

Figure 2b: Carpentras, France

Figure 2c: Albany, NY, USA

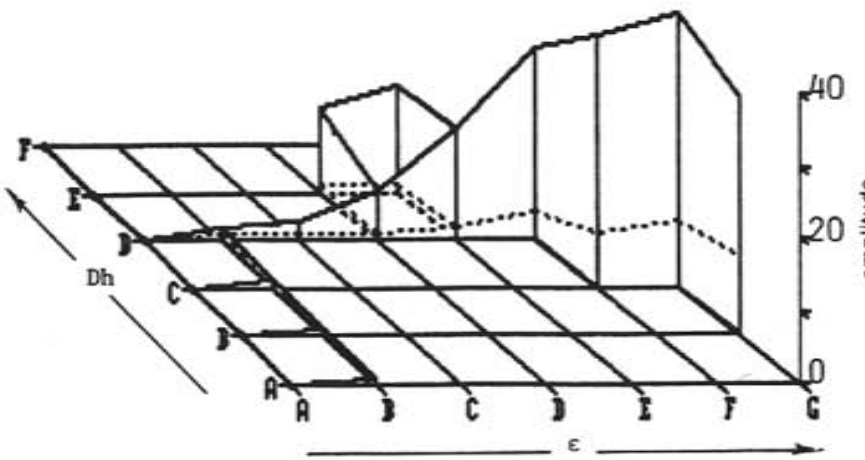

Figure 2d: San Antonio, TX, USA

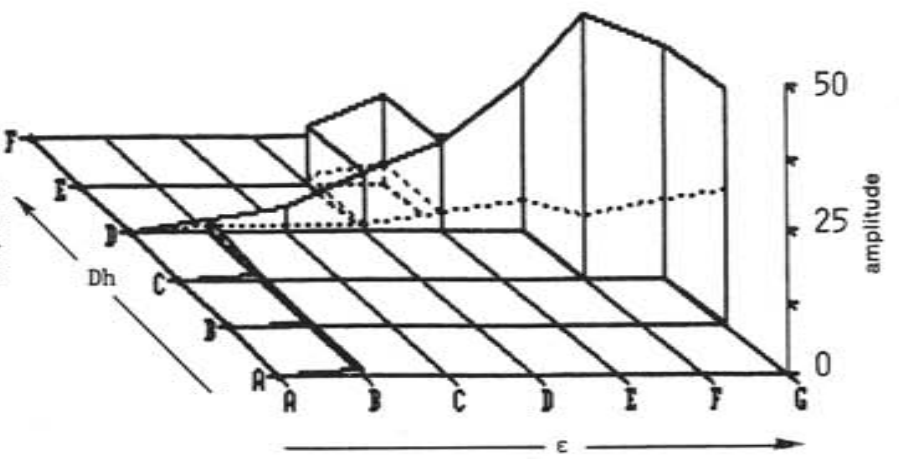

Fig. 2. Variations of circumsolar brightening coefficient, F_1 (solid lines) and horizon brightening, F_2 (dotted lines) with Dh and ε, for $55° < z < 65°$.

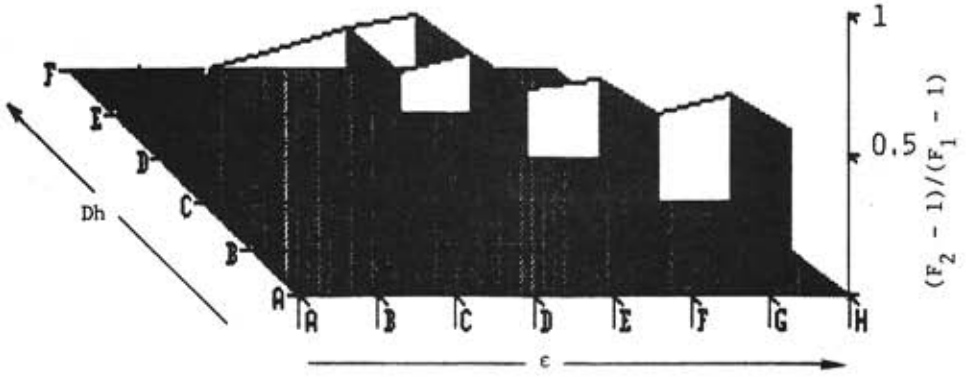

Fig. 3. Variation of the relative magnitudes of horizon and circumsolar brightening with *Dh* and ε for $55° < z < 65°$.

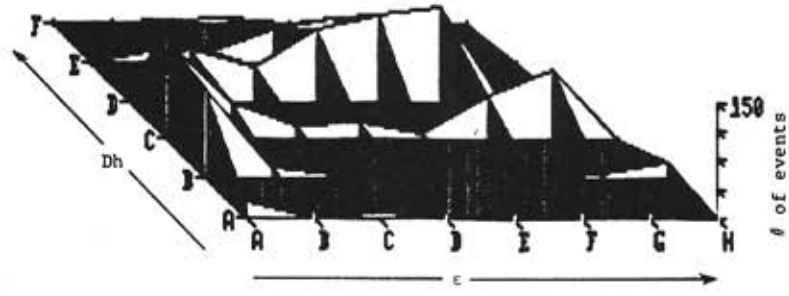

(a)

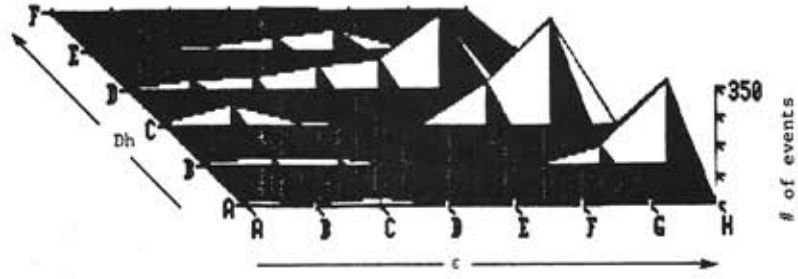

(b)

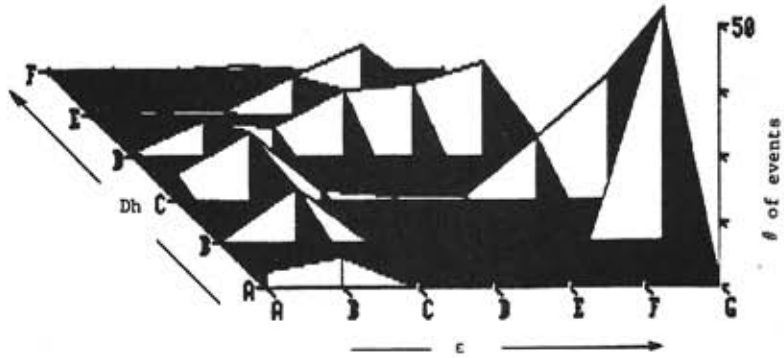

(c)

Fig. 4. Number of hourly events analyzed in each [*Dh*, ε] interval for $55° < z < 65°$; (a) Trappes—21 months of data; (b) Carpentras—24 months of data; (c) Albany—3 months of data.

Table 4(a). Models performance summary for Trappes, France—21 months of hourly data

Model \ Sensor Slope and Orientation	45° South		90° North		90° East		90° South		90° West	
Average* hourly global irradiance KJ/M^2h^{-1}	1060		234		520		656		467	
	RMSE	MBE	RMSE	MBE	RMSE	MBE	RMSE	MBE	RMSE	MBE
	- - Percent of Measured Global - -									
Perez dependent	5.1	-0.4	18.2	7.6	12.9	-1.3	10.2	2.3	14.1	5.4
Perez independent	5.7	-1.2	23.9	14.0	14.4	-1.0	10.4	1.3	15.6	5.9
Isotropic	14.3	-9.1	53.4	33.3	34.0	-5.9	22.4	-10.2	31.2	0.4
Hay	9.3	-5.6	38.0	15.4	23.4	-5.4	14.9	-5.9	21.4	0.1
Klucher	7.6	-3.6	76.5	50.8	30.0	4.6	14.2	-1.2	32.1	12.0

Note: * Average taken over the number of daytime hours studied.

Table 5 summarizes, for each station and sensor orientation, and for independent testing, the improvement achieved with the proposed model over each of the three references, in terms of percent decrease of RMS errors. The "improvement variable," X, is defined as,

$$X = 100(1 - \text{RMSE Perez/RMSE Reference}) \quad (15)$$

An equivalent variable is studied in Table 6, but this time it represents the additional improvement

Table 4(b). Performance summary carpentras, France—24 months of hourly data

Model \ Sensor Slope and Orientation	45° South		90° North		90° East		90° South		90° West	
Average* hourly global irradiance KJ/M^2h^{-1}	1574		230		687		972		715	
	RMSE	MBE	RMSE	MBE	RMSE	MBE	RMSE	MBE	RMSE	MBE
	Percent of Measured Global									
Perez dependent	2.7	-0.7	18.2	8.3	7.6	0.6	5.7	1.2	7.0	0.5
Perez independent	3.9	-1.8	30.0	0.1	10.9	-2.3	7.1	-1.3	10.2	-2.4
Isotropic	10.9	-7.8	47.8	24.0	20.8	-6.9	16.0	-10.0	21.4	-7.7
Hay	6.0	-4.2	36.9	-6.5	14.7	-7.0	10.0	-5.9	14.0	-7.1
Klucher	5.0	-2.9	74.3	49.1	18.2	4.5	9.2	-1.6	18.0	3.2

Note: * Average taken over the number of daytime hours studied

Table 4(c). Performance summary Albany, New York, USA—3 months of hourly data

Average* hourly global irradiance KJ/M^2h^{-1}	Sensor Slope and Orientation: 43° South		90° North		90° East		90° South		90° West	
	1401		260		661		781		617	
Model	RMSE	MBE	RMSE	MBE	RMSE	MBE	RMSE	MBE	RMSE	MBE
	Percent of Measured Global									
Perez dependent	2.9	-0.2	12.7	4.2	8.2	-1.1	6.5	1.6	9.4	0.2
Isotropic	8.9	-5.6	37.7	18.8	26.0	-6.2	15.9	-6.6	27.0	-5.7
Hay	5.6	-3.3	30.4	-3.8	16.5	-7.0	10.5	-4.9	18.3	-7.4
Klucher	4.1	-1.5	60.0	-38.8	22.5	3.9	10.7	-1.8	24.3	5.0

Note: * Average taken over the number of daytime hours studied

achievable when a dependent test is performed. This variable, Y, is given by,

$$Y = 100(1 - \text{RMSE Perez Dependent}/\text{RMSE Perez Independent}) \quad (16)$$

It is interesting to note, as in Section 3.1, that the largest improvement is found for the two stations which have the most different climatic and geographical environments compared to Albany, NY.

3.2.2 *Real time performance.* The difference between measured and modeled radiation values is plotted for selected orientations against time of day for five typical insolation conditions encountered

Table 4(d). Performance summary San Antonio, Texas, USA—4 months of hourly data

Average* hourly global irradiance KJ/M^2h^{-1}	Sensor Slope and Orientation: 30° South		90° North		90° East		90° South		90° West	
	1946		216		771		1523		884	
Model	RMSE	MBE	RMSE	MBE	RMSE	MBE	RMSE	MBE	RMSE	MBE
	Percent of Measured Global									
Perez dependent	2.2	0.5	19.4	8.8	6.7	-1.6	4.6	-2.2	4.9	0.3
Perez independent	2.1	-0.3	26.4	-15.7	10.9	-7.4	7.0	-5.0	8.0	-5.3
Isotropic	5.9	-4.6	33.3	-10.6	21.7	-13.7	16.3	-13.3	19.2	-12.8
Hay	3.0	-1.6	56.0	-40.3	18.9	-14.8	10.8	-8.9	15.2	-11.8
Klucher	2.6	-1.0	39.8	9.3	15.7	-6.6	11.0	-8.4	13.0	-5.9

Note: * Average taken over the number of daytime hours studied

in Albany, New York. The solid lines correspond to the isotropic model, while Klucher, Hay, and Perez models are represented by *x*-lines, +-lines and *o*-lines respectively.

Figures 5(a), (b), and (c) illustrate the case of a winter clear day (February 4, 1980) for the 43° south, the east vertical and north vertical surfaces. Winter, thin overcast conditions, prevailed on February 3, 1980. Results are plotted on Figs. 6(a) and (b) for the 53° south and the north sensors respectively. Figures 7(a) and (b) illustrate variable conditions with several clear occurrences in the morning (February 13, 1980); results are shown for the vertical south and north surfaces, respectively.

The cases of a clear summer day and a high turbidity hazy summer day are illustrated by Figs. 8(a)

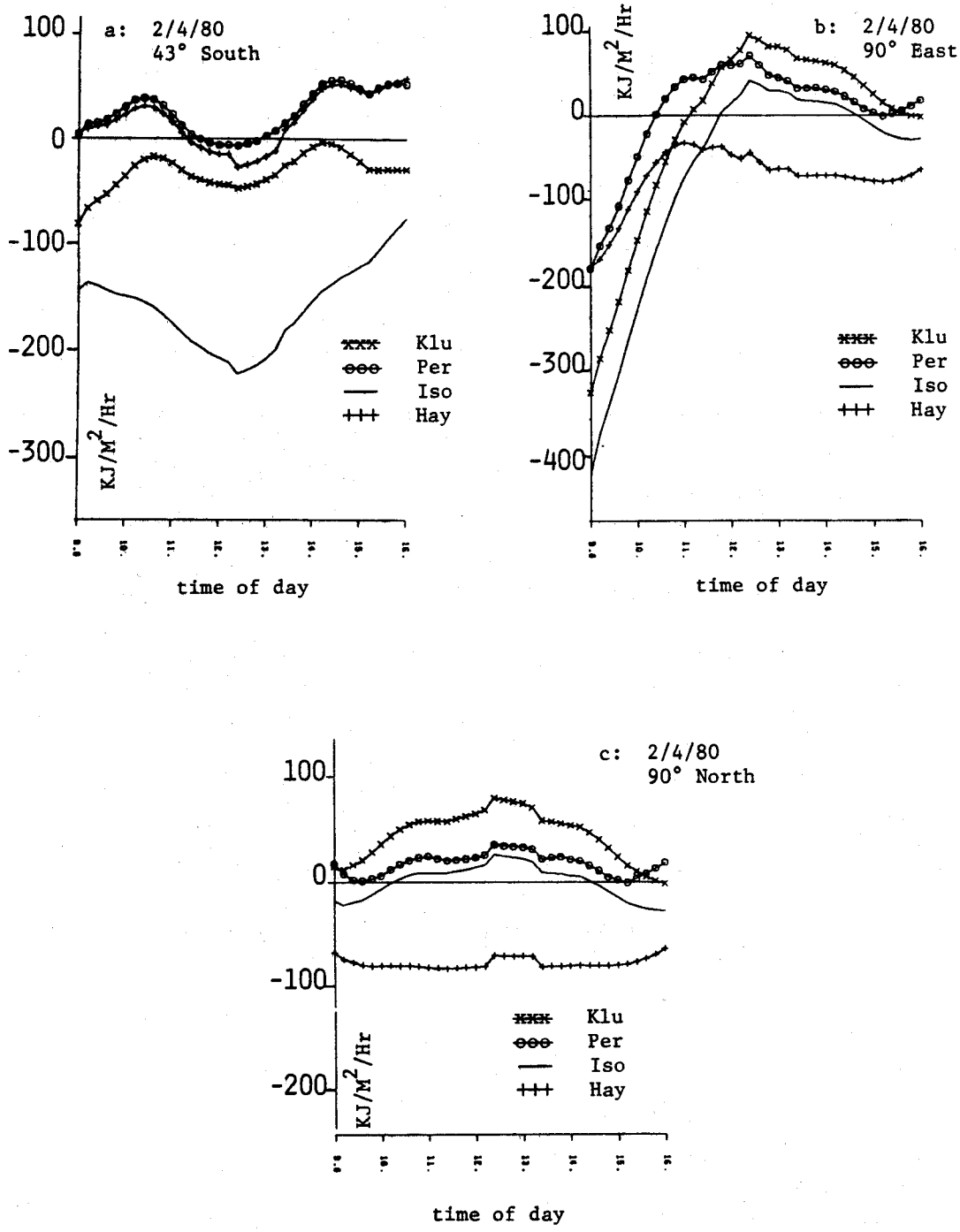

Fig. 5. Daily variations of the difference between modeled and measured irradiance values on a clear, winter day, based on one-minute data in Albany, NY, February 4, 1980.

Table 5. Percent reduction of RMS error, using the proposed model for independent tests: (1 − (RMSE Perez independent)(RMSE Reference Model)$^{-1}$) × 100

	Sensor Slope and Orientation														
	Sloping* South			90 degs. North			90 degs. East			90 degs. South			90 degs. West		
Reference	Iso	Hay	Klu	Iso	Hay	Klu	Iso	Hay	Klu	Iso	Hay	Klu	Iso	Hay	Klu
Albany	67%	48%	29%	66%	58%	79%	68%	50%	66%	59%	38%	39%	65%	49%	61%
Trappes	61%	39%	25%	56%	37%	64%	58%	39%	52%	54%	31%	27%	51%	27%	51%
Carpentras	65%	36%	23%	45%	28%	64%	48%	26%	40%	56%	29%	22%	53%	27%	43%
San Antonio	65%	33%	24%	27%	46%	37%	44%	35%	30%	58%	29%	39%	51%	41%	30%

Note: All tests are independent but for Albany, NY

* 45° for Trappes and Carpentras, 43° for Albany, 30° for San Antonio

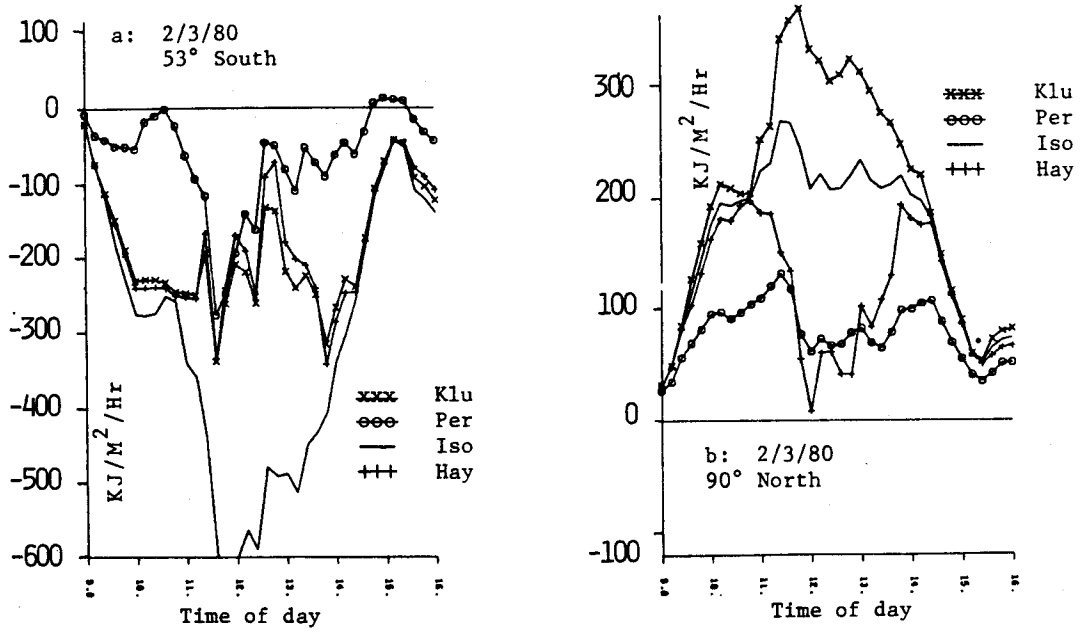

Fig. 6. Daily variations of modeled minus measured irradiance on a thin overcast, winter day based on February 3, 1980 one-minute data, in Albany, NY.

Table 5. Percent reduction of RMS error, using the proposed model for independent tests: (1 − (RMSE Perez independent)(RMSE Reference Model)$^{-1}$) × 100

	Sensor Slope and Orientation														
	Sloping* South			90 degs. North			90 degs. East			90 degs. South			90 degs. West		
Reference	Iso	Hay	Klu	Iso	Hay	Klu	Iso	Hay	Klu	Iso	Hay	Klu	Iso	Hay	Klu
Albany	67%	48%	29%	66%	58%	79%	68%	50%	66%	59%	38%	39%	65%	49%	61%
Trappes	61%	39%	25%	56%	37%	64%	58%	39%	52%	54%	31%	27%	51%	27%	51%
Carpentras	65%	36%	23%	45%	28%	64%	48%	26%	40%	56%	29%	22%	53%	27%	43%
San Antonio	65%	33%	24%	27%	46%	37%	44%	35%	30%	58%	29%	39%	51%	41%	30%

Note: All tests are independent but for Albany, NY

* 45° for Trappes and Carpentras, 43° for Albany, 30° for San Antonio

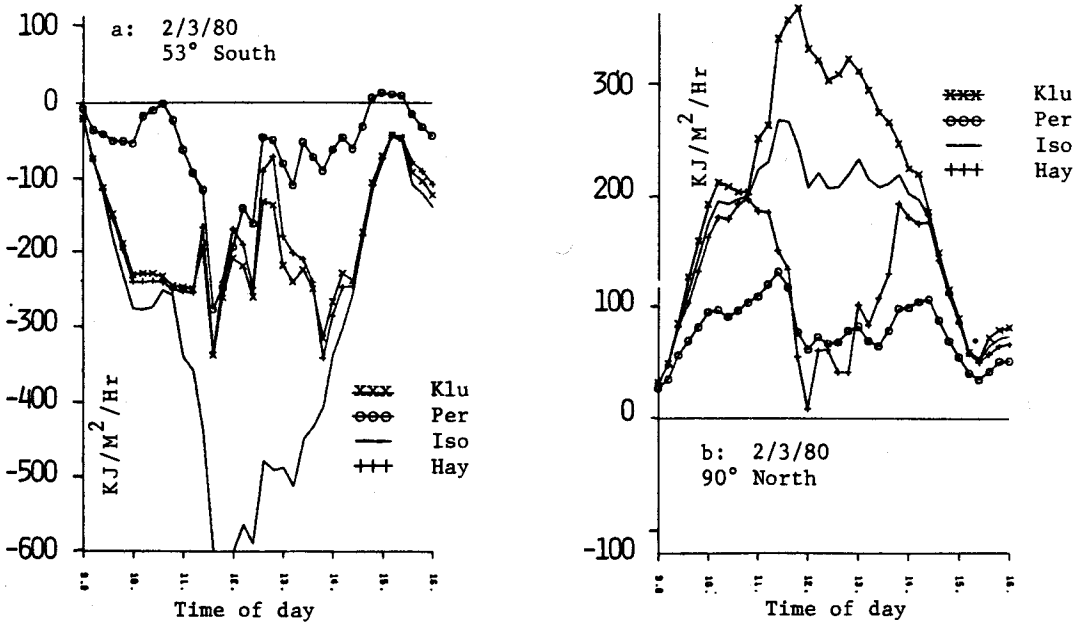

Fig. 6. Daily variations of modeled minus measured irradiance on a thin overcast, winter day based on February 3, 1980 one-minute data, in Albany, NY.

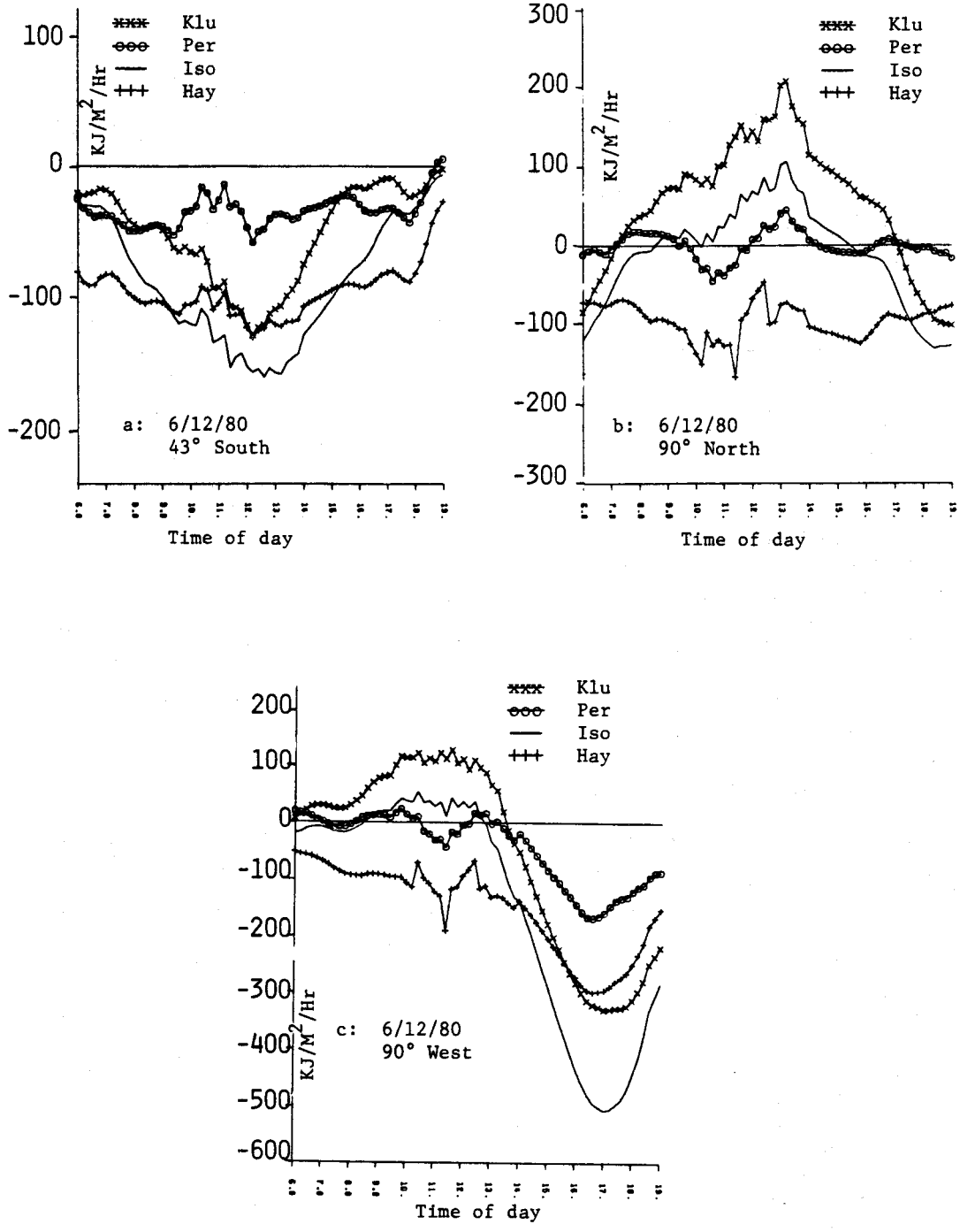

Fig. 8. Daily variations of modeled minus measured irradiance on a clear summer day, based on June 12, 1980 one-minute data in Albany, NY.

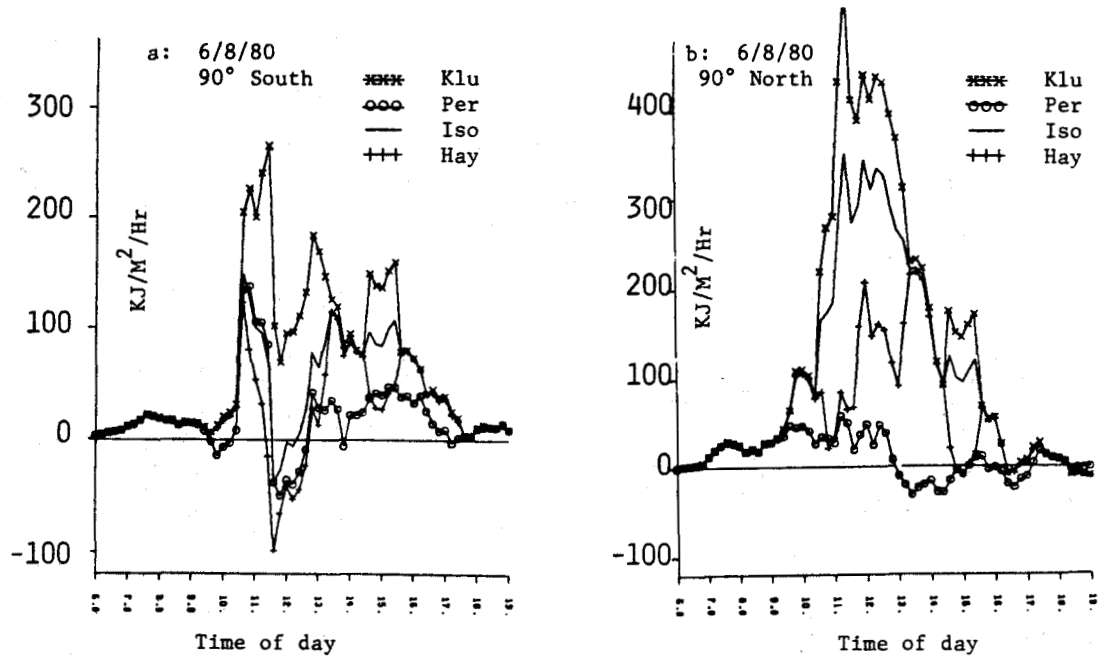

Fig. 9. Daily Variations of modeled minus measured irradiance on a high turbidity summer day, June 8, 1980, based on one-minute data from Albany, NY.

through (c) (June 8, 1980, 43° south, vertical north and west sensors, respectively) and Figs. 9a and b (June 12, 1980, vertical north and south sensors).

It will be noted that all curves presented have been smoothed using a five point averaging method.

4. DISCUSSION

4.1 *Model configurations—parametrization of sky conditions*

The experimental relationship established between F_1, F_2 and the parameters describing sky conditions is found to be similar for all stations. Circumsolar brightening is found to be the dominant anisotropic effect for all conditions (Fig. 2—F_1), but horizon brightening becomes important for clear sky events (Fig. 2—F_2). This is consistent with previous observations[19], where Mie scattering (i.e., forward scattering) dominates in aerosol charged atmospheres, whereas Rayleigh scattering (i.e., multiple scattering, retroscattering, near the horizon) prevails for clear conditions.

Two points of interest will be noted:

(1) A sky description scheme based only on the relative importance of direct radiation (e.g., Hay, Klucher) will overlook several interesting configurations, such as the circumsolar radiance enhancement observed for bright atmospheres where there is no or little direct beam (high Dh, low ε).

(2) The proposed (Dh, ε) grid appears to account globally for most "intermediate" sky configurations. This is best seen through the following example:

The climatic difference between the stations of Trappes and Carpentras is obvious when comparing Figs. 4(a) and (b). Distribution of hourly events in Carpentras shows a large majority of clear to very clear occurrences (high ε, medium to low Dh), whereas events distribution in Trappes reveals numerous overcast and "intermediate conditions," e.g., broken clouds of all types, thin overcast. However the circumsolar/horizon brightening patterns observed in Figs. 2(a) and 2(b), and described in the previous section, are very similar. This is particularly interesting for the middle (high Dh, low to medium ε) portion of these graphs. A wide range of possible "intermediate" sky configurations from several locations exhibit a comparable long term radiance distribution. Hooper and Brunger[20] made a similar observation based on long-term radiance measurements.

Hence, based on the above and observed model performance, it is reasonable to state that the proposed weather parameterization constitutes an adequate basis to describe prevailing radiance distribution in the atmosphere, in most instances.

4.2 *Overall performance*

Both the model physical framework and the sky condition parameterization are assessed through analysis of the independent tests presented above. Performance against ground-shielded data from three widely different solar environments show that they both constitute an adequate approach to the modelization of irradiance on a slope.

Indeed, after fair testing, substantial performance improvement over existing anisotropic models is found for all orientations and all stations when using the RMS error as a standard (Table 5). Per-

formance improvement based on MB error is also remarkable for almost all stations and sensor orientations.

4.3 *Site/climate dependency*

Site dependency is not found in the first approach to be a major stumbling block for the model. However, the F_1/F_2 pattern differences between stations, and the margin for performance improvement from independent to dependent testing are certainly worth additional investigation.

Two possible causes had been originally advanced[8] to explain performance and model configuration differences between sites. These are the following: (1) Climatical/geographical reasons and (2) instrumentation differences. It appears at this point that the influence of the latter is secondary because of the following reasons:

(a) As the most sensitive instrumentation difference between sites is the method for excluding ground-reflection, variations in the quantity of horizon brightening observable for each site should be explained on this basis. However, Trappes and Albany, where two opposite methods for removing ground-reflected irradiance are used—sky shields vs ground shields—exhibit very similar patterns for horizon brightening. Nevertheless, a more complete investigation (e.g., side by side comparison) is needed to eliminate any doubts regarding this matter.

(b) Most observed differences can be logically associated with climatic/geographical differences. These are as follows:

(1) Clear sky horizon brightening is found to be the most pronounced for the highest station, San Antonio, Texas. Indeed, the multiple and retroscattering occurring near the horizon should play an increasing role as altitude increases and radiance from the top of the atmosphere decreases.

(2) Horizon brightening is found to be more intense for the two driest stations (Carpentras and San Antonio). The higher ground albedo associated with dry climate vegetation, and the resulting intensified retroscattering, could explain this observation.

(3) Performance improvement from an Albany-derived model to a station-derived model is larger when climatic differences are more pronounced (e.g., Trappes vs. Carpentras—compare climatic differences: Fig. 4(c) with Figs. 4(a) and 4(b).

The logical follow-up of this work is to analyze the model configuration obtained for a set of specific climate/altitude/environment stations, and to assess the validity of interpolation between sites.

4.4 *Performance vs. reference models—Perez model's limitations*

Real time analysis reveals specific points of interest, contrasting the Perez model's performance with that of the selected reference standards.

The first important point to be noted is that the isotropic model is inadequate for applications requiring dynamic simulations. This is best seen on February 3 for the south-facing 53° slope, where the error generated exceeds 600 JK/m^2/hr (35%) around noon time. It will be noted that an error of that magnitude will persist from sunrise to sunset for tracking flat plate collectors and would likely be increased for low concentrators.

The strength of the proposed design compared to the two anisotropic references is twofold:

(1) The weather condition parametrization includes both direct and diffuse radiation, treated as independent variables, rather than direct radiation only. This may be seen clearly on Fig. 6 to a lesser extent on Figs. 7 and 8. There was almost no direct radiation present on February 3 before 11 AM and after 2 PM, although diffuse radiation was intense. Only the proposed model differed noticeably from the isotropic configuration and could account for part of the existing anisotropy.

(2) This model can go from a circumsolar enhancement configuration to a circumsolar + horizon enhancement configuration depending on the type of sky condition, whereas the Hay model is purely circumsolar; and while the Klucher model includes both circumsolar and horizon brightening, the two terms are not allowed to vary independently. The lack of horizon brightening in the Hay model will cause it to underestimate on clear days for surfaces which do not face the sun (see Fig. 5(b), afternoon, Fig. 5(c) and Fig. 8(c)); it will also underestimate on clear days for all orientations when the zenith angle is small (see Figs. 8(a)–8(c)). On the other hand, the structure of the Klucher model is responsible for its tendency to overestimate for slopes that do not face the sun, particularly on high turbidity days when forward scattering is the only noticeable effect. This is particularly visible on Fig. 9(b) where the overestimate exceeds 100% between 11 AM and 12 PM.

It will also be noted that the Klucher model is bound by design to generate energy values larger than the isotropic values (this may be seen in all tables and daily plots). Additionally, there is a limit by which isotropic values can be exceeded by this model (this limit is equal to 2.7 for $F = 1$, $z = 90°$ and $\theta = 0°$). Consequently, it will not perform as well as either the Hay or the Perez model when directional scattering is very intense—see for example Fig. 5(b) between 9 AM and 11 AM.

The proposed design also reaches its limits, which are most apparent when looking at the real time plots, since there still exists some deviation between modeled and measured values. This performance limitation may be assessed by looking at dependent tests results on Tables 4(a)–4(d). The best achievable RMS errors over a long term period will typically be of the order of 11 to 18 Watts/m^2 for all orientations. Any improvement beyond this point would likely require a more complex ap-

proach to diffuse radiation modeling. However, it will be remarked that simple model design modifications presently under study have been observed to push that limitation another step further. This involves notably differential horizon brightening as a function of azimuth.

4.5 *Model status, developmental work in progress*

There are two points of interest which are now being investigated, or which will require additional work. These are the following:

(1) Establishment of a comprehensive climate/geography/environment/model configuration relationship, based on existing or new data bases at selected sites (e.g., based on classifications such as [19]), as well as investigation of potential site interpolations.

(2) Model design improvements, such as framework modifications as mentioned above, or sky condition parametization based on another combination of the three selected variables—notably, the use of z as dependent rather than independent variable will be investigated. Design improvements will be limited to those requiring no more input parameters than presently used. Also, model end-use simplifications will be investigated. These will noticeably include the use of analytical functions rather than three-dimensional matrices for the coefficients F_1 and F_2, as soon as final model configurations are obtained from extended data analysis.

CONCLUSION

The model, which has been presented, is based on three basic ideas: (1) a geometrical representation of the sky dome incorporating variable circumsolar and horizon atmosphere brightening, (2) a parametric description of the insolation conditions, based on available radiative quantities, and (3) an experimentally-derived law governing the variations of circumsolar and horizon brightening with the insolation conditions.

Model performance is found to be adequate when independently tested against hourly tilted irradiance data sets from Trappes and Carpentras, France, and San Antonio, Texas. Ground-reflected irradiance was either removed at the acquisition site, or independently measured, thereby eliminating assumptions on that matter. Results reveal a systematic performance improvement by this model over the isotropic model and the models of Hay and Klucher, which were used as references. The isotropic RMS errors are typically reduced by 40–60% while Hay's and Klucher's are typically reduced by 25–40% and 20–60%, respectively.

Within this study's context, site-dependency is not found to be a major stumbling block for either the insolation parametrization method or the model itself. This is quite apparent by looking both at the Albany derived model performance and at the similar experimentally-derived laws obtained from the two widely different climate environments of Trappes and Carpentras.

However, there exists a substantial margin for performance improvement, as demonstrated by the results of dependent model tests. These suggest that climate (hence vegetation) and altitude have an influence on the model's configuration and performance which can be interpreted on a deterministic basis. A systematic analysis of their influence, involving several climate/altitude pilot sites will certainly be worth the effort, as typical long-term RMS error could be reduced down to about 15 Wm^{-2} for fixed surfaces of any orientations. This performance improvement is likely to be even more noticeable when considering tracking flat plate or low concentration captors.

Acknowledgement—This work was supported by USDOE contract #DEFG0577ET20182 and by the Atmospheric Sciences Research Center's Energy Group.

REFERENCES

1. IEA Solar Heating and Cooling Programme, Task IX Solar radiation and pyranometry studies. International Energy Agency, Paris, France.
2. C. C. Y. Ma and M. Iqbal, Statistical comparison of models for estimating solar radiation on inclined surfaces. *Proc. of ASES*, Minneapolis, Minnesota, 871 (1983).
3. P. S. Lunde, Prediction of the performance of solar heating systems utilizing annual storage. *Solar Energy*, **22**, 69 (1979).
4. D. Menicucci and Fernandez, Verification of Photovoltaic System modeling codes based on system experimental data. *Proc. XVIIth IEE Photovoltaic Specialists Conference*, Kissimmee, Fla. (1984).
5. V. M. Puri, R. Jimenez and M. Menzer, Total and non-isotropic diffuse insolation on tilted surfaces. *Solar Energy* **25**, 85 (1980).
6. J. E. Hay and J. A. Davies, Calculation of the the solar radiation incident on an inclined surface. *Proc. 1st Canadian Solar Radiation Data Workshop*. J. E. Hay and T. K. Won, Toronto, pp. 59–72 (1980).
7. T. M. Klucher, Evaluation of models to predict insolation on tilted surfaces. *Solar Energy*, **23**, 111 (1978).
8. R. Stewart and R. Perez, Validation of an anisotropic model estimating insolation on Tilted Surfaces. Proc. of ASES, Anaheim, California, 639–644 (1984).
9. R. R. Perez, J. T. Scott and R. Stewart, An anisotropic model for diffuse radiation incident on slopes of different orientations, and possible applications to CPCs. *Proc. of ASES*, Minneapolis, Minnesota, 883–888 (1983).
10. M. Kano, Effect of a turbid layer on Radiation Emerging from a Planetary Atmosphere. Doctoral Dissertation, University of California, Los Angeles (1964).
11. A. Zelenka, Personal Communication, Swiss Meteorological Institute, Zurich, Switzerland (1984).
12. Direction de la Meteorologie, Service Meteorologique Metropolitain, Stations #260 (Trappes) and 874 (Carpentras), Paris, France.
13. Solar Energy Meteorological Research and Training Site Region V, San Antonio, Texas (1981).
14. Solar Energy Meteorological Research and Training Site Region II, Albany, New York (1980).

15. B. Y. H. Liu and R. C. Jordan, The interrelationship and characteristic distribution of direct, diffuse and total solar radiation. *Solar Energy*, **4**, 1 (1960).
16. A. Lebru, Cahier du CSTB 1847, #239. Centre Scientifique et Technique du Batiment, SophiaAntipolis, France (1983).
17. R. C. Temps and K. L. Coulson, Solar radiation incident upon slopes of different orientations, *Solar Energy*, **19**, 179 (1977).
18. K. L. Coulson, *Solar and Terrestrial Radiation*, pp. 84–100. Academic Press, New York (1975).
19. R. C. Callino and M. S. Vojtesak, Solar Climates of the United States based on Long-Term monthly averaged daily insolation values, *Solar Energy* **31**, 283 (1983).
20. M. A. Rosen, F. C. Hooper and A. P. Brunger, The characterization and modelling of the diffuse sky radiance. *Proc. of ISES*, Montreal, Canada (1985).

Solar Energy Vol. 39, No. 3, pp. 221–231, 1987
Printed in the U.S.A.

0038-092X/87 $3.00 + .00

A NEW SIMPLIFIED VERSION OF THE PEREZ DIFFUSE IRRADIANCE MODEL FOR TILTED SURFACES

RICHARD PEREZ† and ROBERT SEALS
Atmospheric Sciences Research Center, SUNY at Albany, Albany, NY 12222, U.S.A.

PIERRE INEICHEN†
Universite de Geneve, Groupe de Physique Appliquee, Geneve 4, CH-1211 Switzerland

RONALD STEWART†
Atmospheric Sciences Research Center, SUNY at Albany, Albany, NY 12222, U.S.A.

DAVID MENICUCCI
Sandia National Laboratories, Albuquerque, NM 87185, U.S.A.

Abstract—A new, more accurate and considerably simpler version of the Perez[1] diffuse irradiance model is presented. This model is one of those used currently to estimate short time step (hourly or less) irradiance on tilted planes based on global and direct (or diffuse) irradiance. It has been shown to perform more accurately than other models for a large number of locations worldwide. The key assumptions defining the model remain basically unchanged. These include (1) a description of the sky dome featuring a circumsolar zone and horizon zone superimposed over an isotropic background, and (2) a parameterization of insolation conditions (based on available inputs to the model), determining the value of the radiant power originating from these two zones. Operational modifications performed on the model are presented in a step by step approach. Each change is justified on the basis of increased ease of use and/or overall accuracy. Two years of hourly data on tilted planes from two climatically distinct sites in France are used to verify performance accuracy. The isotropic, Hay and Klucher models are used as reference. Major changes include (1) the simplification of the governing equation by use of reduced brightness coefficients; (2) the allowance for negative coefficients; (3) reduction of the horizon band to an arc-of-great-circle; (4) optimization of the circumsolar region width; and (5) optimization of insolation conditions parameterization.

1. INTRODUCTION

It is a current practice, for evaluating the energy received by a tilted surface, to decompose the solar radiation into three components which are treated independently[1]: Direct beam, sky diffuse and ground-reflected.

Models differ generally in their treatment of the sky diffuse component which is considered as the largest potential source of computational error[2]. While the treatment of the direct component is straightforward and virtually error-free for flat surfaces, that of the ground reflected component may also be a cause of computational errors which are in most instances, however, of lesser overall impact than that caused by a poor description of the sky hemisphere.

In a separate paper, the authors investigate this last point and describe simple guidelines to account adequately for the ground reflected component[3]. The model discussed in this paper focuses on the treatment of the sky diffuse component.

Originally developed to handle instantaneous events[1, 4], the Perez model, as it has become to be known, has been more extensively used for hourly applications. Although it requires no more input than the most simple model assuming isotropic sky[5], i.e. global and direct or diffuse irradiance, it has been found to perform substantially better than that as well as other widely used anisotropic models [e.g. 6–8] when tested against independent data sets [e.g. 9–12].

The model was recently incorporated into Sandia National Laboratories' (SNL) photovoltaic simulation program, PVFORM[13]. However, more widespread application of this model has been subject to question because of (1) the fact that it was quite more complex to use than other models and (2) the fact that it had not yet been validated for an extended set of environments.

The first point is addressed to a large extent in this paper: A new simpler and slightly higher performance, version of the model is presented.

The second of these concerns is being addressed by Sandia National Labs who currently conducts an extensive measurement program geared to validate and/or configure the model for different key climatic environments[14]. The impacts of atmospheric moisture and aerosol content, regional albedo, altitude and local skylines are notably investigated. Results will be reported subsequently.

2. METHODS

2.1 *Background information on original model*

The Perez diffuse irradiance model incorporates two basic components. The first is a geometric de-

† Member ISES.

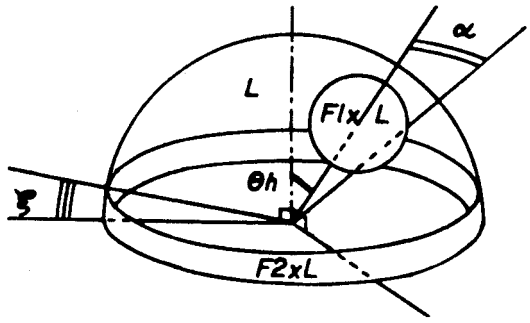

Fig. 1. Perez model's representation of the sky hemisphere

scription of the sky hemisphere superimposing a circumsolar disc and horizon band on an isotropic background (Fig. 1). This configuration was chosen to account for the two most consistent anisotropic effects in the atmosphere: Forward scattering by aerosols and multiple Rayleigh scattering and retroscattering near the horizon. Assuming that radiances in the circumsolar and horizon regions are, respectively, equal to F_1 and F_2 times that of the background, then the diffuse irradiance D_c, impinging on a plane of slope s, is obtained from the horizontal diffuse D_h using

$$D_c = D_h \left[\frac{0.5(1 + \cos(s)) + a(F_1 - 1) + b(F_2 - 1)}{1 + c(F_1 - 1) + d(F_2 - 1)}\right], \quad (1)$$

where a and b are the solid angles occupied, respectively, by the circumsolar region and the horizon band weighted by their average incidence on the slope. The parameters c and d are the equivalent of a and b for the horizontal. These are specified in the nomenclature.

The second component is empirical and establishes the value of the brightness coefficients F_1 and F_2 as a function of the insolation conditions. These conditions are parameterized by three quantities which describe, respectively, the position of the sun, the brightness of the sky dome, and its clearness. These quantities are, respectively, (1) the solar zenith angle Z; (2) the horizontal diffuse irradiance D_h; and (3) the parameter ϵ equal to the sum of D_h and direct normal I divided by D_h. It will be noted that these three quantities require no more input than is normally required by other models to compute hourly irradiance on a slope.

As an example of this parameterization, a scatter plot is presented in Fig. 2 which shows the distribution, in the (D_h, ϵ) plane at $Z \simeq$ constant of hourly observations recorded during a three-year period in Trappes and Carpentras, France[15]. In this figure, D_h has been normalized to extraterrestrial global and is referred to as "delta". This shows the dependent character of D_h and ϵ for high ϵ's (clear skies) and their independent nature for low ϵ's (overcast and partly cloudy cases).

For practical applications the (Z, D_h, ϵ) space was divided into 240 sky condition categories (5 for Z, 6 for D_h and 8 for ϵ). For each category, a pair of (F_1, F_2) coefficients was established. These coefficients were obtained from the least square fitting of eqn (1) to actual data recorded on sets of sloping pyranometers.

2.2 *Summary of changes from original to present model configuration*

The rationale behind each modification was to render the model less complex to use while either maintaining or improving its accuracy. This was judged by testing each version of the model against the three-year data sets from Trappes and Carpentras, France, including hourly global irradiance

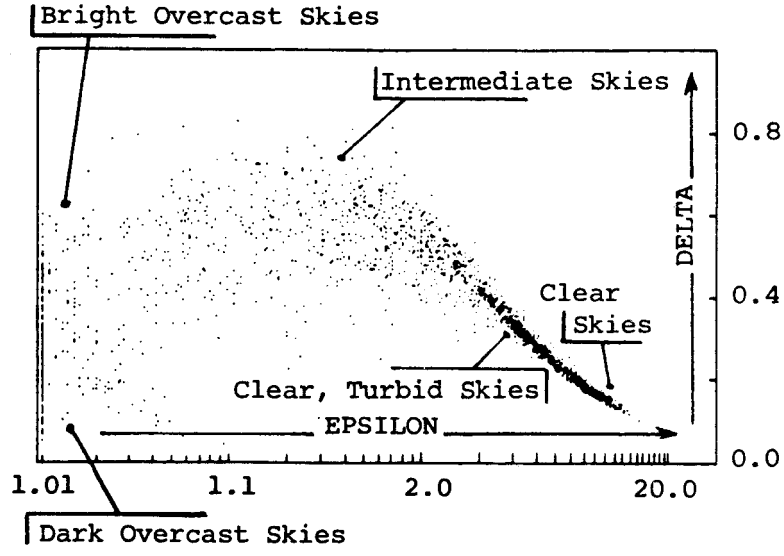

Fig. 2. Distribution of observed hourly events in Trappes and Carpentras (two years of data), in the D_h, ϵ plane for $Z \in [45°, 55°]$.

measurements on five tilted surfaces. The results of these tests are presented in the next section.

2.2.1 *Use of reduced brightness coefficients.* An important drawback of eqn (1) is its non-linearity with respect to F_1 and F_2 as defined earlier. The determination of these coefficients through least square fitting calls notably for a series of approximations and for solving sets of non-linear equations which may require considerable computation.

A major step toward simplification was taken by rewriting the model's governing equation using redefined brightness coefficients. Equation (1) may be written as [16]

$$D_c = D_h \left(\frac{D_c^i + D_c^c + D_c^h}{D_h^i + D_h^c + D_h^h} \right), \qquad (2)$$

where the superscripts i, c and h refer, respectively, to the diffuse contribution, on the horizontal or the slope, of the isotropic background of the circumsolar and the horizon regions. Noting that the denominator of the right-hand side of eqn (2) is equal to D_h, this may be written as

$$D_c = D_h \left(\frac{D_c^i}{D_h} + \frac{D_c^c D_h^c}{D_h D_h^c} + \frac{D_c^h D_h^h}{D_h D_h^h} \right). \qquad (3)$$

Further, one notes that D_c^c/D_h^c equal to a/c, that D_c^h/D_h^h is equal to b/d and that D_c^i is, by definition, given by

$$D_c^i = 0.5\,(1 + \cos(s))\,(D_h - D_h^c - D_h^h). \qquad (4)$$

Finally, if D_h^c/D_h is set equal to F_1' and D_h^h/D_h to F_2', eqn (3) becomes

$$D_c = D_h[0.5(1 + \cos(s))\,(1 - F_1' - F_2') + F_1'(a/c) + F_2'(b/d)]. \qquad (5)$$

Equation (5) is linear with respect to the terms F_1' and F_2' defined as reduced brightness coefficients. Conceptually they represent the respective normalized contributions of the circumsolar and horizon regions to the total diffuse energy received on the horizontal, whereas the original coefficients represent the increase in radiance over the background in both regions. For instance, a value of 0.5 for F_1' indicates that 50% of horizontal diffuse behaves approximately as direct radiation, whereas a value of F_2' equal to 0.2 indicates that a vertical surface will access an additional amount of energy equal to 20% of the horizontal diffuse radiation.

The relationship between the reduced coefficients and the original ones are the following:

$$F_1' = c(F_1 - 1)/[1 + c(F_1 - 1) + d(F_2 - 1)], \qquad (6)$$

$$F_2' = d(F_2 - 1)/[1 + c(F_1 - 1) + d(F_2 - 1)]. \qquad (7)$$

It will be noted that eqns (5) and (1) define exactly the same model framework. As before, the new coefficients may be derived empirically from experimental data recorded on sloping surfaces.

2.2.2 *Allowance for negative coefficients.* In its original setup the model did not allow for coefficients smaller than one (i.e. negative reduced coefficients). In other words the model returned to an isotropic configuration whenever observations could not be explained by an increase in radiance in either of the anisotropic regions. This setup explained most situations except overcast occurrences when the top of the sky dome is the brightest region[17].

Although negative coefficients are physically meaningless (since by definition this would mean negative energy received from a region in the dome), the use of negative F_2' coefficients is equivalent, as far as flat plate surfaces are concerned, to adding a third brighter region at the top of the sky hemisphere. This new setup yields noticeable performance improvements particularly for climates where cloudy conditions prevail.

2.2.3 *Geometric framework modifications.* (a) *Horizon band*: The original configuration called for a 6.5° elevation horizon band. A rigorous definition of the term b in eqn (1) or (5) is rendered complex by such assumption. This was partly circumvented in the original model by accounting only for the half horizon band facing the slope, thus causing a discontinuity between the horizontal and slopes approaching 0°.

A much simpler configuration is now proposed whereby all the energy of the horizon band is contained in an infinitesimally thin region at 0° elevation. Equation (5) becomes

$$D_c = D_h[0.5(1 + \cos(s))\,(1 - F_1') + F_1'(a/c) + F_2' \sin(s)]. \qquad (8)$$

(b) *Circumsolar region*: The circumsolar region was originally set at 15° half angle. A much simpler approach would be to assume that all circumsolar energy originates from a point source; In this case eqn (8) may be simply written as follows:

$$D_c = D_h[0.5(1 + \cos(s))\,(1 - F_1') + F_1'(\cos(\theta_c)/\cos(Z)) + F_2 \sin(s)]. \qquad (9)$$

However, unlike for the horizon band, this simplification causes small performance deterioration, noticeable for the non-south orientations—for which low sun incidence events and therefore the physical size of the circumsolar region have a larger impact. A 25° half-angle circumsolar region was found to provide the best overall performance and is used as a basis to illustrate the impact of the other simplifications and changes described hereafter. The 0° point source option will be proposed as an alternative version of this model. Its operational configuration is reported in Section 3. For infor-

mation, performance validation results using the model with 35°, 25°, 15° and point source circumsolar regions are presented in Table 5.

It is important at this point to remind the reader that the circumsolar representation used in this model (fixed width, homogeneous circular zone) is acceptable only for collecting elements with wide field of view (e.g. flat plate collectors). It would be inaccurate to use this representation as is to compute radiance (or luminance) in specific points of the sky dome. This would require a more detailed description of the forward scattered radiation, accounting for actual radiance profiles and for their variations with insolation conditions (e.g. see [18]). The same is true for the horizon brightening representation used in this model. An expanded version of the model, suited for such applications, is currently under development.

2.2.4 *Optimization of insolation parameterization.*

(a) *Replacement of D_h by Δ*: The second quantity selected to describe insolation conditions (horizontal diffuse irradiance, D_h) is not totally independent from the first quantity (solar zenith angle). Independence between these two dimensions describing, respectively, the position of the sun and the brightness of the sky may be achieved by selecting a new second dimension, Δ, defined as

$$\Delta = (D_h m)/I_0,$$

where m is the relative air mass and I_0 the extraterrestrial radiation. Normalization with respect to I_0 also renders this dimension independent of the users' unit.

(b) *Redefinition of the Δ, ϵ, Z grid*: The discrete sky condition 3D space associated with the original model is composed of 240 categories.

Each of these specifies a pair of coefficients. This approach was chosen primarily to facilitate observational analysis of experimental data. It has the advantage of requiring no computation for querying F_1' and F_2' for a given sky condition; however, the user must carry a table of 480 terms.

An alternate approach would consist of using analytical functions for F_1' and F_2'. Although simpler in concept, the fully analytical approach was rejected because of the added computational time caused by a rather complex formulation. This complexity is due mostly to the variable ϵ which requires a five degree polynomial (i.e. a 24 term expression if the variations with Δ and Z are assumed linear) to approach the precision of the original grid-based approach.

A compromise is proposed here, whereby F_1' and F_2' are expressed as analytic functions of Δ and Z while an eight-category discrete axis is kept for ϵ. The partition of that axis is optimized to provide the same mean variation of F_1' and F_2' in each category, based on the four-year experimental data set pooled from the two French sites. The analytic function in each ϵ category is of the form $e + fZ + g\Delta$, where e, f, g are constants. Indeed, variations with Z and Δ are found to be well-explained by independent linear approximations.

3. RESULTS

3.1 *New model formulation*

The new governing equation of the model is given in section 2.2.3. [eqn (8)]. All terms were defined above and are summarized in the nomenclature. The reduced coefficients $F_1'(Z, \Delta, \epsilon)$ and $F_2'(Z, \Delta, \epsilon)$ are given in Table 1. A simpler, slightly less accurate version of this new model [eqn (9)], is also introduced; the corresponding brightness coefficients are given in Table 2.

Scatter plots in Figs. 3, 4 and 5 illustrate the variations of F_1' and F_2' with respect to Z, Δ and ϵ, respectively. Variations with Z were plotted for ϵ values comprised between 2.5 and 5 corresponding to intermediate to clear and turbid skies. Variations with Δ were plotted for $\epsilon < 1.05$, that is, for overcast

Table 1. Generic circumsolar (F_1') and horizon brightening (F_2') coefficients developed from Trappes and Carpentras data for the 25° circumsolar model

ϵ bin #	Upper limit	Cases^ (%)	25° circumsolar region F_{11}'	F_{12}'	F_{13}'	F_{21}'	F_{22}'	F_{23}'
1	1.056	24.8	−0.011	0.748	−0.080	−0.048	0.073	−0.024
2	1.253	9.32	−0.038	1.115	−0.109	−0.023	0.106	−0.037
3	1.586	7.17	0.166	0.909	−0.179	0.062	−0.021	−0.050
4	2.134	7.88	0.419	0.646	−0.262	0.140	−0.167	−0.042
5	3.230	10.85	0.710	0.025	−0.290	0.243	−0.511	−0.004
6	5.980	18.57	0.857	−0.370	−0.279	0.267	−0.792	0.076
7	10.080	15.17	0.734	−0.073	−0.228	0.231	−1.180	0.199
8	—	6.96	0.421	−0.661	0.097	0.119	−2.125	0.446

$$F_1' = F_{11}'(\epsilon) + F_{12}'(\epsilon)^*\Delta + F_{13}'(\epsilon)^*Z$$
$$F_2' = F_{21}'(\epsilon) + F_{22}'(\epsilon)^*\Delta + F_{23}'(\epsilon)^*Z$$

^ Percent of total cases for 2 years each of Trappes and Carpentras, France.

Table 2. Generic circumsolar (F_1') and horizon brightening (F_2') coefficients developed from Trappes and Carpentras data for the point source circumsolar model

ϵ bin #	Upper limit	Cases^ (%)	Point source circumsolar region					
			F_{11}'	F_{12}'	F_{13}'	F_{21}'	F_{22}'	F_{23}'
1	1.056	24.08	0.041	0.621	−0.105	−0.040	0.074	−0.031
2	1.253	9.32	0.054	0.966	−0.166	−0.016	0.114	−0.045
3	1.586	7.17	0.227	0.866	−0.250	0.069	−0.002	−0.062
4	2.134	7.88	0.486	0.670	−0.373	0.148	−0.137	−0.056
5	3.230	10.85	0.819	0.106	−0.465	0.268	−0.497	−0.029
6	5.980	18.57	1.020	−0.260	−0.514	0.306	−0.804	0.046
7	10.080	15.17	1.009	−0.708	−0.433	0.287	−1.286	0.166
8	—	6.96	0.936	−1.121	−0.352	0.226	−2.449	0.383

$$F_1' = F_{11}'(\epsilon) + F_{12}'(\epsilon)^*\Delta + F_{13}'(\epsilon)^*Z$$
$$F_2' = F_{21}'(\epsilon) + F_{22}'(\epsilon)^*\Delta + F_{23}'(\epsilon)^*Z$$

^ Percent of total events for 2 years each of Trappes and Carpentras, France

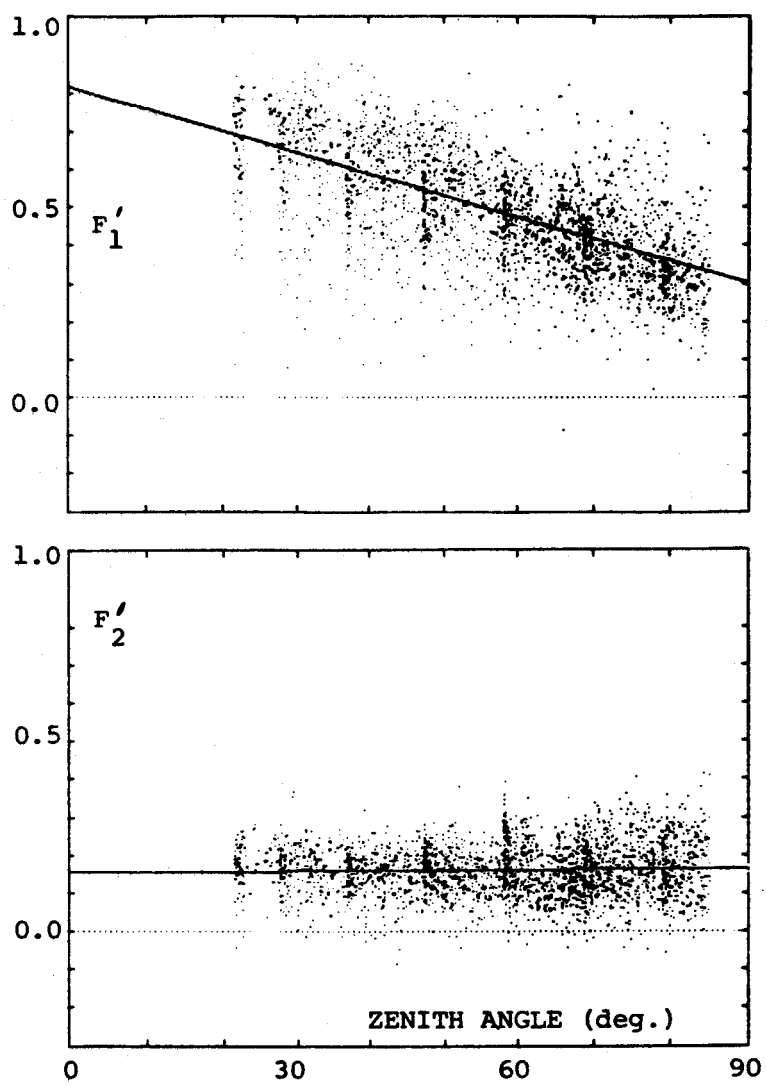

Fig. 3. Variations of F_1' and F_2' with solar zenith angle for $\epsilon \in [2.5, 5]$. Results based on two years of data from Trappes and Carpentras.

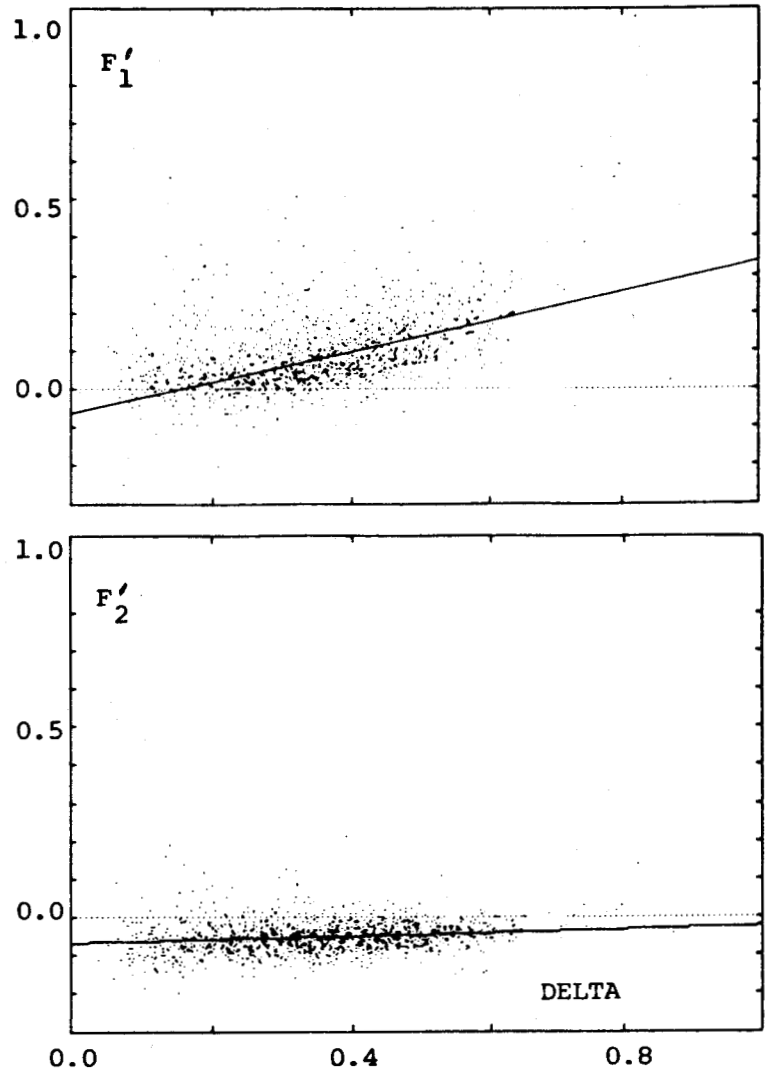

Fig. 4. Variations of F_1' and F_2' with Δ for $\epsilon < 1.05$. Results are based on two years of data from Trappes and Carpentras.

conditions, while variations with ϵ were plotted for zenith angles ranging from 45° to 55°.

The use of linear approximations for explaining the variations of F_1' and F_2' with Δ and Z for given ϵ intervals are clearly justified by these plots. Variations with ϵ are more difficult to express with simple analytic expressions.

These plots confirm past observations made about the brightness coefficients: (1) evidence of circumsolar brightening for bright overcast skies; (2) maximum of circumsolar brightening for partly cloudy to clear highly turbid atmospheres; (3) decrease of circumsolar brightening and marked increase of horizon brightening for low turbidity clear skies; (4) fairly low scatter in experimentally derived F_1' and F_2'—this is particularly interesting for intermediate skies given the large number of possible sky configurations falling into that category. It will be noted, concerning this last point, that much of the dispersion for $\epsilon < 2$, (see Fig. 5), may be explained by variations of Δ.

These results are based on the analysis of a composite data file from Trappes and Carpentras, France, including two years of hourly measurements for each site (Ref. [12]). The measurements include global irradiance, direct irradiance and global irradiance on a 45° tilt south plane and vertical south, west, north and east planes. Ground-reflected irradiance was available from sky-shielded vertical pyranometers facing north and south and was effectively removed from the tilted global measurements as described in [10].

The sites of Trappes and Carpentras represent two different climatic environments (respectively, marine temperate and Mediterranean). They constitute, therefore, an acceptable basis to use the model for climates ranging between these two extremes.

The reader is cautioned, however, that this model has not yet been validated for all possible solar environments. An active program is now underway[14] which will either validate existing for-

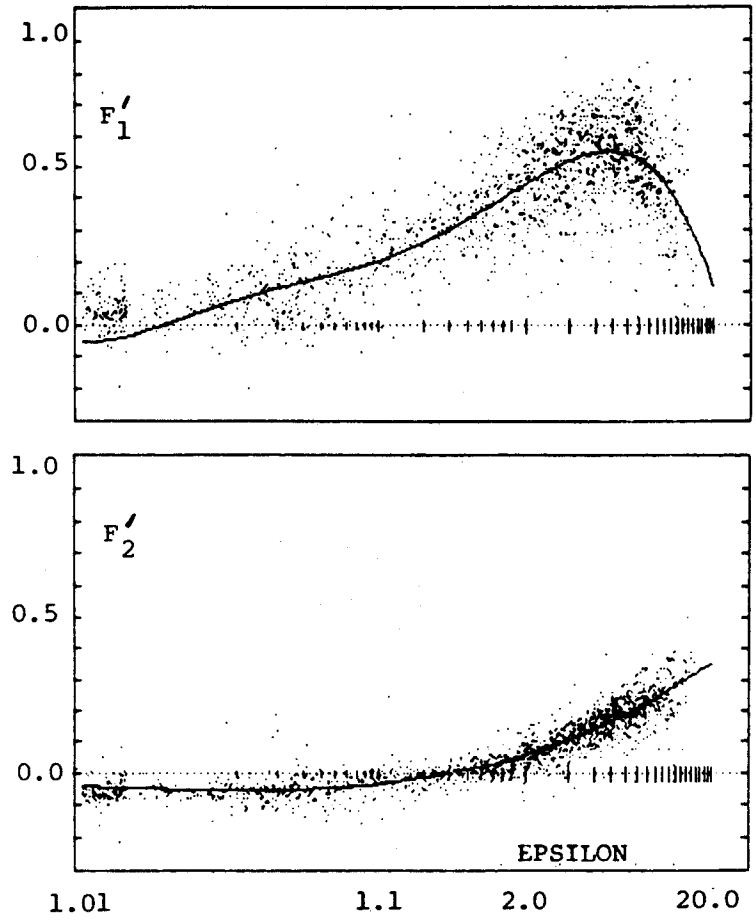

Fig. 5. Variations of F_1' and F_2' with ϵ for $Z \in [45°, 55°]$. Results are based on two years of data from Trappes and Carpentras.

mulations or provide sets of coefficients applicable to several key environments in the United States. This program investigates in particular the effects of altitude, regional albedo and seasonal local aerosol content on model configuration and performance.

3.2 *Model performance validation*

The value of the changes to the Perez model is considered from two perspectives. First, we examine the objective performance improvement in predicting diffuse radiation on sloping surfaces, and second, we examine the practical gain in terms of usability of the simplified model.

3.2.1 *Predictive performance-test results.* The main criteria used for model evaluation are the RMS and mean bias errors resulting from the actual and modeled diffuse. Test data are identical to that used to establish the coefficients, that is, two years of hourly data from both Trappes and Carpentras. In this respect the test of the Perez model may not be considered as independent. However, the pool of data is so large and the climates of the two sites so different that tests may be held as valid given the present status of knowledge in this area. More information on this aspect of the model will be obtained when SNL data becomes available for analysis[14].

Testing the model is a two-step process. First, the coefficients F_1 and F_2 must be generated. During this step, we may also observe the distribution of events with ϵ to optimize partitioning. Second, using the coefficients so generated, the model is used to calculate hourly radiation impinging on various surfaces. The errors generated are compared to three widely used models for reference. These are the isotropic[2], the Hay[3] and Klucher[4] models.

The Perez model has been tested at each step of the simplification discussed above. These results, based on Trappes and Carpentras data, are summarized in Table 3. Further, the original and the new model configurations' performances are compared for Albany, NY. Results are reported in Table 4. This is based on two years of SEMRTS hourly data[19].

The line labelled "Perez 1" is the original version of the model. Perez 2 through 7 are successive changes introduced in the model. The first step toward simplification is the introduction of a simpler governing equation (Perez 2). Note the slight loss

Table 3. Model performance test statistical results. Perez 1: original model; Perez 2 = Perez 1 + eqn (5); Perez 3 = Perez 2 + allowance for negative coefficients; Perez 4 = Perez 3 + eqn (8); Perez 5 = Perez 4 + 25° circumsolar region; Perez 6 = Perez 5 + use of Δ instead of D_h; Perez 7 = new model (25° circumsolar). Results are based on two years of hourly data from Trappes and Carpentras

Model	South 45°	North vertical	East vertical	South vertical	West vertical	Composite error
			RMS ERRORS ($kJ.m^{-2}.hr^{-1}$)			
Isotropic	163.1	119.8	159.0	155.4	151.0	150.4
Hay	94.3	87.9	112.7	98.4	101.7	99.3
Klucher	78.4	178.2	140.2	92.8	141.7	131.3
Perez 1	49.9	46.7	61.8	60.7	59.6	56.1
Perez 2	50.5	46.4	61.3	61.4	59.3	56.1
Perez 3	50.5	42.8	59.6	58.4	57.3	54.1
Perez 4	50.0	43.1	59.5	58.2	56.8	53.9
Perez 5	49.9	40.0	59.2	56.7	56.1	52.8
Perez 6	48.9	38.6	57.8	55.3	53.6	51.3
Perez 7	49.3	37.9	57.5	55.6	52.9	51.1
			MEAN BIAS ($kJ.m^{-2}.hr^{-1}$)			
Isotropic	−109.8	69.9	−37.4	−85.0	−27.5	72.5
Hay	−60.6	10.3	−38.9	−49.6	−26.9	41.2
Klucher	−39.1	121.1	30.6	−11.8	41.6	61.6
Perez 1	−8.5	24.4	−0.8	11.1	13.2	13.9
Perez 2	−8.6	25.1	0.8	11.8	14.3	14.5
Perez 3	−13.0	18.1	−6.2	4.8	7.3	11.1
Perez 4	−11.1	18.5	−6.5	3.8	7.0	10.7
Perez 5	−12.6	17.4	−6.3	6.1	7.5	10.9
Perez 6	−13.3	17.5	−5.8	5.5	7.9	11.0
Perez 7	−14.1	17.6	−6.5	4.7	7.1	11.2
Average Global	1369.2	232.5	619.1	848.6	610.6	
Average Diffuse	593.3	213.3	320.6	368.2	310.7	

Table 4. Model performance test statistical results for Albany, New York. Results are based on two years of hourly data

Model	South 43°	North vertical	East vertical	South vertical	West vertical	Composite error
			RMS ERRORS ($kJ.m^{-2}.hr^{-1}$)			
Isotropic	115.4	104.7	143.6	103.5	152.1	125.5
Hay	74.1	84.2	96.2	75.9	102.1	87.2
Klucher	51.2	158.4	134.2	79.5	141.7	120.1
Original Perez	40.8	36.3	55.1	68.8	63.2	54.3
New Perez *	39.9	31.5	53.2	61.9	60.0	50.7
New Perez ^	41.2	28.1	50.3	61.3	57.3	49.1
			MEAN BIAS ($kJ.m^{-2}.hr^{-1}$)			
Isotropic	−72.5	56.5	−23.7	−36.2	−18.4	46.2
Hay	−32.4	2.2	−31.6	−9.6	−23.9	23.3
Klucher	−12.3	102.3	35.0	27.8	41.7	53.6
Original Perez	4.1	14.6	−4.2	31.6	6.6	16.0
New Perez *	−3.6	5.8	−15.3	18.0	−4.4	11.2
New Perez ^	−5.5	4.6	−15.0	19.7	−4.2	11.8
Average Global	1350.4	233.9	584.4	794.5	579.6	
Average Diffuse	550.1	219.3	299.5	312.0	294.3	

* point source circumsolar; ^ 25° circumsolar region

on south surfaces. This loss seems a reasonable trade-off with the much simpler model equation.

Step 3 reflects the allowance for negative coefficients. The table of mean bias errors emphasizes the importance of this step. The RMS errors also experience a considerable benefit from this simple change. It will be noted that all performance gains from negative coefficients results from better handling of overcast conditions.

Another simplifying change in the model is the reduction of the physical horizon band to a linear quantity. In addition to greatly simplifying model implementation, this has also provided a small overall performance improvement as shown in Perez 4.

Setting the circumsolar half angle to 25 degrees, an increase from the original 15 degrees, provided the overall best results for the two test sites. This change is included in Perez 5—performance variations as a function of circumsolar region definition are also reported, for information, in Table 5. Another noticeable performance gain (Perez 6) resulted from the use of Δ instead of D_h.

The final change for this study is the consolidation of Δ and Z as functional components of the model coefficients, F_1' and F_2'. This is a fairly large evolutionary step for the model, and a slight accuracy loss is encountered on the south surfaces while slightly improving overall performance. This last step also includes optimization of ϵ axis partitioning.

3.2.2 *Computational improvement.* In assessing the computational improvement of the model, we will consider two points. First, the issue of model complexity. The model should be easy to implement and use for personal computer applications. It should also be simple enough to allow hand calculations if necessary. Second, we address the generation of coefficients, F_1' and F_2'. A research organization should be able to develop these coefficients locally, rather than depend on a generic set intended to satisfy a broad climate spectrum.

Determination of brightening coefficients for a given event: In the old version, F_1' and F_2' were each stored in a three-dimensional matrix of 240 elements. Obtaining F_1' and F_2' required a mapping of the continuous variables Δ, ϵ and z into this discrete space. On average, this would require eight comparisons for the mapping (2.5 for Δ, 3.5 for ϵ and 2 for Z), and two table readings.

For the new model, F_1' and F_2' are determined by two simple functions. We must still map ϵ to a discrete space requiring an average of 3.5 comparisons. Then, a total of six table look-up are required.

On a computer, the differences between the original and the new methods are negligible in terms of time: logically, the new method is much more straightforward. Both methods require initialization: the old needs two arrays of 240 elements each while the new needs six arrays of eight elements each. When computed by hand, or on a calculator, the user would probably read the values from a chart.

Model framework: The old model framework was a function of the type

$$R = (a + bF_1 + cF_2)/(1 + dF_1 + eF_2),$$

whereas the new model is a function of the type

$$R = a' + F_1'b' + F_2'c',$$

where a', b' and c' are all simple functions. Implementing the new model is far simpler than the old particularly if one uses the point source version. Although, the savings in computer time for a single run is probably not noticeable.

In general, the model has become simple enough that its use is practical under almost any circumstances.

Generation of Coefficients set: Most users will never need to generate coefficients for F_1' and F_2',

Table 5. Variations of model performance with size of circumsolar region. Results are based on two years of hourly data from Trappes and Carpentras

Circumsolar region sustaining half angle	South 45°	North vertical	East vertical	South vertical	West vertical	Composite error
			RMS ERRORS ($kJ.m^{-2}.hr^{-1}$)			
0°	49.3	43.8	61.8	57.6	56.0	54.1
15°	48.4	40.6	58.8	55.8	53.6	51.9
25°	49.2	37.9	57.4	55.5	52.8	51.0
35°	51.6	36.5	57.8	55.9	53.9	51.7
			MEAN BIAS ($kJ.m^{-2}.hr^{-1}$)			
0°	−10.4	19.3	−6.1	2.5	6.6	10.6
15°	−11.2	18.2	−6.7	3.3	6.5	10.5
25°	−14.0	17.6	−6.4	4.6	7.0	11.1
35°	−18.3	18.2	−4.0	8.0	8.8	12.9

as a well-rounded generic and/or environment-dependant set(s) will be made readily available[14]. However, research facilities with access to a solar data base may want to develop their own coefficients for a specific environment. This process is now greatly simplified. A program to solve a system of non-linear equations used to be required. This could consume considerable computing resources, and could generate non-converging solutions. Coefficient generations now involves only solving sets of linear equations.

4. CONCLUSIONS

A summary of the modifications performed on the Perez model to increase its simplicity, while maintaining or improving accuracy has been presented. While the key assumptions defining the model remain unchanged, substantial "operating" modifications have made the model fairly simple to implement and use for microcomputer-based applications, well in line with other, less accurate models.

Together with increased simplicity, the proposed changes result in improved accuracy on all tested orientations and slopes. Improvements were found to be most noticeable for vertical surfaces particularly for the north-facing one. A simplified "point source" version of this new model is also proposed. It also features improved accuracy on the original model, but to a lesser degree for non-south surfaces.

Each simplification was validated based on two years of hourly data from Trappes and Carpentras, France: two environmentally distinct sites featuring, respectively, humid oceanic and dry Mediterranean climates. Conclusions reached for these two sites were substantiated with data from Albany, New York.

The generic models established for the two French sites now feature an improvement of approximately 2.5–3 to 1 over the isotropic model. RMS errors for all orientations are kept under 16 W m^{-2} while mean bias errors are kept under 5 W m^{-2} for the two sites tested.

It will finally be noted that the main focus of this paper was to introduce a simpler version of a model which has already been extensively validated. Further questions remain concerning the potential impact of altitude, regional/seasonal albedo and local atmospheric moisture and particulate content on the model configuration (i.e. intensities of horizon and circumsolar brightening) and on its performance. However, it is not thought, based on existing validations, that these should have such an effect as to drastically change the performance hierarchy (i.e. isotropic versus Hay versus Klucher versus Perez) shown in Table 3. These questions are currently being addressed and will be the object of upcoming communications.

Acknowledgements—This work was supported by Sandia National Laboratories under Contract No. 56-5434. Parallel work funded by New York State ERDA and previous work funded by SERI were helpful to the development of this research. The authors acknowledge the critical and constructive comments of A. Zelenka of the Swiss Meteorological Institute.

NOMENCLATURE

z Solar zenith angle
F_1 Original circumsolar brightness coefficient
F_2 Original horizon brightness coefficient
D_c Diffuse irradiance impinging on a tilted surface
D_h Diffuse irradiance on the horizontal
s Plane tilt angle
a Solid angle occupied by the circumsolar region, weighted by its average incidence on the slope. In this study a is approximated as follows:

$$a = 2(1 - \cos\alpha)\chi_c$$

where α is the circumsolar region half angle and χ_c is given by

$$\chi_c = \psi_h \cos\theta_c \text{ if } \theta_c < \pi/2 - \alpha.$$
$$\chi_c = \psi_h\psi_c \sin(\psi_c\,\alpha)$$

if $\theta_c \in [\pi/2 \pm \alpha]$ and $\chi_c = 0$, otherwise, where θ_c is the incidence angle on the tilted plane, ψ_h is defined below (see term c) and $\psi_c = \{(\pi/2 - \theta_c + \alpha)/\alpha\}/2$

b Solid angle occupied by the horizon region, weighted by its average incidence on the slope. This is approximated as follows:

$$b = 2\xi'/\pi \sin\xi',$$

where ξ is the angular thickness of the horizon band and ξ' is given by

$$\xi' = (\pi - \xi)/\pi + \xi/2$$

c Solid angle occupied by the circumsolar region, weighted by its average incidence on the horizontal. In this study, c is approximated as follows:

$$c = 2(1 - \cos\alpha)\chi_h,$$

where χ_h is given by

$\chi_h = \cos Z$ if $Z < \pi/2 - \alpha$.
$\chi_h = \psi_h \sin(\psi_h\,\alpha)$, otherwise,
where ψ_h is given by
$\psi_h = (\pi/2 - z + \alpha)/2\alpha$ if $Z > \pi/2 - \alpha$
$\psi_h = 1$, otherwise

d Solid angle occupied by the horizon band weighted by its average incidence on the horizontal. d is given by

$$d = (1 - \cos 2\xi)/2$$

ϵ Sky clearness parameter given by

$$\epsilon = (D_h + I)/D_h,$$

where I is the direct normal incidence irradiance
Δ New sky brightness parameter given by

$$\Delta = D_h\, m/I_0$$

where m is the relative air mass and I_0 the normal incidence extraterrestrial radiation. (A constant value was used in this study.)

F_1' New circumsolar brightness coefficient

F_2' New horizon brightness coefficient

REFERENCES

1. R. R. Perez, J. T. Scott and R. Stewart, An anisotropic model for diffuse radiation incident on slopes of different orientations, and possible applications to CPCs. *Proc. of ASES*, Minneapolis, MN (1983), pp. 883–888.
2. D. Menicucci and J. Fernandez, Verification of photovoltaic system modeling codes based on system experimental data. *Proc. XVIIth IEE Photovoltaic Specialists Conference*, Kissimmee, FL (1984).
3. P. Ineichen, R. Perez and R. Seals, The importance of correct albedo determination for adequately modeling energy received by tilted surfaces. *Solar Energy* (in Press).
4. R. Perez and R. Stewart, Real time comparison of models estimating irradiation on sloping surfaces. *Proc. of ASES*, Anaheim, Ca. (1984).
5. B. Y. H. Liu and R. C. Jordan, The long-term average performance of flat-plate solar energy collectors. *Solar Energy* **7**, 53 (1963).
6. J. E. Hay and J. A. Davies, Calculation of the solar radiation incident on an inclined surface. *Proc. 1st Canadian Solar Radiation Data Workshop*, Toronto (1980) (Edited by J. E. Hay and T. K. Won), pp. 59–72.
7. T. M. Klucher, Evaluation of models to predict insolation on tilted surfaces. *Solar Energy* **23**, 111, 114 (1978).
8. M. H. Pepin-Bosc, D. Goetz and S. Janicot, Evaluation du rayonnement diffus du ciel. *Meteorologie et Energie Renouvelable Conference Proc.* AFME, Valbonne, France (1984).
9. R. Hulstrom and R. Bird, Solar irradiance available to various photovoltaic systems. Solar Energy Research Institute, Golden, CO, SERI/TI-215-2525 (1985).
10. R. Perez, R. Stewart, C. Arbogast, R. Seals and J. Scott, An anisotropic hourly diffuse radiation model for sloping surfaces—Description, performance validation, site dependency evaluation. *Solar Energy* **36**, 6 (1986).
11. International Energy Agency, Task IX, Subtask B, Solar Radiation Model Validation, Calculation of Solar Irradiances for Inclined Surfaces. Draft Report, IEA, Paris, France (1986).
12. B. Bourges, Analyse de Modeles de Calcul d'Eclairement Solaire sur Plans Inclines. Rapport CSTB—AR-MINES # 3.850.3168. Ecole des Mines de Paris, Paris, France (1985).
13. D. F. Menicucci, PVFORM Version 3.0, A photovoltaic system simulation program for stand-alone and grid-interactive applications. Sandia National Laboratories, Laboratories, Albuquerque, NM (1985).
14. Sandia National Laboratories Project #56-5434, SNL, Albuquerque, NM.
15. Direction de la Meteorologie, Service Meterologique Metropolitan, Stations #260 (Trappes) and 874 (Carpentras), Paris, France.
16. A. Zelenka, personal communication. Swiss Meteorological Institute, Zurich, Switzerland (1984).
17. CIE Committee E-3.2, Natural daylight—Official recommendations; 13th CIE Session Compte-Rendu, p. 11. Commission Internationale de l'Elairage, Paris, France (1955).
18. K. Coulson, *Solar and Terrestrial Radiation*, pp. 86–93. Academic Press, New York (1975).
19. USDOE Solar Energy Meteorology Research and Training Site, Region II, Albany, NY. Hourly data summaries, 1980–1981.

Distribution

Attn : Ron Bayes
4040 Morningstar Drive
Salt Lake City
UT 84117

Attn : Thomas J. Geever
8914 Villanova Ave.
Los Angeles
CA 90045

Attn : Walt Hart
5741 S. Jasmine
Englewood
CO 80111

Attn : Mr. G. Hoffmann
Tuev Rheinland
Box 101750
500 Cologne
West Germany

Attn : S. J. Phillips
50 Todd Avenue
COMO
WA 6152
Australia

Attn : Steve Verchinski
2700 Espanola NE
Albuquerque
NM 87110

Attn : Larry Workenpin
502 Stroop Ave.
Ridgecrest
CA 93555

A. N. Williams and Associates
Attn : A. Nash Williams, P.E.
P.O. Box 492
Bonsall
CA 92003

ARCO Solar, Inc.
Attn : Kim W. Mitchell
P.O. Box 2105
Chatsworth
CA 91313

Attn : Charles Brent
Box 5172
Hattiesburg
MS 39406

Attn : Bob Hammond
5225 Morgan Trail
Chino Valley
AZ 86323

Attn : Tom Hoff
Waukegan Rd.
Apt. 2A
Deerfield
IL 60015

Attn : Dr. Osamah Jamjoom
P.O. Box 8372
Jeddah 682-6445
Saudi Arabia

Attn : George C. Royal
2532 I Street NW
Washington, D.C.
20037

Attn : Arthur T. White
6411 Valley Circle Terr.
Canoga Park
CA 91307

3M Corporation
Attn : Allen Zderad
3M Center
Bldg 235-BC-05
St. Paul
MN 55144

ALCAD, Inc.
Attn : Jim McDowall
73 Defco Park Road
Wharton Brook Industrial Park
North Haven
CT 06473

Acurex Corporation
Attn : Les Doss III
555 Clyde Avenue
P.O. Box 7555
Mountain View
CA 94039

Aerospace Corporation
Attn : Edward J. Simburger, P.
2350 E. El Segundo Blvd.
El Segundo
CA 90245

Alabama Power Company
Attn : John T. Bambarger, P.E.
600 North 18th St.
P.O. Box 2641
Birmingham
AL 35291-0650

American Power Technology
Attn : Dave Brewer
4440 Del Monte
San Diego
CA 92107

Arizona Public Service Co.
Attn : Tom Lepley
P.O. Box 21666
Station 5629
Phoenix
AZ 85036

Arizona State University
Attn : Mehdi N. Bahadori
College of Architecture
Tempe
AZ 85287

Ascension Technology
Attn : Russell Miles
P.O. Box 121
Lincoln Center
MA 01773

Auburn University
Attn : Ali F. Imece, M.S.
Electrical Engineering Dept.
Auburn
AL 36849

BDM Corporation
Attn : Tim Lambarski
1801 Randolph Road SE
Albuquerque
NM 87106

Alabama Power Co.
Attn : Greg Reardon
P.O. Box 2641
Birmingham
AL 35291

Alpha Solarco
Attn : Pete Tyjewski
11536 Gondola Drive
Sharonville
OH 45241

Anco Engineers, Inc.
Attn : Nicholas Puga
9937 Jefferson Blvd.
Culver City
CA 90232-3591

Arizona Solar Energy Comm.
Attn : Robert L. Sears, P.E.,
1700 W. Washington
Executive Tower Room 502
Phoenix
AZ 85007

Arizona State University
Attn : Mehdi N. Bahadori, Ph.D
College of Architecture and
Environmental Design
Tempe
AZ 85287

Asian Institute of Technology
Attn : Dr. F. Lasnier
Division of Energy Technology
G.P.O. Box 2754
Bangkok 10501
Thailand

Auroville International USA
Attn : Joel Goodman
P.O. Box 162489
Sacramento
CA 95816

Battelle Columbus Laboratories
Attn : Gerald T. Noel
505 King Avenue
Columbus
OH 43201-2693

Bechtel Group, Inc.
Attn : Walter J. Stolte
50 Beale Street
P.O. Box 3965
San Francisco
CA 94119

Black and Veatch
Attn : Sheldon L. Levy
1500 Meadow Lake Parkway
Kansas City
MO 64114

Bluepoint Associates Ltd.
Attn : Art Dickerson
245 Hacienda Avenue
San Luis Obispo
CA 93401

Boeing Computer Services
Attn : Henry Mayorga
565 Andover Park West
Tukwila
WA 98188

CBNS
Attn : Leonard S. Rodberg
Queens College, CUNY
Flushing
NY 11367

Cal State Polytechnic Univ.
Attn : William B. Stine, Ph.D.
School of Engineering
3801 West Temple Avenue
Pomona
CA 91768-4062

Cal Tran
Attn : Roy Mode
1120 N Street
Sacramento
CA 95814

California Micro Utility
Attn : Rick Rodgers
Fort Cronkhite
Bldg. 1065
Sausalito
CA 94965

City of Austin Elec. Utility
Attn : John Hoffner
P.O. Box 1088
Austin
TX 78767

City of Austin Electric Util.
Attn : David C. Panico
P.O. Box 1088
Austin
TX 78767

City of Palo Alto
Attn : Scott Akin
Utilities Department
P.O. Box 10250
Palo Alto
CA 94303

Cochise Engineering Consult.
Attn : Bruce Johnson, P.E.
822 Calle Jinete
Sierra Vista
AZ 85635

Colorado Mountain College
Attn : Steve McCorney
Solar Program
3000 County Road 114
Glenwood Springs
CO 81601

Colorado Technical College
Attn : Chris Boyd
655 Elkton Drive
Colorado Springs
CO 80901

Colorado Technical College
Attn : Donald Mueller
655 Elkton Drive
Colorado Springs
CO 80901

Commission of European Comm.
Attn : Dr. G. Riesch
Joint Research Centre
Ispra Establishment
21020 Ispra
(Varese)
Italy

Council of Energy Res. Tribes
Attn : Glen Lane
1580 Logan St.
Denver
CO 80203

Dennis A. DeHaven Associates
Attn : Dennis A. DeHaven
11 South Middletown Rd.
P.O. Box 1790
Media
PA 19063

El Paso Electric
Attn : Margaret Andriola Danao
P.O. Box 982
El Paso
TX 79960

Energy Systems, Inc.
Attn : Lloyd Algie
1535 Meyerside Dr. Unit 6
Mississauga, Ontario
Canada P.C. L5T-1M9

Florida Power and Light
Attn : Gary L. Michel
P.O. Box 14000
Juno Beach
FL 33408

Florida Solar Energy Center
Attn : Henry M. Healey
300 State Road 401
Cape Canaveral
FL 32920

Georgia Institute of Tech.
Attn : Sheldon M. Jeter
School of Mechanical Eng.
Atlanta
GA 30332

Georgia Power Co.
Attn : Dennis L. Keebaugh
7 Solar Circle
Shenandoah
GA 30265

DeVry Institute of Technology
Attn : Anthony Meola
2149 West Dunlap Ave.
Phoenix
AZ 85021

Design Professionals, Inc.
Attn : George Bolling
4301 Carlisle Blvd. NE
Albuquerque
NM

Electric Power Research Inst.
Attn : John Schaefer
P.O. Box 10412
3412 Hill View Ave.
Palo Alto
CA 94303

Evans International
Attn : Lynn Hurlbert
3128 West Clarendon
Phoenix
AZ 87017

Florida Solar Energy Center
Attn : Gobind H. Atmaram, Ph.D
300 State Road 401
Cape Canaveral
FL 32920

Fysisch Laboratorium
Attn : E. A. Alsema
Rijksuniversiteit
P.O. Box 80 000
3508 TA
Utrecht
Netherlands

Georgia Institute of Tech.
Attn : George J. Vachtsevanos,
School of Electrical Eng.
Atlanta
GA 30332

Hawaii Natural Energy Inst.
Attn : Art Seki
University of Hawaii at Manoa
2540 Dole St.
Honolulu
HI 96822

Hughes Aircraft Corporation
Attn : John A. Castle
P.O. Box 9399
Bldg. A1 M/S 4C843
Long Beach
CA 90810-0399

Hughes Aircraft Corporation
Attn : John Ingersoll
Bldg. E11 MS V123
P.O. Box 902
El Segundo
CA 90245

Indian Institute of Technology
Attn : J. C. Joshi
Centre of Energy Studies
Hauz Khas
New Delhi - 110016
India

Institut for Physikalische
Attn : Dipl.-Phys. S. Nann
Elektronik
Postfach 80 11 40
D-7000
Stuttgart 80
West Germany

Integrated Power Corp.
Attn : Doug Danley
Systems Engineering Manager
7524 Standish Pl.
Rockville
MD 20855

Intersol Power Corp.
Attn : Nicholas J. Ganiaris
11901 W. Cedar Ave.
Lakewood
CO 80228

Intersol Power Corporation
Attn : Derek C. Cass
11901 W. Cedar Avenue
Lakewood
CO 80228

Iowa State University
Attn : A. G. Potter
215 Coover Hall
Ames
IA 50010

Jacksonville Electric Author.
Attn : George S. Rizk
233 West Duval St.
Jacksonville
FL 32202

Jet Propulsion Laboratory
Attn : Russell S. Sugimura
California Institute of Tech.
Mail Stop 507/201
4800 Oak Grove Drive
Pasadena
CA 91109

Jet Propulsion Laboratory
Attn : L. Wen
MS 507-201
4800 Oak Grove Drive
Pasadena
CA 91103

Jim Cullen Associates
Attn : Jim Cullen
P.O. Box 732
Laytonville
CA 95454

Johnson Controls, Inc.
Attn : Dr. Kathryn R. Bullock
P.O. Box 591
Milwaukee
WI 53201

Kansas City Power and Light
Attn : Dave Martin
P.O. Box 679 4th floor
Kansas City
MO 64141

Kuwait Institute for
Attn : Saud Ayyash
Scientific Research
Energy Department
P.O. Box 24885
13109 Safat
Kuwait

Martin Marietta Energy System
Attn : Stephen I. Kaplan
P.O. Box Y
Oak Ridge
TN 37831

Mass. Institute of Technology
Attn : Louis Bucciarelli
E51-201B
Cambridge
MA 02139

McFall-Konkel & Kimball
Attn : Robert E. Sidwell
2160 South Clermont St.
Denver
CO 80222

Meridian Corporation
Attn : Robert V. Russo
5113 Leesburg Pike
Suite 700
Falls Church
VA 22041

MicroComputer Design Tools
Attn : Ray Bahm
2513 Kimberly Court NW
Albuquerque
NM 87120

Mobil Solar Corporation
Attn : Anthony Norbedo
16 Hickory Drive
Wapahm
MA 02254

Murdoch University
Attn : Prof. P. J. Jennings
School of MPS
Murdoch, WA 6150
Australia

NMSEI
Attn : Steve Durand
Box 3 SOL
Las Cruces
NM 88003

New York Power Authority
Attn : Mark Kapner, P.E.
10 Columbus Circle
New York
NY 10019

Massachusetts Trans. Center
Attn : Harry Zuckerberg
MS DTS54
Transportation Systems Center
Kendall Square
Cambridge
MS 02142

Meridian Corporation
Attn : Anil Cabraal, Ph.D
5113 Leesburg Pike
Suite 700
Falls Church
VA 22041

Meridian Corporation
Attn : Lawrence T. Slominski
5113 Leesburg Pike, Suite 700
Falls Church
VA 22041

Midwest Research Institute
Attn : Matthew Imamura
425 Volker Blvd.
Kansas City
MO 64110

Mohawk Valley Community Coll.
Attn : Dr. Timothy J. Schwob
Div. of Technology and Bus.
1101 Sherman Drive
Utica
NY 13501

NCAT
Attn : Ray Schott
3040 Continental Dr.
P.O. Box 3838
Butte
MT 59702

NMSEI
Attn : Paul Hutchinson
Box 3 SOL
Las Cruces
NM 88003

North American PV
Attn : George Wilson
6400 Airport Rd, Suite A
El Paso
TX 79725

North Carolina St. Univ.
Attn : A. Almahdi
4408 Bleeker Ct.
Raleigh
NC 27606

Northern Arizona University
Attn : Jerry Hatfield
NAU Box 15600
Flagstaff
AZ 86011

Northern States Power
Attn : Mark Rogers
Research Department
414 Nicollet Mall
Minneapolis
MN 55401

ONSITE Energy
Attn : R. Alan Cowan
P.O. Box 9217
838 S.W. 1st, Suite 520
Portland
OR 97204

Old Dominion University
Attn : A. Sidney Roberts, Jr.,
Department of Mechanical Eng.
Norfolk
VA 23508

Ontario Research Foundation
Attn : John Savage
Sheridon Park
Postal Code L5K1B3
Mississanga
Ontario
Canada

Pacific Gas and Electric
Attn : Stephen L. Hester
3400 Crow Canyon Road
San Ramon
CA 94583

Pacific Gas and Electric
Attn : J. W. Maitland Horner
77 Beale Street
San Francisco
CA 94106

Pacific Gas and Electric
Attn : Chuck Whitaker
3400 Crow Canyon Rd.
San Ramon
CA 94583

Philadelphia Electric Co.
Attn : Donald Fagnan
Research and Testing Division
2301 Market Street
Philadelphia
PA 19101

Photron Canada, Inc.
Attn : Ron LaPlace
P.O. Box 136
Colinton, Alberta
TOG ORO Canada

Platte River Power Authority
Attn : Carol J. Dollard
Timberline & Horsetooth Roads
Fort Collins
CO 80525

Public Service Elec. and Gas
Attn : John L. Del Monaco, P.E
80 Park Plaza, T-16A
P.O. Box 570
Newark
NJ 07101

Public Service Elec. and Gas
Attn : Paul P. Perkins
80 Park Plaza, T16A
P.O. Box 570
Newark
NJ 07101

Public Service Elec. and Gas
Attn : Harry T. Roman
80 Park Plaza
P.O. Box 570
Newark
NJ 07101

Rainmakeer Cooling, Inc.
Attn : Leonard R. Bachman, AIA
1518 Castlerock
Houston
TX 77090

Regional Economic Research
Attn : Steve Ettinger
12520 High Bluff Drive
Suite 220
San Diego
CA 92130

SAIC
Attn : Richard Sterrett
MS #5
P.O. Box 2351
La Jolla
CA 92038

Salt River Project
Attn : Gary L. Powell, Ph.D.
P.O. Box 1980
Phoenix
AZ 85001

San Diego Gas and Electric
Attn : Don E. Fralick, P.E.
110 W. "A" Street
P.O. Box 1831
San Diego
CA 92112

Sci-Tech International
Attn : Ugur Ortabasi
5673 W. Las Positas Blvd.
Suite 205
Pleasanton
CA 94566

Solar Connection
Attn : Michael Orians
P.O. Box 1138
Morro Bay
CA 93442

Solar Electric Specialties
Attn : Jim Welch
649 Remmington
Fort Collins
CO 80524

Solar Engineering Services
Attn : Tim Ball
P.O. Box 7122
Olympia
WA 98507

Solarex Corporation
Attn : Eric E. Daniels
1335 Piccard Drive
Rockville
MD 20850

Rockwell International Corp.
Attn : T. C. Evatt
Rocketdyne Division
6633 Canoga Avenue
Canoga Park
CA 91304

Sab Nife Inc.
Attn : Arne O. Nilsson
George Washington Highway
P.O. Box 100
Lincoln
RI 02865

San Diego Gas & Electric
Attn : Eric Pulliam
P.O. Box 1831
San Diego
CA 92112

San Luis Valley Solar Energy
Attn : Tom Enos
512 Ross Ave.
Alamosa
CA 81101

Scientific Analysis, Inc.
Attn : John Allen Gunn, P.E.
6012 E. Shirley Lane
Montgomery
AL 36117

Solar Electric Co., Inc.
Attn : Ron Richmond
404 Piikoi St. Suite 267-B
Honolulu
HI 96814

Solar Energy Research Inst.
Attn : Richard DeBlasio
1617 Cole Blvd.
Golden
CO 80401

Solar Systems Design Inc.
Attn : Corey Mayer
RD1 Box 462A
Voorheesville
NY 12186

Solarex Corporation
Attn : Ramon Dominguez, P.E.
1335 Piccard Drive
Rockville
MD 20850

Solarex Corporation
Attn : Richard Keller
6510 W. 91st Avenue, Suite 102
Denver
CO 80030

Solavolt International
Attn : Bill Bailey
P.O. Box 2934
Phoenix
AZ 85062

Sonoma State University
Attn : Prof. Rocky Rohwedder
Energy Management and Design
Richnert Park
CA 94928

Southern Company Services
Attn : J. Timothy Petty
P.O. Box 2625
Birmingham
AL 35202

Spire Corporation
Attn : Steve Hogan
Patriots Park
Bedford
MA 01730

State University of NY/Albany
Attn : Richard Perez (50)
ASRC
1400 Washington Ave.
Albany
NY 12222

Swedish State Power Board
Attn : Dr. Bjorn Karlsson
DEVELOPMENT
Alvkarleby Laboratory
S-810 71
Alvkarleby
Sweden

Tennessee Valley Authority
Attn : David J. Chaffin, P.E.
SP2SD-C
Chattanooga
TN 37402-2801

Solarize Inc.
Attn : John Berdner
1450 Harbor Blvd.
Suite D
West Sacramento
CA 95691

Solavolt International
Attn : Paul Garvison
P.O. Box 2934
Phoenix
AZ 85062

Southern Company Services
Attn : J. Grott
P.O. Box 2625
Birmingham
AL 35202

Sovonics Solar Systems
Attn : Ronald C. Cull
4440 Warrensville Center Road
Cleveland
OH 44128

Stanford University
Attn : Albert Keicher
Member, Technical Staff
SLAC, P.O. Box 4349
Stanford
CA 94305

Stone and Webster Engineering
Attn : John V. Burns
P.O. Box 2325
Boston
MA 02107

Tel Aviv University
Attn : Prof. J. Appelbaum
Faculty of Engineering
Tel Aviv 69978
Israel

Tennessee Valley Authority
Attn : Jeff Jansen
Solar Group
Architectural Design Branch
400 Commerce Ave.
Knoxville
TN 37902

Tennessee Valley Authority
Attn : Sharon Ogle
1S 72A Signal Place
Chattanooga
TN 37402

Tennessee Valley Authority
Attn : Joan M. Wood
217 Power Building
Solar Electric Section
Chattanooga
TN 37401

U.S. Army Corps of Engineers
Attn : Linda Lawrie
P.O. Box 4005
Champaign
IL 61820

U.S. Department of Energy/HQ
Attn : Dr. A. D. Krantz
Division of PV Energy Systems
Room 5B066 Forrestal Bldg.
1000 Independence Ave. SW
Washington, D.C.
20585

Univ. of Texas at Arlington
Attn : Jack Fitzer
Electrical Engineering Dept.
Arlington
TX 76019

University of Arizona
Attn : Francisco Luttmann
Nuclear and Energy Engineering
Tucson
AZ 85721

University of Arizona
Attn : Adrian Tylin
Department of Nuclear Eng.
Engineering Bldg., Room 104
Tucson
AZ 85721

University of Delaware
Attn : Allen M. Barnett
Electrical Engineering Dept.
Newark
DE 19711

Tennessee Valley Authority
Attn : Barnabas Seaman
Commercial and Industrial Br.
25 55B Signal Place
Chattanooga
TN 37402-2801

U.S. Army Corps of Engineers
Attn : Dwight A. Beranek, P.E.
12565 W. Center Rd.
Omaha
NE 68144-3869

U.S. Department of Energy
Attn : Gary G. Hoffmann
Western Area Power Admin.
P.O. Box 3402
Golden
CO 80401

USA-CERL
Attn : Roch Ducey
Box 4005
Champaign
IL 61820

University of Alabama JEC
Attn : Leonard Adcock
Test Facility
Huntsville
AL 35899

University of Arizona
Attn : Donald E. Osborn
College of Engineering
Solar and Energy Research Fac
Harvill Bldg. Box 11 Room 151
Tucson
AZ 85721

University of Cape Town
Attn : Dr. A. A. Eberhard
Energy Research Institute
Private Bag
Rondebosch 7700
South Africa

University of Illinois
Attn : Ted Funk
Regional Office
1209 Wenthe Drive
Effingham
IL 62401

University of Lowell
Attn : Stuart L. Frye
One University Ave.
Lowell
MA 01854

University of Queensland
Attn : Peter Jolly
SERC
St. Lucia
Queensland
Australia

University of Wyoming
Attn : Prof. Badrul Chowdhury
EE Dept.
University Station Box 3295
Laramie
WY 82071

Virginia Power / CTA
Attn : Wendy Thompson
P.O. Box 26666
Richmond
VA 23261

WATSON Simulation Laboratory
Attn : Larry D'Andrea
University of Waterloo
Waterloo
Ontario N2L3G1

William Lamb Co.
Attn : Joel Davidson
10615 Chandler Blvd.
North Hollywood
CA 91601

6221	E. C. Boes
6223	G. J. Jones
6223	R. N. Chapman (10)
6223	J. W. Strachan
6224	D. E. Arvizu
6226	D. F. Menicucci (50)
3141	S. A. Landenberger (5)
3151	W. I. Klein (3)
3154-1	C. L. Ward (8) DOE/OSTI
8524	J. A. Wackerly
6220	A. V. Poore

University of New Mexico
Attn : Dr. W. A. Gross
Department of Mechanical Eng.
Albuquerque
NM 87131

University of Wisconsin
Attn : Dr. Sandy Klein
Dept. of Mechanical Eng.
Madison
WI 53706

Virginia Polytechnic Institute
Attn : Saifur Rahman, Ph.D.
Electrical Engineering Dept.
Blacksburg
VA 24061

Virginia Power Co.
Attn : J. W. Greene
P.O. Box 26666
Richmond
VA 23261

Wichita State University
Attn : Dr. Ward Jewell
Dept. of Electrical Eng.
Box 44
Wichita
KS 67208-1595

World Crafts Foundation
Attn : Hans Guggenheim
318 Shawnut Avenue
Boston
MA 02118

XYTEC
Attn : Bruce Blevins
4110 Tesota
Las Cruces
NM 88001